



UNIVERSIDADE DA BEIRA INTERIOR
Engenharia

Adaptive Methods for Color Vision Impaired Users

Maria Madalena Gonçalves Ribeiro

Tese para obtenção do Grau de Doutor em
Engenharia Informática
(3º de ciclo de estudos)

Orientador: Prof. Doutor Abel João Padrão Gomes

Covilhã, julho de 2017

To my daughters, Carolina and Carlota

Acknowledgments

Imprimis, to Professor Abel Gomes. I express my heartfelt thanks by the exceptional guidance along this research project, for the availability, by teaching me in finding the ways and by the priceless encouragement.

To the Instituto Politécnico de Castelo Branco by the support, notwithstanding the huge budgetary constraints. In particular, to ESART, I present the recognition and gratitude to the School Board of Directors, which made possible a sabbatical for a semester.

To my dear friend Miguel Afonso, by his willingness in clarifying the color vision in the perspective of Physics.

To Marco Bernardo, who understands the issues related to the color vision deficiency, for his precious help in the questionnaires improvement.

To Paulo Silveira, Isabel Castanheira and Carla S. Pedro, by the earnest collaboration with the statistical study.

To Ana Sofia Marcelo, Daniel Raposo and Fernando Raposo, who suggested and lent me relevant bibliography.

To the authors that answered to my help requests, about some issues found in their articles. Particularly, I would like to thank Françoise Viénot, João Brisson Lopes, Manuel Menezes de Oliveira Neto and Alina Mereuta who gently sent me relevant documents for this doctoral work.

To Orlando Pereira and David Flatla, by the exchange of ideas about technical issues. Thank you for the support.

To the CVD people, who collaborated by manifesting their opinion during the usability study. Their collaboration was crucial my findings, so my sincere acknowledgments.

To my parents, for teaching me how to set new goals, making me believe that I would reach them.

To my dear husband, Luis Miguel, by his understanding about the meaning of this endeavor, by his support in fostering the family balance.

To Carolina and Carlota, my beloved daughters, due to the care that I did not give them. I know that you rationally understand the absences of a busy mother, but there is no way of explaining it to your young hearts.

To Who that hands me the strength, giving me the floor, even when it seems to disappear.

Abstract

Color plays a key role in the understanding of the information in computer environments. It happens that about 5% of the world population is affected by color vision deficiency (CVD), also called color blindness. This visual impairment hampers the color perception, ending up by limiting the overall perception that CVD people have about the surrounding environment, no matter it is real or virtual. In fact, a CVD individual may not distinguish between two different colors, what often originates confusion or a biased understanding of the reality, including web environments, whose web pages are plenty of media elements like text, still images, video, sprites, and so on.

Aware of the difficulties that color-blind people may face in interpreting colored contents, a significant number of recoloring algorithms have been proposed in the literature with the purpose of improving the visual perception of those people somehow. However, most of those algorithms lack a systematic study of subjective assessment, what undermines their validity, not to say usefulness. Thus, in the sequel of the research work behind this Ph.D. thesis, the central question that needs to be answered is whether recoloring algorithms are of any usefulness and help for colorblind people or not.

With this in mind, we conceived a few preliminary recoloring algorithms that were published in conference proceedings elsewhere. Except the algorithm detailed in Chapter 3, these conference algorithms are not described in this thesis, though they have been important to engender those presented here. The first algorithm (Chapter 3) was designed and implemented for people with dichromacy to improve their color perception. The idea is to project the reddish hues onto other hues that are perceived more regularly by dichromat people.

The second algorithm (Chapter 4) is also intended for people with dichromacy to improve their perception of color, but its applicability covers the adaptation of text and image, in HTML5-compliant web environments. This enhancement of color contrast of text and imaging in web pages is done while keeping the naturalness of color as much as possible. Also, to the best of our knowledge, this is the first web recoloring approach targeted to dichromat people that takes into consideration both text and image recoloring in an integrated manner.

The third algorithm (Chapter 5) primarily focuses on the enhancement of some of the object contours in still images, instead of recoloring the pixels of the regions bounded by such contours. Enhancing contours is particularly suited to increase contrast in images, where we find adjacent regions that are color indistinguishable from dichromat's point of view. To our best knowledge, this is one of the first algorithms that take advantage of image analysis and processing techniques for region contours.

After accurate subjective assessment studies for color-blind people, we concluded that the CVD adaptation methods are useful in general. Nevertheless, each method is not efficient enough to adapt all sorts of images, that is, the adequacy of each method depends on the type of image (photo-images, graphical representations, etc.).

Furthermore, we noted that the experience-based perceptual learning of colorblind people throughout their lives determines their visual perception. That is, color adaptation algorithms

must satisfy requirements such as color naturalness and consistency, to ensure that dichromat people improve their visual perception without artifacts. On the other hand, CVD adaptation algorithms should be object-oriented, instead of pixel-oriented (as typically done), to select judiciously pixels that should be adapted. This perspective opens an opportunity window for future research in color accessibility in the field of in human-computer interaction (HCI).

Keywords

Color vision deficiency, color adaptation, human-computer interaction, accessibility, inclusion.

Resumo

A cor desempenha um papel fundamental na compreensão da informação em ambientes computacionais. Porém, cerca de 5% da população mundial é afetada pela deficiência de visão de cor (ou *Color Vision Deficiency* (CVD), do Inglês), correntemente designada por daltonismo. Esta insuficiência visual dificulta a percepção das cores, o que limita a percepção geral que os indivíduos têm sobre o meio, seja real ou virtual. Efetivamente, um indivíduo com CVD vê como iguais cores que são diferentes, o que origina confusão ou uma compreensão distorcida da realidade, assim como dos ambientes web, onde existe uma abundância de conteúdos média coloridos, como texto, imagens fixas e vídeo, entre outros.

Com o intuito de mitigar as dificuldades que as pessoas com CVD enfrentam na interpretação de conteúdos coloridos, tem sido proposto na literatura um número significativo de algoritmos de recoloração, que têm como o objetivo melhorar, de alguma forma, a percepção visual de pessoas com CVD. Porém, a maioria desses trabalhos carece de um estudo sistemático de avaliação subjetiva, o que põe em causa a sua validação, se não mesmo a sua utilidade. Assim, a principal questão à qual se pretende responder, como resultado do trabalho de investigação subjacente a esta tese de doutoramento, é se os algoritmos de recoloração têm ou não uma real utilidade, constituindo assim uma ajuda efetiva às pessoas com daltonismo.

Tendo em mente esta questão, concebemos alguns algoritmos de recoloração preliminares que foram publicados em atas de conferências. Com exceção do algoritmo descrito no Capítulo 3, esses algoritmos não são descritos nesta tese, não obstante a sua importância na conceção daqueles descritos nesta dissertação. O primeiro algoritmo (Capítulo 3) foi projetado e implementado para pessoas com dicromacia, a fim de melhorar a sua percepção da cor. A ideia consiste em projetar as cores de matiz avermelhada em matizes que são melhor percebidos pelas pessoas com os tipos de daltonismo em causa.

O segundo algoritmo (Capítulo 4) também se destina a melhorar a percepção da cor por parte de pessoas com dicromacia, porém a sua aplicabilidade abrange a adaptação de texto e imagem, em ambientes web compatíveis com HTML5. Isto é conseguido através do realce do contraste de cores em blocos de texto e em imagens, em páginas da web, mantendo a naturalidade da cor tanto quanto possível. Além disso, tanto quanto sabemos, esta é a primeira abordagem de recoloração em ambiente web para pessoas com dicromacia, que trata o texto e a imagem de forma integrada.

O terceiro algoritmo (Capítulo 5) centra-se principalmente na melhoria de alguns dos contornos de objetos em imagens, em vez de aplicar a recoloração aos pixels das regiões delimitadas por esses contornos. Esta abordagem é particularmente adequada para aumentar o contraste em imagens, quando existem regiões adjacentes que são de cor indistinguível sob a perspetiva dos observadores com dicromacia. Também neste caso, e tanto quanto é do nosso conhecimento, este é um dos primeiros algoritmos em que se recorre a técnicas de análise e processamento de contornos de regiões.

Após rigorosos estudos de avaliação subjetiva com pessoas com daltonismo, concluiu-se que os métodos de adaptação CVD são úteis em geral. No entanto, cada método não é suficientemente eficiente para todos os tipos de imagens, isto é, o desempenho de cada método depende do tipo

de imagem (fotografias, representações gráficas, etc.).

Além disso, notamos que a aprendizagem perceptual baseada na experiência das pessoas daltônicas ao longo de suas vidas é determinante para perceber aquilo que vêem. Isto significa que os algoritmos de adaptação de cor devem satisfazer requisitos tais como a naturalidade e a consistência da cor, de modo a não pôr em causa aquilo que os destinatários consideram razoável ver no mundo real. Por outro lado, a abordagem seguida na adaptação CVD deve ser orientada aos objetos, em vez de ser orientada aos pixels (como tem sido feito até ao momento), de forma a possibilitar uma seleção mais criteriosa dos pixels que deverão ser sujeitos ao processo de adaptação. Esta perspectiva abre uma janela de oportunidade para futura investigação em acessibilidade da cor no domínio da interação humano-computador (HCI).

Palavras-chave

Deficiência na visão da cor, adaptação da cor, interação humano-computador, acessibilidade, inclusão.

Resumo alargado

Os algoritmos de recoloração e adaptação de cor para pessoas com deficiência na visão de cor (*color vision deficiency* (CVD), do inglês), também designadas por pessoas daltónicas, é um tema importante de investigação do domínio da acessibilidade e da interação humano-computador (*human-computer interaction* (HCI), do inglês). No decurso do trabalho de investigação, constatou-se a existência de um número significativo de algoritmos de recoloração na literatura e, salvo algumas exceções, observou-se que os algoritmos propostos não são acompanhados por uma avaliação subjetiva que os permita validar. De certa forma, este facto mostra que a aprendizagem perceptual das pessoas daltónicas não é tida em conta na conceção de algoritmos de recoloração, que são habitualmente propostos por pessoas tricromatas e não por pessoas daltónicas. Na verdade, uma pessoa daltónica aprende a identificar um vermelho porque todos lhe dizem que essa cor é um vermelho. No entanto, ele/ela não vê o vermelho como um tricromata. Na verdade, um vermelho é visto como um verde, ainda que esse vermelho não seja nem um vermelho nem um verde, mas sim uma espécie de amarelo escuro (acastanhado), simplesmente porque um dicromata só vê amarelos e azuis.

Enquadramento e Motivação

Como se sabe, as pessoas que possuem os tipos mais comuns de dicromacia (i.e., deuteranopia ou protanopia) só veem azuis (uma cor primária) e amarelos (uma cor secundária). Estas pessoas têm dificuldade em distinguir os vermelhos dos verdes, pois os seus cones vermelhos (no caso da protanopia) ou os cones verdes (no caso da deuteranopia) não funcionam ou não existem na retina. No caso de tritanopia, são os cones azuis que não funcionam ou não estão presentes na retina das pessoas afetadas. Neste caso, as pessoas só veem vermelhos e cianos, com mais ou menos quantidade de saturação e de luz.

Surpreendentemente, depois de um conjunto exaustivo de experiências, descobrimos que este tipo de daltónicos só vê dois tons no espaço de cor HSV, 240-azul e 60-amarelo, embora o espectro de luz abranja outros azuis e amarelos. Como consequência, o seu espaço de cor é limitado a um triângulo de cor, que resulta do corte do cone HSV em duas partes idênticas. Por outras palavras, todas as cores vistas por tricromatas são percebidas pelos dicromatas como 240-azul e 60-amarelo, com maior ou menor saturação e brilho.

A questão é, então, como melhorar a perceção da cor de alguém que só vê amarelos e azuis, com maior ou menor saturação e brilho, mantendo a naturalidade da cor tanto quanto possível, do ponto de vista de uma pessoa dicromata? Tem alguma utilidade efetiva? De facto, a recoloração facilmente entra em conflito com a aprendizagem perceptual dos indivíduos, uma vez que eles estão habituados a ver o mundo de uma certa maneira. De alguma forma, estas questões foram o ponto de partida do trabalho de investigação subjacente a esta tese de doutoramento.

Declaração de Tese

No decurso deste trabalho de investigação sobre métodos de adaptação de cor para pessoas com daltonismo, percebemos que a aprendizagem percetual de cada indivíduo é determinante para a sua perceção da realidade. Algumas pessoas veem o mundo em tons de amarelo e azul, outras em tons de ciano e vermelho, mas a maioria delas vê em todos os matizes, não obstante se é de uma forma distorcida ou não.

Ao mudar as cores das imagens e do texto através de algoritmos, poderemos interferir com essa perceção que as pessoas com daltonismo têm sobre a realidade. De facto, é o que acontece com a maioria dos algoritmos existentes na literatura. As pessoas com deuteranopia veem os verdes como verdes distorcidos. Portanto, faz muito mais sentido vê-los dessa forma do que mudar a cor das folhas de uma árvore numa fotografia para azul, pois isso irá romper com a aprendizagem percetual desse indivíduo.

Assim sendo, este trabalho de investigação assenta sobre a seguinte declaração de tese:

É possível encontrar um método adaptativo para pessoas daltónicas que é capaz de melhorar a sua perceção visual (i.e., que lhes permita ver mais objetos/elementos de imagem do que em circunstâncias habituais, sem adaptação), sem interferir com a sua aprendizagem percetual.

Como se pode verificar ao longo desta dissertação, mostramos que de facto isso é possível, mas não de forma universal, pois cada método é mais adequado para certas categorias de imagens do que para outras. Tentámos cobrir um domínio representativo de imagens, pelo que foram consideradas imagens pertencendo a cinco categorias: visualização da informação (infovis), fotografias de cenas interiores (*indoor*), fotografias de cenas exteriores (*outdoor*), visualização científica (scivis), e sinalética.

Questões de Investigação

Tendo em consideração o problema geral da adaptação de cor em imagens para melhoria da percepção visual de pessoas com daltonismo, as principais questões de investigação que precisam ser respondidas são as seguintes:

É possível aumentar a percepção visual de um indivíduo com daltonismo pela aplicação de um processo de recoloração a uma imagem, sem interferir com a sua aprendizagem percetual?

Em determinadas circunstâncias, uma pessoa daltónica não consegue distinguir dois objetos adjacentes numa imagem, mesmo quando esses objetos são representados com cores suficientemente distintas. Isto acontece pois essas duas cores são distintas para um tricromata, mas vistas como iguais para um indivíduo com daltonismo. A recoloração resolve este problema facilmente, embora acarrete efeitos colaterais que conflituam com a aprendizagem percetual, porque geralmente é um processo que se aplica aos pixels da imagem, independentemente dos

objetos existentes na cena representada. A questão é então, como mitigar estes efeitos secundários no processo de recoloração. A nossa estratégia para resolver este problema consiste em manter a naturalidade da cor tanto quanto possível e, em simultâneo, aumentar o contraste entre os diferentes objetos constituintes da cena. Isto leva-nos a uma outra pergunta.

É possível que um indivíduo com daltonismo veja objetos que não são inicialmente distinguíveis numa determinada imagem original, sem interferir com a sua aprendizagem perceptual?

Tanto quanto sabemos, não há nenhum algoritmo capaz de fazer esta tarefa corretamente. A razão reside no facto de tal procedimento requerer a definição dos contornos de objetos de uma cena representada na imagem. A nossa estratégia consistiu em usar técnicas de análise e processamento de imagem para detetar os contornos de objetos das imagens, realçando-os sempre que necessário. Esta abordagem tem a vantagem de minimizar as alterações nas imagens, indo de encontro ao que está estabelecido pela aprendizagem perceptual do indivíduo daltónico.

Os algoritmos de recoloração são efetivamente úteis para as pessoas daltónicas?

A nossa resposta é afirmativa, desde que os métodos de adaptação preservem a aprendizagem perceptual dos indivíduos daltónicos. Na maioria dos algoritmos existentes na literatura parece não existir qualquer preocupação relativamente à preservação da aprendizagem perceptual dos indivíduos daltónicos. De facto, apenas um trabalho de investigação nesta área se faz acompanhar de um efetivo estudo de avaliação subjectiva. Neste trabalho, realizou-se uma série de estudos de avaliação subjetiva, a partir dos quais foi possível concluir que os algoritmos de adaptação são úteis desde que não colidam de forma significativa com a aprendizagem perceptual do indivíduo daltónico. Além disso, depois de terminar este trabalho, concluímos que a adaptação de cor em imagens deve ser realizada seletivamente, i.e., em objetos específicos nas imagens. Em particular, os algoritmos de adaptação devem identificar as cores ou as áreas que são confundidas com outras ou que ficam mesmo invisíveis para os indivíduos daltónicos, agindo então em conformidade.

Trajetos do Trabalho de Investigação

No início do trabalho de investigação subjacente à presente dissertação, tivemos a intenção de investigar as dificuldades visuais de pessoas daltónicas quando interagem com navegadores web, em particular com a cor do texto e imagens. A ideia era projetar e desenvolver um *add-on* de recoloração como uma extensão para as funcionalidades de um navegador, o que fizemos em devido tempo. Rapidamente, percebemos que não há diferença na recoloração de imagem e texto; a única diferença é o meio, não o algoritmo de recoloração.

Entretanto, procedeu-se à revisão da literatura sobre métodos de adaptação de cor para pessoas com deficiência na visão de cor (CVD). Considerámos também algoritmos de simulação CVD, a fim de observar como as pessoas daltónicas veem o mundo, em termos de cor. Curiosamente, encontramos algumas dezenas desses algoritmos, embora a maioria não inclua qualquer estudo

de avaliação subjetiva, a fim de validar a sua eficácia perceptual na eliminação de ambiguidades da cor. Porém, implementámos alguns desses algoritmos de recoloração focados na dicromacia, de modo a obter uma melhor compreensão do problema em questão. Criámos e implementámos também alguns novos algoritmos, sendo um destes descrito no Capítulo 3. Assim, concluímos a primeira fase do nosso trabalho de investigação.

A segunda etapa do trabalho de investigação envolveu a conceção e desenvolvimento de um método de adaptação de cor (recoloração), tendo como premissa o respeito pela aprendizagem perceptual dos dicromatas. A percepção visual de seres humanos está estreitamente relacionada com a experiência de aprendizagem prévia, que intimamente relaciona os objetos com as suas cores típicas; por exemplo, é bastante difícil imaginar uma laranja azul na natureza. A interpretação sobre o que observamos é extremamente dependente da aprendizagem baseada nas experiências passadas, sendo construída ao longo das nossas vidas. Curiosamente, depois de entrevistar alguns indivíduos com dicromacia, percebemos que estes são capazes de reconhecer e identificar as cores vivas pelos respetivos nomes; por exemplo, são capazes de identificar alguns vermelhos, embora não consigam ver os vermelhos como os tricromatas veem os vermelhos. A fim de não interferir com a sua aprendizagem perceptual e experiência prévia, adotámos a estratégia de mudar as cores o menos possível. Este objetivo foi atingido através do *aumento do contraste* das cores da imagem, e ao mesmo tempo mantendo a *naturalidade da cor*, bem como a *consistência no mapeamento de cor*. O Capítulo 4 descreve um algoritmo de recoloração que satisfaz estes três requisitos.

Na terceira fase da investigação, adotámos uma abordagem distinta para adaptação de cor em imagens estáticas. Na verdade, a maioria dos algoritmos de mapeamento de cor são orientados aos píxeis, sendo que todos eles são recoloridos da mesma forma, não havendo qualquer distinção entre eles na imagem. Ao invés, decidimos considerar o conteúdo de imagens em termos de seus objetos constituintes, encontrando primeiro os seus contornos ou limites. Depois, só os píxeis desses contornos entre objetos adjacentes são realçados, se necessário, de modo a reforçar a sua identidade. Tais contornos ou limites são determinados utilizando métodos baseados em arestas, próprios do domínio de análise e processamento de imagem. Tanto quanto sabemos, este é o primeiro algoritmo deste tipo a ser utilizado em métodos de adaptação para deficiência na visão da cor que se foca no realce de contornos, como descrito no Capítulo 5.

Finalmente, e após a submissão dos três artigos mais importantes produzidos no âmbito do trabalho de investigação de doutoramento a revistas especializadas, deu-se início à escrita desta dissertação.

Contribuições

De uma forma geral, pode dizer-se que as principais contribuições do trabalho de investigação que nos levou à escrita desta tese de doutoramento são as seguintes:

- Uma nova técnica de recoloração que tem em conta o espaço de cor bi-dimensional de dicromatas. Tal como poderá ver ao longo desta dissertação, e considerando o espaço cónico HSV percebido por tricromatas, em que os matizes de cor se distribuem ao longo de 360 graus, o espaço de cor de dicromatas corresponde ao triângulo que resulta da

interseção entre o cone HSV e o plano definido pelo ápice do cone e pelos matizes 60-amarelo e 240-azul, com maior ou menor saturação e brilho. A nossa técnica permite também mapear diretamente as coordenadas RGB para tricromatas em coordenadas RGB para dicromatas. Esta técnica foi incorporada no algoritmo RGBeat (veja-se Capítulo 4), que cumpre os três requisitos acima mencionados: melhoria do contraste, preservação da naturalidade da cor e preservação da consistência de cor.

- Uma das primeiras técnicas de adaptação de cor que se baseia no realce de contornos (veja-se Capítulo 5). Isto foi feito utilizando técnicas de deteção de contornos de objetos em imagens, como é habitual no domínio da análise e processamento de imagem. A ideia principal consiste em aumentar o contraste dos contornos (ou parte deles) de objetos que, supostamente, são confundidos com outros objetos adjacentes na imagem. Desta forma, a imagem permanece quase intocada, embora as pessoas com daltonismo vejam aumentada a sua perceção visual, uma vez que acabam por ver mais objetos numa cena do que conseguiriam ver sem adaptação.
- A abertura de uma janela de oportunidade para o prosseguimento da investigação, depois de descobrir que os atuais métodos de adaptação não são ainda suficientemente eficientes na melhoria da perceção visual das pessoas daltónicas. Isto acontece porque a maioria desses métodos são orientados aos píxeis (i.e., todos os píxeis da imagem são tratados da mesma forma), em vez de serem orientados aos objetos, ou seja, não têm em consideração o modo como as pessoas com daltonismo veem o mundo circundante.

A lição a tirar deste trabalho de investigação é que deve ser alterada a metodologia adotada no âmbito das novas técnicas de adaptação de cor para pessoas daltónicas. Esta metodologia tem que ser sustentada no espaço de cor das pessoas daltónicas, sem ignorar a aprendizagem perceptual sobre a cor ao longo das suas vidas.

Publicações

Este trabalho não foi financiado por qualquer bolsa ou projeto de investigação. No entanto, o registo e a participação em conferências foram parcialmente financiados pela Universidade da Beira Interior, através de verbas internas do Curso de Doutoramento em Engenharia Informática, assim como pelo Instituto Politécnico de Castelo Branco, onde a doutoranda é docente. Este trabalho deu origem às seguintes submissões a revistas científicas da especialidade:

Ribeiro, M. and Gomes, A. Recoloring Algorithms for Colorblind People: A Survey. *ACM Computing Surveys* (submitted), 2017.

Abstract: The color is a powerful communication component everywhere, not only as part of the message and its meaning but also as a way of discriminating contents therein. However, 5% of world population suffer from a visual impairment, known as color vision deficiency (CVD), commonly known as colorblindness, which constrains the color perception. This handicap adulterates the way the color is perceived, compromising the reading and understanding of the message contents. This fact becomes even more serious due to the increasing availability of

multimedia contents in computational environments, mainly on the web and other resources provided by the Internet, as well due to the growing on graphical software and tools. This issue becomes even more meaningful with the widespread of the small portable display devices, where the content size is quite reduced. Aware of this problem, a significant number of research works related to the CVD condition have been described in the literature in the last two decades, in particular, those aimed at improving the readability of contents via color enhancing, independently of they include text, images or both. This survey mainly intends to reveal the state-of-the-art on recoloring algorithms for still images, as well to identify the current trends in the assessment and correction techniques for colorblind people.

Ribeiro, M. and Gomes, A. RGBeat: A Recoloring Algorithm for Deutan and Protan Dichromats. *IEEE Transactions on Visualization and Computer Graphics* (submitted), 2016.

Abstract: It is widely accepted that people with deutan and protan dichromats only see blues and yellows, so that they cannot distinguish reds from greens very well. In fact, we will see that deutan and protan dichromats only see exactly two hues in the HSV color space, 240-blue (240°) and 60-yellow (60°). Thus, their color space is limited to a color triangle that cuts off the HSV color cone into two identical parts. With this in mind, we propose here a novel recoloring algorithm for deutan and protan dichromats to enhance their color perception, particularly in HTML5-compliant web environments. This is accomplished by enhancing color contrast of text and imaging in web pages, while keeping the naturalness of color as much as possible. Also, as far as we know, this is the first web recoloring approach for dichromat people that takes into consideration both text and image recoloring in an integrated manner. Moreover, it is also one of the first color adaptation methods that increases the visual perception of deutan and protan dichromats relative to original images.

Ribeiro, M. and Gomes, A. Contour Enhancement Approach for Dichromat People. *IEEE Transactions on Visualization and Computer Graphics* (submitted), 2017.

Abstract: A variety of recoloring methods have been proposed in the literature to remedy the problem of confusing red-green colors faced by dichromat people (as well by other color-blinded people). The common strategy to mitigate this problem is to remap colors to other colors. But, it is clear this does not guarantee neither the necessary contrast to distinguish the elements of an image, nor the naturalness of colors learnt from past experience of each individual. In other words, the individual's perceptual learning may not hold under color remapping. With this in mind, we introduce the first algorithm that selectively enhances the required object contours in still images, instead of recoloring the pixels of the regions bounded by such contours or even the entirety of such contours. This is particularly adequate to increase contrast in images where we find adjacent regions that are color-indistinguishable from the dichromacy's point of view.

Outros artigos publicados no decurso do trabalho de investigação conducentes à presente dissertação são os seguintes:

— Ribeiro, M. and Gomes, A. *Adaptação de Cor para Dicromatas na Visualização de Imagens.*

In Proceedings of the 20th Encontro Português de Computação Gráfica (EPCG'2012), Viana do Castelo, Portugal, pp. 99-102, October 2012.

— Ribeiro, M. and Gomes, A. *Recoloração de Web Conteúdos para Daltónicos - Recoloração de Imagens*. In Proceedings of the 2nd International Conference in Design e Graphic Arts (CIDAG'2012), Tomar, Portugal, pp. 470-473, October 2012.

— Ribeiro, M. and Gomes, A. *A Skillet-Based Recoloring Algorithm for Dichromats*. In Proceedings of the 15th IEEE International Conference on E-Health Networking, Application and Services (IEEE HealthCom'2013), Lisbon, Portugal, pp. 654-658, October 2013.

— Ribeiro, M. and Gomes, A. *Adaptação da Cor da Tipografia em Páginas Web para Pessoas com Deficiência na Visão da Cor*. In Proceedings of the 4º Encontro de Tipografia, Idanha-a-Nova, Portugal, pp. 83-88, September 2013.

— Ribeiro, M. and Gomes, A. *Creating Accessibility to Web Contents for Colorblind People*. In Proceedings of the 5th International Conference on Applied Human Factors and Ergonomics (AHFE'2014), Kraków, Poland, Vol. 10, pp. 646-656, AHFE International, July 2014.

Organização da Tese

Apesar de vários artigos publicados durante o programa de doutoramento, esta tese inclui apenas os resultados dos artigos mais relevantes que foram submetidos ou publicados, em devido tempo. A tese está então organizada da seguinte forma:

Capítulo 1. Este é o presente capítulo, que relata a motivação subjacente a este trabalho, bem como a *declaração de tese*, as principais questões de investigação, as contribuições científicas decorrentes do trabalho de investigação, assim como as publicações que levaram à elaboração desta tese.

Capítulo 2. Este capítulo leva a cabo uma revisão da literatura sobre métodos e algoritmos de adaptação de cores para as pessoas com daltonismo. Este estudo revelou-se essencial para identificar o estado-da-arte em métodos de recoloração, suas lacunas e pontos fortes, vantagens e desvantagens, na procura de novas soluções, assim como abordagens e metodologias alternativas.

Capítulo 3. Neste capítulo é apresentado um método de adaptação de cor baseado na estratégia de mapeamento de cor. Este método segue uma abordagem convencional de algoritmos de recoloração com base no espaço de cor HSV. O objetivo principal é projetar as cores avermelhadas numa outra gama de matizes, por forma a poderem ser melhor vistas por pessoas com dicromacia.

Capítulo 4. Este capítulo descreve um método de adaptação de cor igualmente baseado na estratégia de mapeamento de cor. De certa forma, este método introduz uma nova técnica de mapeamento que leva em consideração o equilíbrio entre os seguintes requisitos percetuais: naturalidade da cor, a consistência de cor e o realce de contraste. Além disso, a recoloração foi concebida no espaço de cor HSV, embora sendo diretamente realizada no espaço de cor RGB.

Capítulo 5. Este capítulo apresenta um método inovador de adaptação de cor que envolve apenas uma estratégia de realce de contornos, com base em técnicas de análise e processamento de imagem. Especificamente, é usado o filtro de Sobel para detetar os contornos de objetos numa imagem. De seguida, os contornos dos objetos (e não os seus interiores) são sujeitos a um processo recoloração, de forma seletiva.

Capítulo 6. Este capítulo conclui a tese, onde se discutem também os resultados obtidos. No final, são ainda deixadas algumas questões em aberto e sugestões para trabalho futuro.

Contents

1	Introduction	1
1.1	Context and Motivation	1
1.2	Thesis Statement	2
1.3	Research Questions	2
1.4	The Course of the Research Work	3
1.5	Contributions	4
1.6	Publications	5
1.7	Thesis Organization	7
2	Adaptive Methods for Color Vision Deficiency – a Survey	9
2.1	Introduction	9
2.2	Color Perception	10
2.2.1	Color Vision Deficiency	10
2.3	CVD Adaptation Methods for Anomalous Trichromacy	13
2.3.1	<i>LMS</i> Based Methods	13
2.3.2	RGB Based Methods	15
2.3.3	HSx Based Methods	16
2.3.4	CIE Based Methods	17
2.3.5	Methods for Anomalous Trichromacy: a Discussion	22
2.4	CVD Adaptation Methods for Dichromacy	24
2.4.1	LMS Based Methods	24
2.4.2	RGB Based Methods	26
2.4.3	HSx Based Methods	29
2.4.4	CIE Based Methods	34
2.4.5	Methods for Dichromacy: a Discussion	42
2.5	CVD Adaptation Methods for Monochromacy	45

2.5.1	CIE Based Methods	45
2.5.2	Methods for Monochromacy: a Discussion	45
2.6	Critical Analysis and Trends for the Future	46
2.7	Conclusions	47
3	ShrinkInverse: Creating Accessibility to Web Contents for Colorblind People	49
3.1	Introduction	49
3.2	Background	49
3.2.1	RGB Color Model	49
3.2.2	HSV Color Model	50
3.2.3	HSL Color Model	50
3.3	The ShrinkInverse Algorithm	51
3.4	The Recoloring Algorithm	53
3.5	Experimental Results	54
3.5.1	Setup	54
3.5.2	Comparative Analysis	54
3.5.3	Time Performance	54
3.5.4	Comparative Recoloring	54
3.6	Further Remarks	57
4	RGBeat: A Recoloring Algorithm for Deutan and Protan Dichromats	59
4.1	Introduction	59
4.2	Recoloring Algorithm	59
4.2.1	Leading Idea	59
4.2.2	HSV Color Domain of Deuteranopy and Protanopy	60
4.2.3	Recoloring Procedure	61
4.3	Text Recoloring Algorithm for HTML Documents	65
4.4	Image Recoloring Algorithm for HTML Documents	66
4.5	Results	67

4.5.1	Setup	67
4.5.2	Methodology	67
4.5.3	Qualitative Evaluation	67
4.5.4	Quantitative Evaluation	68
4.5.5	Time Performance-Based Evaluation	73
4.6	Subjective Evaluation	74
4.6.1	The Universe of CVD People	75
4.6.2	The Questionnaire	76
4.6.3	Data Collecting	76
4.6.4	Data Analysis	76
4.7	Contributions	79
4.8	Further Remarks	80
5	Contour Enhancement Algorithm for Improving Visual Perception of Deutan and Protan Dichromats	83
5.1	Introduction	83
5.2	Contour Enhancement Algorithm	83
5.2.1	Dichromat Image Generation	84
5.2.2	Gaussian Blur Filter	86
5.2.3	Grayscale Conversion	86
5.2.4	Contour Detection	86
5.2.5	Contour Highlighting	87
5.3	Results	89
5.3.1	Setup	89
5.3.2	Perceived Region Rate	89
5.3.3	Contrast	90
5.3.4	Naturalness	91
5.4	Subjective Evaluation	91
5.4.1	The Universe of CVD People	91

5.4.2	The Questionnaire	93
5.4.3	Data Scoring and Collecting	94
5.4.4	Data Analysis	96
5.5	Conclusions	97
6	Conclusions	99
6.1	The Revisited Problem	99
6.2	Contributions	99
6.3	Research Limitations	100
6.4	Future Work	101
6.5	Closure of the Research Work	101
	Bibliografia	I

List of Figures

2.1	Taxonomy of color vision deficiencies.	11
2.2	Color gamut seen by: (a) trichromat people (regular color vision); and (b)-(d) anomalous trichromat people, with (b) protanomaly, (c) deuteranomaly, and (d) tritanomaly. The images (b)-(d) were obtained through the simulation algorithm due to [1] with degree of severity of 0.5.	12
2.3	Flowers seen by: (a) trichromat people (regular color vision); and (b)-(d) anomalous trichromat people, with (b) protanomaly, (c) deuteranomaly, and (d) tritanomaly. The images (b), (c), and (d) were obtained through the simulation algorithm due to [1] with degree of severity of 0.5.	13
2.4	Color gamut when seen by people with (a) regular color vision; (b) protanopy; (c) deuteranopy and (d) tritanopy. (b) and (c) simulation via [2]; (d) simulation via [3].	13
2.5	Color gamut when seen by people with (a) regular color vision; (b) protanopy; (c) deuteranopy and (d) tritanopy. (b) and (c) simulation via [2]; (d) simulation via [3].	14
2.6	LMS-based recoloring method due to [4]: (a) original image; (b) deuteranope image view; (c) deuteranope image view after recoloring. Images courtesy of [4]. .	14
2.7	LMS-based recoloring method due to [5]: (a) original image; (b) deuteranope image view; (c) deuteranope image view after recoloring. Images courtesy of [5]. .	14
2.8	RGB-based recoloring method due to [6]: (a) original image; (b) deuteranope image view; (c) deuteranope image view after recoloring. Images courtesy of [6].	16
2.9	RGB-based recoloring method due to [7]: (a) original image; (b) deuteranope image view; (c) deuteranope image view after recoloring. Images courtesy of [7].	17
2.10	RGB-based recoloring method due to [8]: (a) original image; (b) deuteranope image view; (c) deuteranope image view after recoloring. Images courtesy of [8].	17
2.11	CIE Lab-based recoloring method due to [9]: (a) original image; (b) deuteranope image view; (c) deuteranope image view after recoloring. Images courtesy of [9].	19
2.12	CIE Lab-based recoloring method due to [10]: (a) original image; (b) deuteranope image view; (c) deuteranope image view after recoloring. Images courtesy of [10].	19
2.13	CIE Luv-based recoloring method due to [11]: (a)(d) original image; (b)(e) deuteranope image view; deuteranope image view after recoloring. Images courtesy of [11].	20
2.14	CIE XYZ-based recoloring method due to [12]: (a) original image; (b) deuteranope image view; (c) deuteranope image view after recoloring. Images courtesy of [12].	20

2.15 LMS-based recoloring method due to [13]: (a) original image; (b) deuteranope image view; (c) deuteranope image view after recoloring. Images courtesy of [13].	25
2.16 LMS-based recoloring method due to [14]: (a) original image; (b) deuteranope image view; (c) deuteranope image view after recoloring. Images courtesy of [14].	25
2.17 RGB-based recoloring method due to [15]: (a) original image; (b) deuteranope image view; (c) deuteranope image view after recoloring. Images courtesy of [15].	26
2.18 RGB-based recoloring method due to [16]: (a) original image; (b) deuteranope image view; (c) deuteranope image view after recoloring. Images courtesy of [16].	28
2.19 RGB-based recoloring method due to [17]: (a) original image; (b) deuteranope image view; (c) deuteranope image view after recoloring. Images courtesy of [17].	29
2.20 HSV-based recoloring method due to [17]: (a) original image; (b) deuteranope image view; (c) deuteranope image view after recoloring. Images courtesy of [17].	32
2.21 HSV-based recoloring method due to [18]: (a) original image; (b) deuteranope image view; (c) deuteranope image view after recoloring. Images courtesy of [18].	32
2.22 (a) HSV-based recoloring method due to [19]: (a) original image; (b) deuteranope image view; (c) deuteranope image view after recoloring. Images courtesy of [19].	33
2.23 CIE Lab-based recoloring method due to [20]: (a) to deuteranope people; (b) to protanope people. 1 st column: original colors; 2 nd column: dichromat view of the colors; 3 rd column: dichromat view of the colors after recoloring. Images courtesy of [20].	36
2.24 CIE Lab-based recoloring method due to [21]: (a) original image; (b) deuteranope image view; (c) deuteranope image view after recoloring. Images courtesy of [21].	36
2.25 CIE Lab-based recoloring method due to [22]: (a) original image; (b) deuteranope image view; (c) deuteranope image view after recoloring. Images courtesy of [22].	36
2.26 CIE Lab-based recoloring method due to [23]: (a) original image; (b) deuteranope image view; (c) deuteranope image view after recoloring. Images courtesy of [23].	36
2.27 CIE Lab-based recoloring method due to [24]: (a) original image; (b) deuteranope image view; (c) deuteranope image view after recoloring. Images courtesy of [24].	40
2.28 CIE Lab-based recoloring method due to [25] is not color consistent because the red colors of both original images (a) and (d) are mapped to different colors in deuteranope images (c) and (f), respectively, after recoloring. The images (b) and (e) show the original images as seen by deuteranope people. Images courtesy of [25].	41
2.29 CIE Lab-based recoloring method due to [26] and [27]:(a) original image; (b) deuteranope image view; (c) deuteranope image view after recoloring by the method due to [26]; (d) deuteranope image view after recoloring by the method due to [27]. Images courtesy of [26] [27].	46

3.1	Color space models	50
3.2	ShrinkInverse recoloring algorithm	52
3.3	Lantana flowers recolored by three distinct methods	55
3.4	Strawberries recolored by three distinct methods	56
4.1	HSV cone sections seen by trichromat and deuteranope people	60
4.2	HSV color space seen by trichromat and deuteranope people	60
4.3	Lantana flowers recolored by three distinct methods	69
4.4	Petunia flowers recolored by three distinct methods	70
4.5	Still images of a dataset with 100 images	71
4.6	Time performance of CEA method	73
4.7	Dataset of images belonging to the categories InfoVis, Indoor and Outdoor	74
4.8	Dataset of images belonging to the categories SciVis and Signage	75
4.9	Distribution of the preference scores of color adaptation methods per category .	77
4.10	Box-and-whisker diagrams of preferences of color adaptation methods	77
5.1	Global schema of the contours enhancement process	84
5.2	The contour enhancement process applied to an hibiscus flower	85
5.3	Image adaptation of an Europe map through the CEA algorithm	87
5.4	Image adaptation of a danger nameplate through the CEA algorithm	88
5.5	Image adaptation of a recycling sign through the CEA algorithm	88
5.6	Perceived region rate before and after image adaptation through CEA	90
5.7	Dataset of images belonging to the categories <i>InfoVis</i> , <i>Indoor</i> and <i>Outdoor</i>	92
5.8	Dataset of images belonging to the categories <i>SciVis</i> and <i>Signage</i>	93
5.9	Distribution of the preference scores of color adaptation methods per category .	95
5.10	Box-and-whisker diagrams of preferences of color adaptation methods	95

List of Tables

2.1	Recoloring methods for anomalous trichromat people.	23
2.2	Recoloring methods for dichromat people.	43
2.3	Summary of the color adaptation methods, for monochromacy.	46
3.1	Average time spent by the image recoloring algorithms	55
4.1	Statistical results for different adaptation color methods	79
5.1	Statistical results for different adaptation color methods	97

Acronyms

CLUT	Color Look Up Table
CSS	Cascading Style Sheets
CVD	Color Vision Deficiency
DOM	Document Object Model
HTML	Hyper Text Markup Language
SOM	Self-Organizing Map
LUT	Look Up Table
WAI	Web Accessibility Initiative
WCAG	Web Content Accessibility Guidelines
W3C	World Wide Web Consortium
WWW	World Wide Web

Chapter 1

Introduction

Recoloring and adaptation algorithms for color vision deficiency (CVD) people (i.e. color-blind people) is an important research topic in accessible computing and computer-human interaction. Despite the existence of a significant number of recoloring algorithms in the literature, in the course of our research work, and with a few exceptions, we noted that these algorithms are not accompanied by subjective assessment studies to validate them. In a way, this fact shows that perceptual learning of color-blind people is not taken into account in the design of recoloring algorithms, which are usually put forward by trichromats, not by color-blind people. In fact, a color-blind individual learns to identify a red because everyone says that such a color is red. However, he/she does not see the red as a trichromat does. In fact, red is seen as green. Truly speaking, such a red is not a red nor green, but a kind of dark yellow (a brownish color), simply because a red-green dichromat only sees yellows and blues.

1.1 Context and Motivation

As known, in general, red-green dichromats only see blues (a primary color) and yellows (a secondary color). They have some difficulties in distinguishing reds from greens, simply because their red cones (protanopes) or green cones (deutanopes) do not work or do not exist in retina. In the particular case of tritanopes, their blue cones are absent or do not work at all; they only see reds and cyans, with more or less saturation and brightness.

Surprisingly, after an exhaustive set of experiments, we found that red-green dichromats only see two hues in the HSV color space, 240-blue and 60-yellow, though the light spectrum covers other blues and yellows. As a consequence, their color space is limited to a color triangle that results from cutting off the HSV cone into two identical parts. In other words, all the colors seen by trichromats are perceived by dichromats as 240-blue and 60-yellow with more or less saturation and brightness.

The question is then how to improve the color perception of someone who only sees yellows and blues, with more or less saturation and brightness, while keeping the naturalness of color as much as possible from the dichromat point of view? Is it of any usefulness? In fact, recoloring easily conflicts with the perceptual learning of the individuals, since they are accustomed to viewing the world in a certain manner. In a way, these questions were the start point of the research work behind this Ph.D. thesis.

1.2 Thesis Statement

In the course of our research work in adaptation methods for color-blind people in computer environments, we realized that the perceptual learning of each person determines his/her insight about reality. Some people see the world in yellows and blues, some in reds and cyans, and most in all hues, no matter whether in a distorted manner or not.

By changing the colors of images and text through algorithms, we risk interfering with the perception that color-blind people have about the reality. In true, this is what happens with most recoloring algorithms in the literature. Red-green dichromats see greens as distorted greens, which are greens after all. Therefore, it does make much sense to change the green of tree leaves of a given scene into blue, because that would break with the perceptual learning of an individual who is dichromat.

Accordingly, our research work sustains on the following thesis statement:

It is feasible to achieve a computational adaptive method for color-blind people that is capable of increasing their visual perception (i.e. to enable them to see more image objects/elements than in adaptation-free circumstances) without undermining their perceptual learning.

As seen throughout this thesis, we show that this is possible, but not in a universal way. That is, each method is more appropriate to certain image categories than others. We tried to use a representative domain of images, thus considering images belonging to five different categories: information visualization (InfoVis), images concerning (indoor and outdoor) photographs, scientific visualization (SciVis), and signage. Anyway, we conclude that depending on the type of image, a method may be more or less suited for a specific category, since it depends on the requirements considered in its inception.

1.3 Research Questions

Taking into consideration the general problem of adapting color in images for improving the visual perception of color-blind people, the principal research questions are the following:

Is it possible to increase the visual perception of a color-blind individual by applying a recoloring process to an image without undermining his/her perceptual learning?

In some circumstances, a color-blind individual cannot distinguish two adjacent objects in an image, even when such objects are pictured with distinct colors. This is so because those two colors —though distinct for a trichromat— are seen as the same color for a color-blind individual. Recoloring solves this problem easily, but it also creates side effects because recoloring usually applies to pixels of an image, independently of the objects in a given scene. The question then is how to mitigate these side effects in the recoloring process. Our strategy to solve this problem is recoloring but maintaining the color naturalness as much as possible, and simultaneously increasing the contrast between the different objects existing in a scene. This leads

us to another question.

Is it possible for a CVD individual to see objects that are not distinguishable from others in a given image without undermining his/her perceptual learning?

To our best knowledge, there is no algorithm capable of doing this task correctly. The reason lies in the fact that such a procedure requires the delineation of the boundaries of objects in a scene. Our strategy here was to use image analysis and processing techniques to detect the boundaries of image objects, highlighting them whenever needed. This has the advantage of minimizing the image changes, in conformity with what dictates the perceptual learning of a color-blind individual.

Are color adaptation algorithms useful for colorblind people?

Our answer is affirmative since they preserve the perceptual learning of CVD people. It happens that most algorithms extant in the literature are not concerned with preserving the perceptual learning of color-blind. In fact, only one of them is accompanied by subjective assessment studies. In our work, we also carried out a series of subjective assessment studies, from which we concluded that color adaptation algorithms are useful since they do not clash with the perceptual learning of color-blind in a significant manner. Furthermore, after finishing this work, we conclude that the color adaptation in images must be performed selectively for specific objects in imaging. In particular, the color adaptation algorithms should identify the colors or areas that are confused with others or that are not visible to color-blind individuals, and then proceed accordingly.

1.4 The Course of the Research Work

At the beginning of the research work underlying the present thesis, we had the intent of investigating the visual difficulties of color-blind people when interacting with web browsers, in particular with color of text and images. The idea was to design and develop a recoloring add-on as an extension to the functionalities of a browser, what we did in due time. Rapidly, we realized that there is no difference in recoloring imaging and text; the only difference is the medium, not the recoloring algorithm.

In the meanwhile, we reviewed the literature on color adaptation methods for CVD people. We also considered CVD simulation algorithms to observe how color-blind people see the world regarding color. Interestingly, we found a few dozens of these algorithms, but the majority of them without any subjective assessment and testing to validate their perceptual efficacy in disambiguating color. Nevertheless, we ended up re-implementing some of those recoloring algorithms —with a focus on dichromacy— to better understand the problem at hand. We also designed and implemented a couple of new recoloring algorithms (without considering perceptual learning), a representative of which is described in Chapter 3. So, we concluded the first stage of our research work.

The second stage of the research work involved the design and development of a color adaptation

method that takes into account the perceptual learning of dichromats. The visual perception of humans has much to do with their previous learning experience that intimately relates objects to their typical colors; for example, it is rather difficult to imagine a blue orange in nature. The interpretation about what we observe is extremely dependent on that past experience-based learning, which is held throughout our lives. Interestingly, after interviewing some dichromat individuals, we realized that they are capable of recognizing and identifying the vivid colors by their names; for example, they are capable of identifying some reds, even considering they cannot see true reds. To not break with their perceptual learning and experience, we adopted the strategy of changing the colors as less as possible. This was accomplished by increasing the *color contrast* of the image and at the same time maintaining the *color naturalness*, as well as its *color consistency*. Chapter 4 describes a recoloring algorithm that satisfies these three perceptual requirements.

In the third research stage, we pursued a distinct approach to color adaptation in still images. In fact, most color adaptation algorithms are pixel-based, so that the pixels are all recolored in the same manner, without any selective criterion of what should be recolored or not. On the contrary, we decided to look at the contents of images regarding their constituent objects, finding first their contours or boundaries. Then, those contours that separate an object from its neighbors are enhanced, if needed, to reinforce their separate identities. Such contours or boundaries are determined using edge-based methods as usual in the field of image analysis and processing. To our best knowledge, this is one of the first color adaptation algorithms that take advantage of contour enhancement, and is described in Chapter 5.

Finally, and following the submission of the three most important articles produced in the scope of the Ph.D. research work to specialized journals, the present thesis was written up.

1.5 Contributions

In a general setting, we can say that the main contributions of the research work that has led us to the write-up of this Ph.D. thesis are the following:

- A novel recoloring technique that takes into account the color planar space of dichromats. As explained throughout the thesis, the color gamut seen by trichromat people, which can be represented by a 3D cone, in which hues are distributed over 360° converges into the 2D dichromat triangular half plane, in which there are only the as 240-blue and 60-yellow hues, with more or less saturation and brightness. Thus, their color triangle space is the result from intersecting the HSV color cone with the plane defined by the cone apex, the 60-yellow hue point and 240-blue hue point of the cone base. Our technique also includes a technique to directly map RGB coordinates for trichromats into RGB coordinates for dichromats. This technique has been incorporated into the RGBeat algorithm (see Chapter 4), which complies with three requirements: contrast enhancement, color naturalness, and color consistency.
- One of the first image adaptation techniques that build upon contour enhancement. This has been accomplished using edge-based techniques to detect object contours in images, as is usual in image analysis and processing. The leading idea is to increase the contrast of

contours (or part of them) of objects that likely are mistaken with their neighbors. In this manner, the image remains almost untouched, and the colorblind people increase their visual perception because they end up seeing more objects in a scene than it would see without adaptation.

- The opening of an opportunity window for further research, after realizing that the current adaptation methods are not efficient enough in improving the visual perception of the color-blind people. This is so because most of those methods are pixel-sensitive, rather than object-sensitive, and do not take into consideration how the color-blind people see the surrounding world, i.e., they mostly ignore the color space of the color-blind people.

The lesson to take of this research work is that we have to change the methodology in the development of new adaptation techniques for color vision deficiency. This methodology must be sustained onto the color space of the color-blind people, or, to be more precise, the methodology must be based on the color space of each color-blind individual, without ignoring their perceptual learning about colors in various circumstances of their lives.

1.6 Publications

This research was not funded by any grant or research project. However, the registration and attendance to conferences were partially supported by Universidade da Beira Interior via its Doctoral School in Computer Science and Engineering, as well by Instituto Politécnico de Castelo Branco, where the doctoral candidate teaches. The work done during these years have given rise to the following submissions to journals:

Ribeiro, M. and Gomes, A. Recoloring Algorithms for Colorblind People: A Survey. ACM Computing Surveys (submitted), 2017.

Abstract: *The color is a powerful communication component everywhere, not only as part of the message and its meaning but also as a way of discriminating contents therein. However, 5% of world population suffer from a visual impairment, known as color vision deficiency (CVD), commonly known as colorblindness, which constrains the color perception. This handicap adulterates the way the color is perceived, compromising the reading and understanding of the message contents. This fact becomes even more serious due to the increasing availability of multimedia contents in computational environments, mainly on the web and other resources provided by the Internet, as well due to the growing on graphical software and tools. This issue becomes even more meaningful with the widespread of the small portable display devices, where the content size is quite reduced. Aware of this problem, a significant number of research works related to the CVD condition have been described in the literature in the last two decades, in particular, those aimed at improving the readability of contents via color enhancing, independently of they include text, images or both. This survey mainly intends to reveal the state-of-the-art on recoloring algorithms for still images, as well to identify the current trends in the assessment and correction techniques for colorblind people.*

Ribeiro, M. and Gomes, A. RGBeat: A Recoloring Algorithm for Deutan and Protan Dichromats. IEEE Transactions on Visualization and Computer Graphics (under revision), 2017.

Abstract: *It is widely accepted that people with deutan and protan dichromats only see blues and yellows, so that they cannot distinguish reds from greens very well. In fact, we will see that deutan and protan dichromats only see exactly two hues in the HSV color space, 240-blue (240°) and 60-yellow (60°). Thus, their color space is limited to a color triangle that cuts off the HSV color cone into two identical parts. With this in mind, we propose here a novel recoloring algorithm for deutan and protan dichromats to enhance their color perception, particularly in HTML5-compliant web environments. This is accomplished by enhancing color contrast of text and imaging in web pages, while keeping the naturalness of color as much as possible. Also, as far as we know, this is the first web recoloring approach for dichromat people that takes into consideration both text and image recoloring in an integrated manner. Moreover, it is also one of the first color adaptation methods that increases the visual perception of deutan and protan dichromats relative to original images.*

Ribeiro, M. and Gomes, A. Contour Enhancement Approach for Dichromat People. IEEE Transactions on Visualization and Computer Graphics (under revision), 2017.

Abstract: *A variety of recoloring methods have been proposed in the literature to remedy the problem of confusing red-green colors faced by dichromat people (as well by other color-blinded people). The common strategy to mitigate this problem is to remap colors to other colors. But, it is clear this does not guarantee neither the necessary contrast to distinguish the elements of an image, nor the naturalness of colors learnt from past experience of each individual. In other words, the individual's perceptual learning may not hold under color remapping. With this in mind, we introduce the first algorithm that selectively enhances the required object contours in still images, instead of recoloring the pixels of the regions bounded by such contours or even the entirety of such contours. This is particularly adequate to increase contrast in images where we find adjacent regions that are color-indistinguishable from the dichromacy's point of view.*

Other articles published in the course of the research are the following:

— Ribeiro, M. and Gomes, A. *Adaptação de Cor para Dicromatas na Visualização de Imagens*. In Proceedings of the 20th Encontro Português de Computação Gráfica (EPCG'2012), Viana do Castelo, Portugal, pp. 99-102, October 2012.

— Ribeiro, M. and Gomes, A. *Recoloração de Web Conteúdos para Daltónicos - Recoloração de Imagens*. In Proceedings of the 2nd International Conference in Design e Graphic Arts (CIDAG'2012), Tomar, Portugal, pp. 470-473, October 2012.

— Ribeiro, M. and Gomes, A. *A Skillet-Based Recoloring Algorithm for Dichromats*. In Proceedings of the 15th IEEE International Conference on E-Health Networking, Application and Services (IEEE HealthCom'2013), Lisbon, Portugal, pp. 654-658, October 2013.

— Ribeiro, M. and Gomes, A. *Adaptação da Cor da Tipografia em Páginas Web para Pessoas com Deficiência na Visão da Cor*. In Proceedings of the 4º Encontro de Tipografia, Idanha-a-Nova,

Portugal, pp. 83-88, September 2013.

— Ribeiro, M. and Gomes, A. *Creating Accessibility to Web Contents for Colorblind People*. In Proceedings of the 5th International Conference on Applied Human Factors and Ergonomics (AHFE'2014), Kraków, Poland, Vol. 10, pp. 646-656, AHFE International, July 2014.

1.7 Thesis Organization

In spite of various articles published during the Ph.D. program, this thesis only includes the results of the most relevant articles that have been submitted or published in due time. The thesis is organized as follows:

Chapter 1. This is the present chapter, which reports the motivation behind this work, as well as the thesis statement, the principal research questions, the scientific contributions that stem from the research work, and the publications that have led to the writeup of this thesis.

Chapter 2. This chapter carries out a review of the literature on color adaptation methods and algorithms for colorblind people. This study has revealed itself essential to identify the current state-of-the-art in recoloring methods, their flaws, advantages, disadvantages, and strengths in the search to find new solutions, approaches, and alternative methodologies.

Chapter 3. This chapter presents a color adaptation method based on a recoloring strategy. This method follows a conventional approach as usual in the field of recoloring algorithms, and builds upon the HSV color space. The main goal is to project the reddish colors into another area of hues, where they could be seen with hues seen by dichromat people.

Chapter 4. This chapter describes a color adaptation method also based on a recoloring strategy. In a way, this method takes into consideration a perceptual balance between color naturalness, color consistency, and contrast enhancement. Besides, the recoloring was conceived in the HSV color space, although being performed directly in the RGB color space.

Chapter 5. This chapter details a novel color adaptation method that only involves a contour enhancement strategy, which is borrowed from the techniques used in image analysis and processing. Specifically, one uses a Sobel filter to detect contours of objects in an image. Then, object contours (not its interior) are subject to a recoloring procedure in a selective manner.

Chapter 6. This chapter concludes the thesis, where we further discuss our findings. Some open issues and suggestions for future work are also put forward in the end.

Chapter 2

Adaptive Methods for Color Vision Deficiency — a Survey

The color is a powerful communication component everywhere, not only as part of the message and its meaning, but also as way of discriminating contents therein. However, 5% of world population suffer from a visual impairment, known as color vision deficiency (CVD), commonly known as colorblindness, which constrains the color perception. This handicap adulterates the way the color is perceived, compromising the reading and understanding of the message contents. This issue becomes even more serious due to the increasing availability of multimedia contents in computational environments, mainly on web and other resources provided by Internet, as well due to the growing on graphical software and tools. Aware of this problem, a significant number of research works related with the CVD condition have been described in the literature in the last two decades, in particular those aimed at improving the readability of contents via color enhancing, independently of they include text, images or both. This survey mainly addresses the state-of-the-art with respect to recoloring algorithms for still images, as well as to identify the current trends in the color adaptation techniques for colorblind people.

2.1 Introduction

The color is a powerful feature that eases communication among humans directly or via documents. The color is present in many aspects of our daily lifes. Early on, the children use crayons to express themselves through forms and colorful scribbles. The color is part of many things of everyday, including the food we eat, the natural and urban landscapes where we live in, and the clothes we wear. We can even say that, in some sense, the color reflects the personality of each individual (the taste, culture and even age).

Nevertheless, about 5% of world population suffers from a handicap named color vision deficit (CVD), commonly known as colorblindness. This impairment has different types and degrees of severity depending on the type and the number of photoreceptor cells of eye affected. This fact impedes, limits or distorts the perception of color, sometimes even reducing the gamut of visible colors, interfering in this manner on visualization of the contents of images and generic documents, and, consequently on the communication and interaction process (i.e., the message, not matter it is implicit or explicit) between humans.

In this context, and for the first time, we put forward a survey about the color adaptation algorithms for CVD people, with a focus on still images, yet they also apply to other media as text and video. Our methodology strikes on the ability of color adaptation methods in preserving the *perceptual learning* of CVD people as much as possible. For example, a deuteranope person sees an orange in a faded green, so it is not a good idea to re-color it in blue because his/her

perceptual experience tell him/her that an orange is not a blue piece of fruit.

To preserve the perceptual learning, the following perceptual requirements must be satisfied:

- **Color naturalness.** Preserving color naturalness means minimizing the perceptual difference between an original color and the color after adaptation. This requirement allows us to not break up with the perceptual learning of the colorblind.
- **Color consistency.** Preserving color consistency means that a given color is always remapped to the same color, independently of the set of colors subject to remapping. This requirement is crucial to avoid the disorientation in the perception of the colorblind.
- **Color contrast.** In the process of color adaptation, preserving or enhancing color contrast is essential to be able to better distinguish adjacent objects in a given image. In some cases, it is even necessary to distinguish objects that are as a single one.

This survey is organized as follows. Section 2.2 introduces the color perception and the color vision deficiency. Sections 2.3, 2.4 and 2.5 focus on color adaptation algorithms for anomalous trichromats, dichromats, and monochromats, respectively. Section 2.6 reviews the state-of-the-art color adaptation methods as a whole, their current trends and challenges, as well as some hints for future work. Section 2.7 draws the most relevant conclusions of our study.

2.2 Color Perception

The color perception involves the eye and nervous system. In the human eye, there are some photosensitive cells in retina, called cone cells. They receive the stimulus from light, being transduced into chemical signals, which are conducted to the brain through neurological structures [28][29]. There are three types of cone cells, being each cone type sensitive to a specific range of light wavelengths of the color spectrum: S-cones (blue-cones) are light sensitive to small wavelengths; M-cones (green-cones) are sensitive to the medium wavelengths; and L-cones (red-cones) are sensitive to long wavelengths [30].

The perception of color is built on the sensitivity of the three types of cones, which originate three different signals to the brain that are therein combined into a single signal concerning a specific color; hence, the so-called tristimulus theory [30][29][31]. When the human color perception works well by combining small, medium and long wavelength signals, we are in presence of a trichromat individual that perceives all colors of the visible spectrum; specifically, he/she is capable of distinguishing about 700 different tones [32].

2.2.1 Color Vision Deficiency

Not all people see the color in a regular way as a trichromat individual. Such visual impairment is known as color vision deficiency (CVD), though it is also known as colorblindness or daltonism, and can be acquired by the way of cortical trauma [33] [34], brain fever [35], disorders, degenerations, dystrophy or diseases of different origin, diabetes *mellitus*, and yet exposition

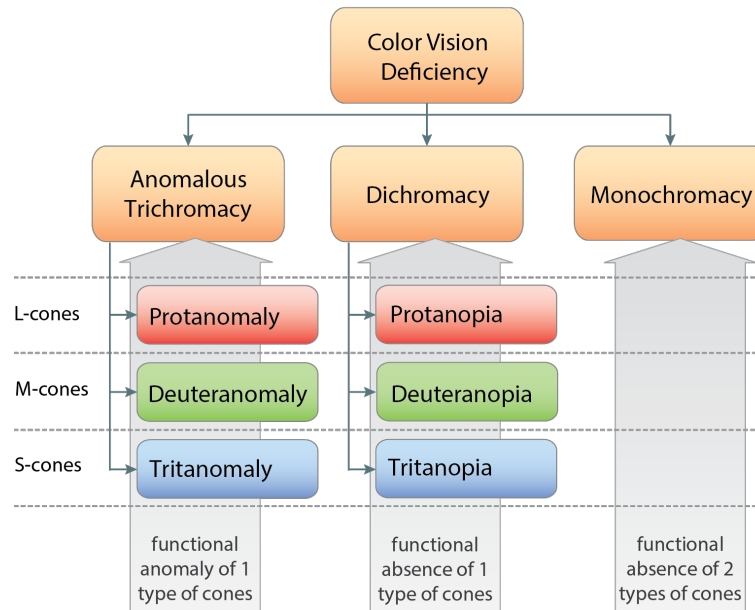


Figure 2.1: Taxonomy of color vision deficiencies.

to toxic agents [36]. However, the most common CVD type originates in genetic alterations of cone cells opsins [30].

Depending on the number of color channels affected, we can classify the CVD into three main categories [37] [38] [30], as shown in Fig. 2.1:

- **Anomalous trichromacy.** In this case, the curve of sensitivity of one type of cone cells is shifted from its regular position, which causes distortion in color perception, though the color gamut is essentially the same as for people without CVD (see Fig. 2.2).
- **Dichromacy.** In this case, one type of cones is missing, so the color space of a dichromat individual is reduced to 2D, with a consequent reduction of his/her color spectrum.
- **Monochromacy.** In this case, two or even three types of cones are missing or do not work at all. Therefore, the color vision is based on rods, which allow for grayscale vision. That is, the color space of a monochromat individual is 1D.

Despite the relative unknown of the community about the CVD condition, it is quite frequent because it has 5% of rate incidence in the population, and about 8% in men [39]. Fortunately, the higher rates of incidence occurs in less severe types (i.e., anomalous trichromats and dichromats).

2.2.1.1 Anomalous Trichromacy

There are three kinds of anomalous trichromacy, depending on the type of mis-functioning cone cell: protanomaly, deuteranomaly or tritanomaly, which are related with the curve of sensitivity of the L-, M- or S-cone cells, respectively [30]. Furthermore, the anomalous trichromacy is ascribed a degree of severity, which varies from 0.1 to 0.9 [4].

Figs. 2.2 and 2.3 illustrate how the anomalous trichromats see. Protanomalous and deuteranomalous people see in a very similar way, but a bit different from tritanomalous people. It is noticeable the vanishment of the most vivid colors when seen by anomalous trichromat people; for example, protanomalous and deuteranomalous people see reddish colors as rusty and close to browns, while tritanomalous people see bright yellows, as well as blues and greens, in a dull way.

2.2.1.2 Dichromacy

Also, there are three subtypes of dichromacy, namely protanopy, deuteranopy, and tritanopy, which refer to the absence of the L-, M- and S-cone cells, respectively, on retina [30]. Protanopes and deuteranopes have difficulties in distinguishing between red and green colors; hence, the so-called red/green colorblindness. Tritanopes do not distinguish blues from greens, and yellows from magentas [30][40].

Figs. 2.4 and 2.5 illustrate how the colors are perceived by dichromats. Their color gamut is quite limited because the 3D color space perceived by a trichromat is reduced to 2D; specifically, protanopes and deuteranopes only see blues and yellows (with more or less lightness), while tritanopes only see reds and cyans (with more or less lightness).



Figure 2.2: Color gamut seen by: (a) trichromat people (regular color vision); and (b)-(d) anomalous trichromat people, with (b) protanomaly, (c) deuteranomaly, and (d) tritanomaly. The images (b)-(d) were obtained through the simulation algorithm due to [1] with degree of severity of 0.5.

2.2.1.3 Monochromacy

Fortunately, only a few people are monochromat. Monochromacy is the severest type of CVD because two or even three types of cones do not work at all or do not exist. Therefore, there are two types of monochromacy: *blue-cone monochromacy*, when only the S-cone cells are working [41], and *rod monochromacy* when all types of cones are either missing or non-functioning for some reason. The rod monochromacy (or achromatopsia) is characterized by a total lack of color experience, as well as a low vision acuity, so that rod monochromat people only see grayscale shades, as in the scotopic vision [30] [42] [43]. In regards to blue-cone monochromacy, it is characterized by a grayscale vision with some shades of blue [44].



Figure 2.3: Flowers seen by: (a) trichromat people (regular color vision); and (b)-(d) anomalous trichromat people, with (b) protanomaly, (c) deuteranomaly, and (d) tritanomaly. The images (b), (c), and (d) were obtained through the simulation algorithm due to [1] with degree of severity of 0.5.

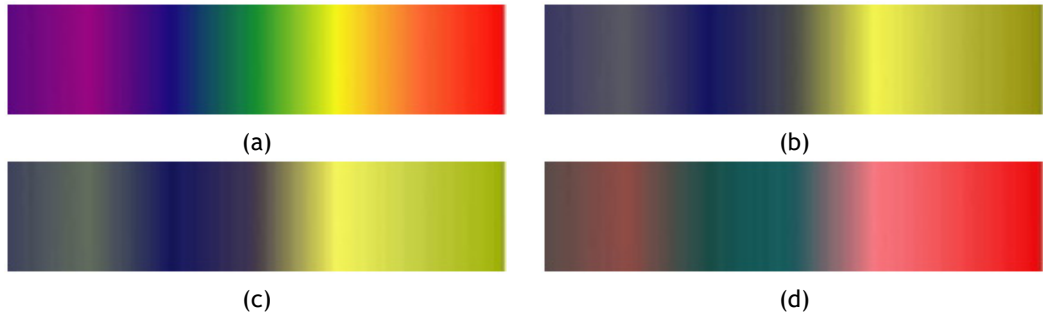


Figure 2.4: Color gamut when seen by people with (a) regular color vision; (b) protanopia; (c) deuteranopia and (d) tritanopia. (b) and (c) simulation via [2]; (d) simulation via [3].

2.3 CVD Adaptation Methods for Anomalous Trichromacy

As noted above, the anomalous trichromacy is characterized by the weakness of sensitivity of a single type of cone cells, either L , or M , or S . This means that anomalous trichromats see all the colors in the visible electromagnetic spectrum, but in a distorted way. Let us then see how this problem has been tackled from the algorithmic point of view.

2.3.1 LMS Based Methods

Let us consider the color (L, M, S) as seen by a trichromat. Let us also take into account that an anomalous trichromat sees the same color as (L, m, S) , with $m < M$, i.e., the anomalous trichromat is deuteranomalous. One uses three 3×3 matrices L , M , and S given by [45] to obtain

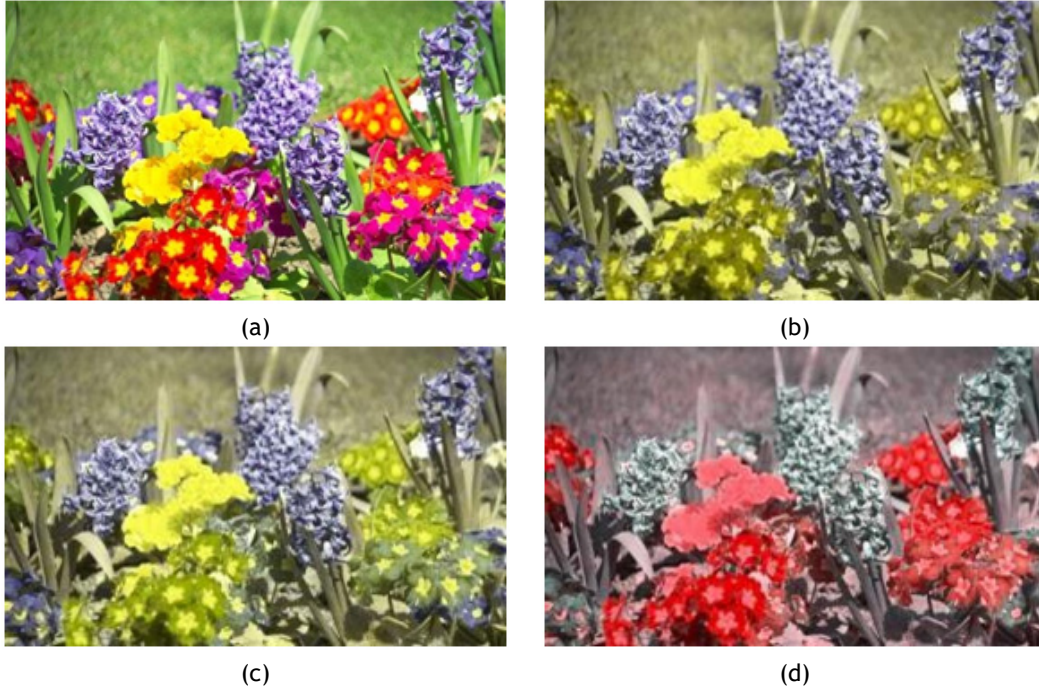


Figure 2.5: Color gamut when seen by people with (a) regular color vision; (b) protanopy; (c) deuteranopy and (d) tritanopy. (b) and (c) simulation via [2]; (d) simulation via [3].



Figure 2.6: LMS-based recoloring method due to [4]: (a) original image; (b) deuteranope image view; (c) deuteranope image view after recoloring. Images courtesy of [4].

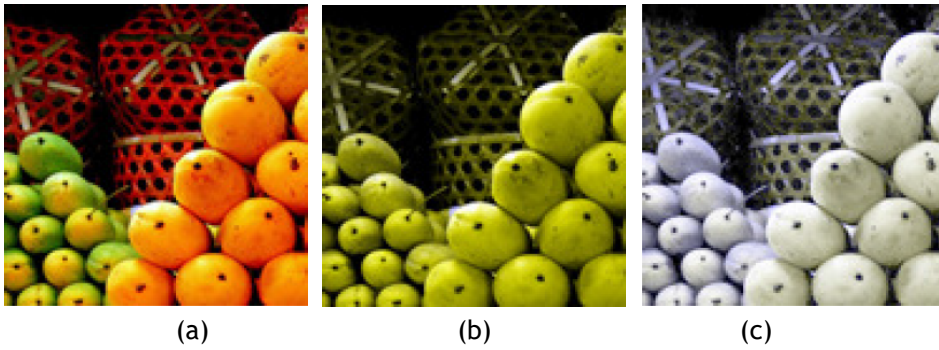


Figure 2.7: LMS-based recoloring method due to [5]: (a) original image; (b) deuteranope image view; (c) deuteranope image view after recoloring. Images courtesy of [5].

the (l, M, S) , (L, m, S) , and (L, M, s) , respectively, from (L, M, S) . For example, in the case of deuteranomalous (those having anomaly in M -type cones), the color correction must be done in order to increase the value of m toward M as much as possible. This is done by applying the

inverse matrix M^{-1} to (L, M, S) , not to (L, m, S) ; otherwise, the individual continues to see (L, M, S) as (L, m, S) . Therefore, given a pixel of a RGB image, the recoloring pipeline for a deuteranomalous is

$$(R, G, B) \rightarrow (L, M, S) \xrightarrow{M^{-1}} (L, M^*, S) \quad (2.1)$$

where $M^* > M$ is a value that, in principle, is perceived as M by a deuteranomalous. However, this increasing color compensation is not so effective for values of M close to the upper bound of M because they overlap at the upper bound of M .

This technique has been developed by Yang et al. [45], after preliminary works of the same research group described in [46], [4], and [47]. In the same line of research, Yang and colleagues [4] [48] developed an algorithm that in meanwhile appeared as part of DIA (Digital Item Adaptation), a module of the standard MPEG-21 framework. In general, the contrast of images is enhanced, except when the colors of the image are already very saturated, being close to the borders of the color space. The colors naturalness is also ensured, since the hue is not altered to other quite different. Both the color consistency is guaranteed, because any is always changed to the same one.

Lee-Santos method [49]. Also, another research group ended up developing this technique afterwards, as described in [49], [5], and [50]. The contribution of this later research group lies in the derivation of the matrices L and M for anomalous trichromats from those proposed by Vienot et al. [2] for dichromats, with the advantage of considering variable degrees of protanomaly and deuteranomaly.

Summing up, increasing the value of either L , M , or S translates into increasing the vivacity of color, which is nothing more than a color compensation strategy. It is clear this is accomplished without changing the color naturalness, but with contrast enhancement since the vivid shades are much better distinguishable than faint shades.

2.3.2 RGB Based Methods

We found only two RGB-based recoloring methods for anomalous trichromacy. The first was exclusively designed for protanomalous people, and is due to [51], while the second is more generic because it applies in principle to any sort of CVD, and was proposed by [6].

Poret et al.' method [51]. These authors start from the assumption that protanomalous people perceive better the dark, saturated red shades than dull, light shades. This explains why they compressed the range $[0, 255]$ of reds (R channel) into $[0, 205]$; this is valid for all colors having some amount of R . Although this strategy may improve the perception of the dull, light red shades, it diminishes the perception of other colors (e.g., the vibrant yellow $(255, 255, 0)$ is changed to a yellowish green $(205, 255, 0)$). Thus, color consistency is maintained, but naturalness is slightly lost.

Flatla-Gutwin method [6]. In turn, [6] proposed a solution that only applies to images with a limited number of colors, as it is common in signage, charts, and the like. It does not apply to photo-realistic images. Nevertheless, their method is customizable for each CVD individual, requiring a diagnosis beforehand, during which one identifies the set of distinctive colors as seen

by such individual. Therefore, this method strikes on the colors that each individual recognizes as distinct, i.e., his/her customized color domain.

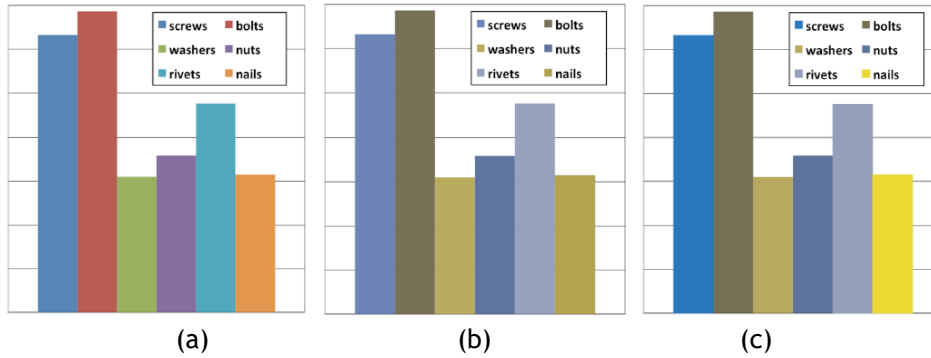


Figure 2.8: RGB-based recoloring method due to [6]: (a) original image; (b) deuteranope image view; (c) deuteranope image view after recoloring. Images courtesy of [6].

Taking into account the domain of colors perceived by a CVD individual, the color adaptation process for each image starts off. First, one extracts the key colors from a given image; for example, if there are a number of red shades, we have a single key red. Second, for each key color, one determines its confusing key colors existing in the same image. Third, one replaces each confusing key color by another color of the customized color domain, giving priority to the most confusing key colors. The second and third steps are then repeated while color confusion persists. It is clear that this recoloring procedure does not maintain neither color consistency nor color naturalness, but it introduces a new way to look at recoloring methods for colorblindness.

2.3.3 HSx Based Methods

Although the RGB is the common color format in display devices, it does not comply with the way the human brain tends to organize the colors. Instead, HSI, HSL and HSV color models, also known as *mind representations of colors* [52], organize colors in terms of hue (H), saturation (S), and brightness (i.e., intensity (I), lightness (L) or value (V)).

In light of this HSx model, we can say that anomalous trichromat people perceive colors in a faded manner, i.e., there is a fading process of the vivacity of hues, also known as decolorization process, which leads to a reduction of the image contrast. This decolorization process translates into less saturated and darker colors (i.e., different chroma), yet the hue remains unchanged.

Therefore, the methods of this category operate in a way to recover the saturation and brightness as much as possible.

2.3.3.1 HSI

Chen-Liao method [7]. Chen and Liao opted for only increasing the saturation in the HSI model, with the goal of enhancing the color purity. However, this recovery of saturation is performed directly on the RGB color space, avoiding the explicit RGB-HSI and HSI-RGB conversions, in order to speed up the time performance. Furthermore, their method maintains color naturalness and

consistency, yet the increasing on saturation of already saturated colors limits their mutual discrimination.

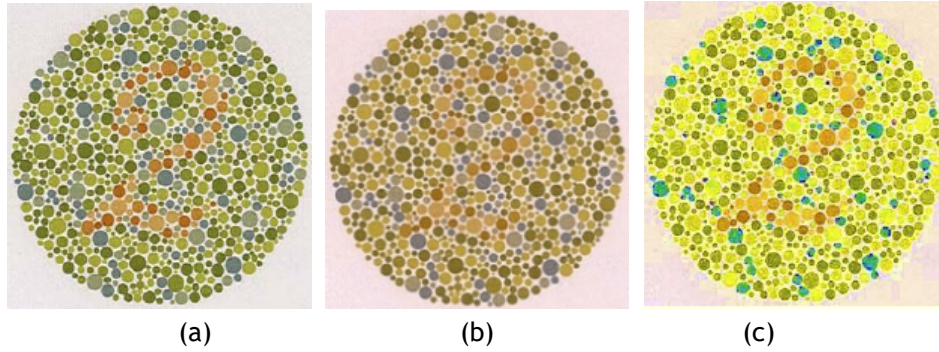


Figure 2.9: RGB-based recoloring method due to [7]: (a) original image; (b) deuteranope image view; (c) deuteranope image view after recoloring. Images courtesy of [7].

2.3.3.2 HSV

Huang et al.'method [8]. On the other hand, Huang et al. [8] only change the hue parameter to enhance the image contrast. In fact, their method is based on a sort of hue stretching, which translates itself into a counter-clockwise rotation of hues. Therefore, the color naturalness may not be hold for all images because the hue rotation may result in a quite different hue. Even worse it is the fact that the color consistency is not preserved at all, because the remapping of a given hue depends on the frequency (i.e., number of times) of each hue in the image. The applicability area of this proposal extends to dichromacy.

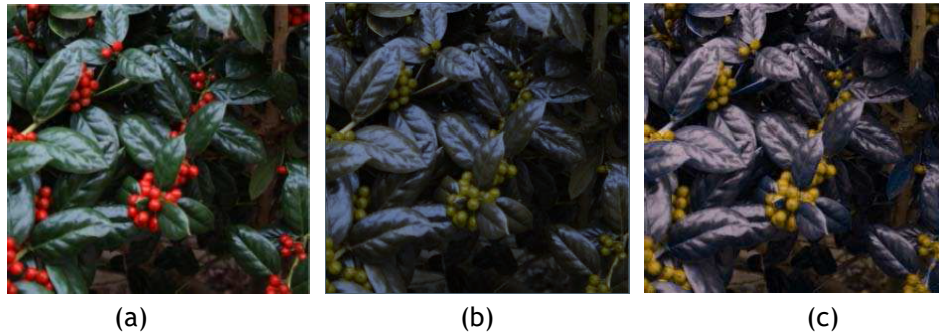


Figure 2.10: RGB-based recoloring method due to [8]: (a) original image; (b) deuteranope image view; (c) deuteranope image view after recoloring. Images courtesy of [8].

2.3.4 CIE Based Methods

Both CIE Lab and CIE Luv are recommended color spaces by CIE [53] because they preserve the perceptual uniformity, i.e., the distance between two colors corresponds to their perceptual difference [54]. This particularity is explored in all works which adopted these colors spaces, since their proposals are quite focused in the color distances, namely to measure the augment of the discrimination among colors or the apprise how different a color is from the original.

2.3.4.1 CIE Lab

In the literature, we find only one recoloring method for anomalous trichromat people that takes advantage of the CIE Lab color space, which is due to Huang et al. [9]. Later on, and based on this method, Yanagida et al. [55] created a color pallet for red-green dichromacy to be used for graphical designers.

Huang et al.'method [9]. This method consists of two major steps. In the first step, one extracts the key colors of an image. Then, they find the optimal mapping that preserves the contrast between each pair of key colors. Such key colors are determined using the K -means algorithm, yet the value of K is calculated by applying the minimum description length (MDL) principle [56]. That is, it is assumed that the color distribution in an image can be approximated by K Gaussian functions. Thus, the color information of an image can be represented by the Gaussian Mixture Model (GMM). This allows us to record not only each key color, but also its cluster of colors.

The second step carries out the optimization procedure. The idea here is preserve the contrast between each pair of key colors relative to trichromat color perception. Taking into consideration each key color is represented by a Gaussian distribution, we need to calculate the “distance” between each pair of Gaussians, which can be calculated using the symmetric Kullback-Leibler (KL) divergence. Besides, Huang et al. introduced a weighting method of colors in order to characterize their importance for CVD people. This distance-and-weighting procedure ensures the maintenance of color contrast, so that the most altered colors due to the CVD condition are those ascribed with heavy weights to be able to recover the original contrast.

Taking into account this method maintains the lightness (L), we draw the conclusion that changes in color occur in the plane ab of CIE Lab, which are rotations on such a color plane. Therefore, this method is not very effective in preserving color naturalness. Besides, the color consistency is not ensured either, because that depends on the key colors determined in the first step (both red and green colors are mapped differently in Fig. 2.11 (c) and Fig. 2.11 (f)).

In [10], the authors proposed some improvements on their previous method, namely to preserve the naturalness and reduce the complexity of the optimization function. In this new formulation, one applies a priority order in the color re-mapping, from the best to the worse perceived colors. Even so, the colors are mapped to quite different colors so that naturalness is not assured at all.

2.3.4.2 CIE XYZ

Similar to LMS, the CIE XYZ color space represents all colors seen by a human viewer, i.e., it is not limited to the color space associated to any display device. In other words, the CIE XYZ color space is device-independent. But, the CIE XYZ is richer than LMS because it includes the luminance Y (i.e., “intensity of light”, not perceived luminance), in addition to two chromaticity parameters X and Z , i.e., we end up to be able to quantify the difference between, for example, a light red and a dark red [57][58].

Mochizuki et al.'method [12]. Let us now consider the color (X, Y, Z) as seen by a trichromat,

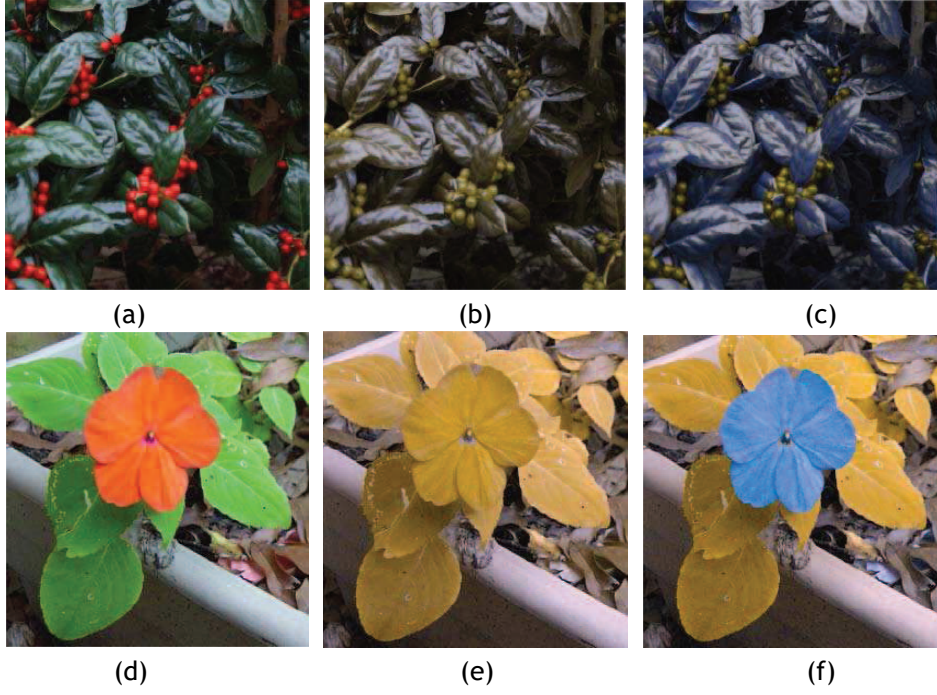


Figure 2.11: CIE Lab-based recoloring method due to [9]: (a) original image; (b) deuteranope image view; (c) deuteranope image view after recoloring. Images courtesy of [9].

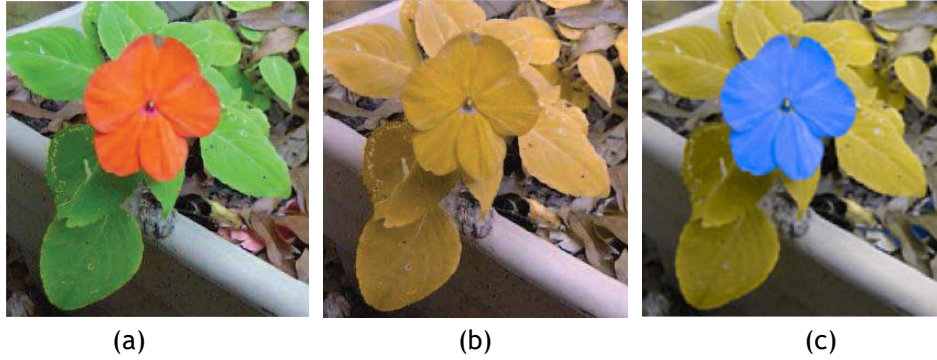


Figure 2.12: CIE Lab-based recoloring method due to [10]: (a) original image; (b) deuteranope image view; (c) deuteranope image view after recoloring. Images courtesy of [10].

and its corresponding color (x, y, z) as seen by an anomalous trichromat, as well as the matrix M that transforms (X, Y, Z) into (x, y, z) . Therefore, the matrix M^{-1} allows us to obtain (X, Y, Z) from (x, y, z) . This means that we can use M^{-1} to get a new color (X^*, Y^*, Z^*) from (X, Y, Z) , that is,

$$(R, G, B) \rightarrow (X, Y, Z) \xrightarrow{M^{-1}} (X^*, Y^*, Z^*) \quad (2.2)$$

where (X^*, Y^*, Z^*) is the adapted color that allows an anomalous trichromat to see (X, Y, Z) as usual for a trichromat.

This recoloring pipeline has only been used by [12] and [59], who belong to the same research group. Later on, this group proposed some improvements to this recoloring process in terms of time performance [60] and color compensation reliability [61].

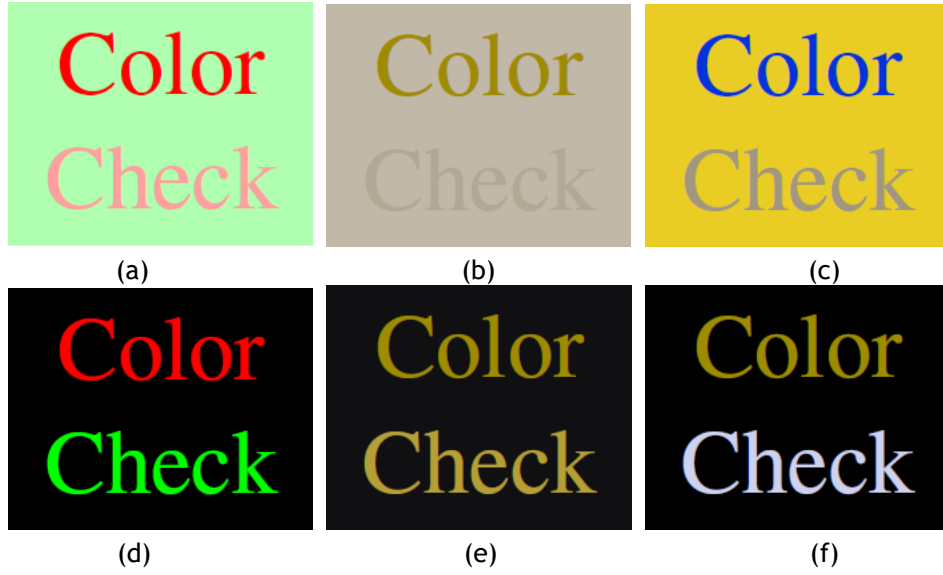


Figure 2.13: CIE Luv-based recoloring method due to [11]: (a)(d) original image; (b)(e) deuteranope image view; deuteranope image view after recoloring. Images courtesy of [11].

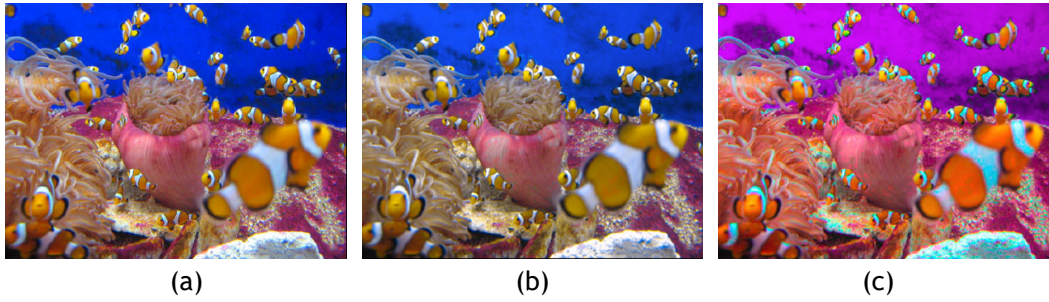


Figure 2.14: CIE XYZ-based recoloring method due to [12]: (a) original image; (b) deuteranope image view; (c) deuteranope image view after recoloring. Images courtesy of [12].

Note that the aforementioned color adaptation strategy may lead to an overlapping of colors in the boundary of the CIE XYZ color space. Even so, the image contrast is enhanced, unless the original image only includes the worst-case colors (i.e., color space boundary colors). The color naturalness is maintained because the colors are not changed for distant colors. Furthermore, the color consistency is *a priori* ensured because a color is always mapped to a unique color.

2.3.4.3 CIE Luv

To our best knowledge, there are three major color adaptation methods that build upon the CIE Luv color space, namely those due to Ichikawa et al. [11], Oshima et al. [62], and Milic et al. [63].

Ichikawa et al.'method [11]. Regarding the CIE Luv color space, we found two works from the same research group [11] [64]. Taking into account that anomalous trichomat people shorten the distance because colors relative to trichomat people, the leading idea of Ichikawa et al.'s method is to recover the original differentiation between colors as much as possible (i.e., augmenting/recovering the distance among colors) in HTML documents, yet minimizing the change

of each color, i.e., to recover the contrast without compromising the naturalness of colors. Later on, these authors re-engineered their method also for images [64].

To this end, they adopted a strategy that consists of two main steps. First, they extract all the colors (C_1, C_2, \dots, C_n) from the HTML document and their mutual relations (i.e., “included” and “even” mutual relations), which give rise to a directed graph representing a kind of color segmentation with connectivity information (i.e., color adjacency and hierarchy).

Second, the original color vector (C_1, C_2, \dots, C_n) is iteratively changed by a genetic algorithm. In each iteration, one generates a population for each color. The generation of each color population obeys to the following. It is known that for bright and dark colors, it is difficult to put in evidence the color difference between spectral colors. In this case, one only changes the lightness, not the chroma. On the contrary, when the lightness is medium, one changes only the chroma, not the lightness. However, these changes must take into account the mutual relations as expressed in the color graph mentioned above. It is clear that the genetic algorithm sustains on a fitness function that attains a minimum after a number of iterations. In the end, one obtains the optimum color vector $(C_1^*, C_2^*, \dots, C_n^*)$ that makes each web page better perceived for anomalous trichromat people.

In short, the method clearly is contrast-oriented, but does not preserve the naturalness neither the consistency of color because the final colors depend on the initial set of colors and their mutual relations.

Oshima et al.’s method Oshima et al. [62] [65] [66]. This method is a follow-up of the work due to Mochizuki et al.’method [12] approached in Section 2.3.4.2 above, but using the CIE Luv color space instead of the CIE XYZ.

The leading idea of this method is to compensate the color weakness based on the difference between the color stimuli for a trichromat observer and color stimuli for a color weak observer (i.e., an anomalous trichromat observer).

A trichromat person cannot distinguish each color from its neighboring colors within a threshold distance in the CIE Luv color space, that is, the neighboring colors inside a spherical sphere. In the case of an anomalous trichromat person, such a undistinguishable neighborhood of colors is an ellipsoid. Oshima et al. were able to find a matrix M that makes a transformation from such a sphere to an ellipsoid, which features the distortion in the color perception inherent to the anomalous trichromacy. Therefore, they were able to compensate the distortion of the color perception of anomalous trichromat people using the matrix M^{-1} as follows:

$$(R, G, B) \rightarrow (L, u, v) \xrightarrow{M^{-1}} (L^*, u^*, v^*) \quad (2.3)$$

where (L^*, u^*, v^*) is the adapted color that allows an anomalous trichromat person to see (L, u, v) as usual for a trichromat person.

This method has the advantage of using the CIE Luv color space, which is perceptually uniform so that the computation of the matrix M is more rigorous than the one due to Mochizuki et al.’method [12]. Consequently, the three perceptual requirements of color consistency, naturalness and contrast are satisfied.

Milic et al.’s method [63]. As known, a CVD individual cannot distinguish certain colors from

one another, which belong to the so-called confusion lines of a given color space [67]. Given a subset of confusion colors, Milic et al. adopted the strategy of keeping only one of them in the confusion line; the remaining ones are shifted perpendicularly to the confusion line.

This method consists of three steps. In the first step, one carries out a color image segmentation based on (u, v) -chromaticity, using then the K-means algorithm to form clusters of colors, whose centers are the representative colors of the input image. Note that this step excludes the lightness (L) from the color segmentation-and-clustering process.

The recoloring process of the representative colors takes place in the second step. When two or more of these colors lie on the same confusion line, all except one should be rotated around the confusion point (i.e., the point of convergence of all the confusion lines) to create room for color differences. That is, each representative color is subject to a color adaptation procedure.

The third step consists in recoloring each pixel of a given image relative to its adapted representative color. In other words, the color differences between every recolored pixel and the remapped center of the cluster (or segment) are preserved relative to the original colors before mapping.

Clearly, this method ensures color contrast because its focus is on creating color differences perpendicularly to confusion lines of the CIE Luv color space. In regards to color naturalness, our opinion is that it is preserved because the rotation of confusing colors is constrained by the severity degree. However, the color consistency is not preserved because the recoloring process depends on the colors and color segments in the original image.

2.3.5 Methods for Anomalous Trichromacy: a Discussion

A brief glance at Table 2.1 shows the following:

- *Anomalous trichromacy types.* Most recoloring methods apply to the three types of anomalous trichromacy. This can be explained by the fact that anomalous trichromats see all colors yet in a distorted way as a consequence of mis-functioning of one type of cones. So, what all we need is to compensate or correct the color distortion caused by such cones, no matter the type of anomalous trichromacy type.
- *Color ranges.* The color range used by a given method is closely related to the color compensation technique. Essentially, we have identified two major color compensation techniques: objective function optimization and matrix-based color remapping. Typically, optimization-based methods use a few or a small set of key (or representative) colors of the input image, using then color interpolation to remap the remaining colors; for example, methods relied on CIE Lab and RGB, as well as some methods based on CIE Luv color spaces use objective functions to iteratively maximize distances between confusing colors (i.e., enhancing the contrast), but at the same time to minimize such color changes to preserve the color naturalness as much as possible. Matrix-based methods use true colors (TC) to remap colors; for example, methods built upon LMS, CIE XYZ, HSV, and HSI color spaces use a color remapping matrix, no matter it is an inverse matrix or a rotation matrix, or else.

Table 2.1: Recoloring methods for anomalous trichromat people.

Reference	Anomalous trichromacy type			Color space	Target medium			Color range	Perceptual requirement		
	PA	DA	TA		N-Ph	Ph	O		CE	CC	NM
[46]	•	•	•	LMS	•	•		TC	•	•	•
[11]	•	•	•	CIE Luv			H	few	•		
[64]	•	•	•	CIE Luv	•			few	•		
[68]	•	•	•	LMS	•	•		TC	•	•	•
[4]	•	•	•	LMS	•	•		TC	•	•	•
[47]	•	•	•	LMS	•	•		TC	•	•	•
[49]	•	•	•	LMS	•	•		TC	•	•	•
[12]	•	•	•	CIE XYZ	•	•		TC	•	•	•
[8]	•	•	•	HSV	•	•		TC	•		
[9]	•	•	•	CIE Lab	•	•		key	•		
[51]	•			RGB	•	•		TC	•		
[59]	•	•	•	CIE XYZ	•	•		TC	•	•	•
[10]	•	•	•	CIE Lab	•	•		key	•		
[5]	•	•	•	LMS	•	•		TC	•	•	•
[50]	•	•	•	LMS	•	•		TC	•	•	•
[60]	•	•	•	CIE XYZ	•	•		TC	•	•	•
[61]	•	•	•	CIE XYZ	•	•		TC	•	•	•
[7]	•	•	•	HSI (RGB)	•	•		TC	•	•	•
[6]	•	•	•	RGB	•			few	•		
[62]	•	•	•	CIE Luv	•	•		TC	•	•	•
[65]	•	•	•	CIE Luv	•	•		TC	•	•	•
[63]	•	•	•	CIE Luv	•	•		key	•		
[66]	•	•	•	CIE Luv	•	•		TC	•	•	•

Abbreviations:

Anomalous trichromacy type: PA (protanomaly); DA (deuteranomaly); TA (tritanomaly).

Target medium: N-Ph (non-photo image); Ph (photo image); O (other): H (HTML document).

Color range: TC (true color); few (few colors); key (key colors).

Properties: CC (color consistency); CE (contrast enhancement); NM (naturalness maintenance).

- *Color spaces.* Most recoloring methods build upon on CIE color spaces. In some extent, this is due to the fact that the color spaces CIE Lab and CIE Luv spaces enjoy the color uniformity property, that is, the distance between colors is given by Euclidean distance. Therefore, Euclidean distance can be used as a metric to measure and ensure color contrast between confusing colors in images as seen by anomalous trichromats. On the other hand, the CIE XYZ space has the advantage of being device-independent, but it is not perceptually uniform when one uses the Euclidean distance. However, it is perceptually uniform when one uses the Riemann metrics (see, for example, [12]).
- *Target media.* All methods, except the one due to Ichikawa et al. [11], were designed for still images. In fact, the general understanding of the scientific community is that a recoloring or color adaptation method is independent on medium, either it is an image, a HTML document, text, or even video; hence, the focus on still images.
- *Perceptual requirements.* All methods focus on recovering the color contrast caused by

the color distortion of the anomalous trichromacy condition. Most of these methods are color-consistent, and are able to preserve the color naturalness. That is, most methods preserve the perceptual learning of anomalous trichromat people. Interestingly, such perceptual learning-preserving methods are those that operate on true colors (TC), which are those that take advantage of matrix-based color remapping. This fact suggests that optimization-based methods are not suited to preserve the perceptual learning of anomalous trichromats. In fact, optimization-based methods depend on the key colors of each image, that is, the recoloring procedure varies from an image to another.

Thus, the main conclusions we can draw from the state-of-the-art methods for anomalous trichromats are the following:

- Matrix-based color remapping methods preserve the the perceptual learning of anomalous trichromat people.
- Optimization-based color remapping methods do not preserve the the perceptual learning of anomalous trichromat people.

In short, it remains to know whether or not it is feasible to design an optimization-based method that preserves the perceptual learning of anomalous trichromat people.

2.4 CVD Adaptation Methods for Dichromacy

As seen above, the color space of trichromat people is 3D because the three sorts of cone cells work well. Considering that dichromacy stems from mis-function or absence of one sort of cone cells, the dichromat color space reduces a 2D plane of colors. As a consequence of the projection 3D colors onto a 2D plane, dichromat people confuse colors because of the color overlapping on the plane. Thus, dichromat-oriented recoloring methods aim at diminishing such confusion by remapping and putting apart the most confusing colors (i.e., reds and greens). This is so because, unlike the anomalous trichromat-oriented recoloring methods, there is no room for color compensation.

2.4.1 LMS Based Methods

Considering that dichromacy stems from the non-functionality or absence of one sort of cone cells, either L-, or M-, or S-cones. Since the parameters of the LMS color space represent the response of the three types of cones of the human eye, the dichromacy sets as zero the coefficient of one the parameters L , M or S , leaving unaltered the coefficients of the other two parameters. In other words, it means that the coefficient of affected channel is lost (e.g., a color (L, M, S) it is seen as $(L, 0, S)$, when seen by a deuteranope individual).

We found three LMS-based recoloring methods for dichromacy, which are due to [69], [13], and [14].

Ma et al.'method [69]. In this work it is proposed a back-propagation neuronal network model for simulating colorblindness cure, which is impractical unless we have means to stimulate the non-responsive cones in the retina or the neurons in the brain. Thus, this proposal suffers from practicability issues that are difficult to overcome given the current state-of-the-art of vision science and technology.

Jefferson-Harvey method [13]. Jefferson and Harvey introduced a method that allows for interactive recoloring for each dichromat individual. Therefore, the method is not automated, since it depends on color space of each dichromat individual. This user dependence is expressed as a 3×3 matrix \mathbf{A}_i , with $i \in \{P, D, T\}$ standing the category of dichromacy, i.e., P for protanapy, D for deuteranopy, and T for tritanopy, as follows:

$$\mathbf{C}_{LMS}^* = \mathbf{C}_{LMS} + \mathbf{A}_i \Delta \mathbf{C} \quad (2.4)$$

where $\Delta \mathbf{C}$ stands for the difference between the original color \mathbf{C}_{LMS} and simulated dichromat color \mathbf{C}_{LMS}' through Brettel et al.'s algorithm [70] [2]. As the sum in Eq. (2.4) shows, the key idea of Jefferson-Harvey algorithm is to transfer the chromatic data of the non-functioning cone type over the two functioning cone types. Thus, this algorithm carries out a kind of color compensation.

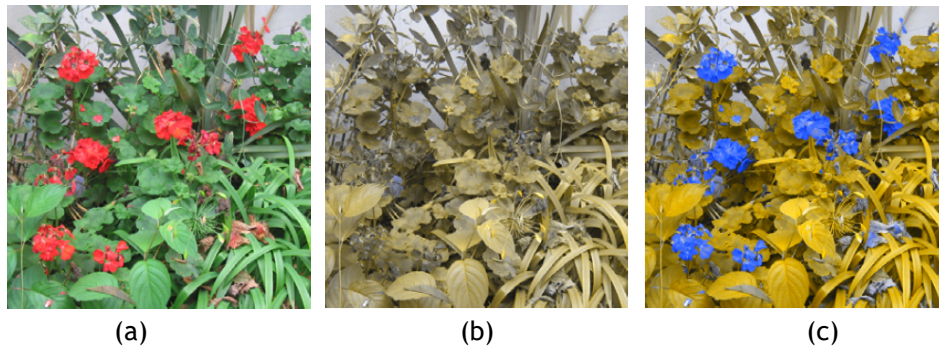


Figure 2.15: LMS-based recoloring method due to [13]: (a) original image; (b) deuteranope image view; (c) deuteranope image view after recoloring. Images courtesy of [13].

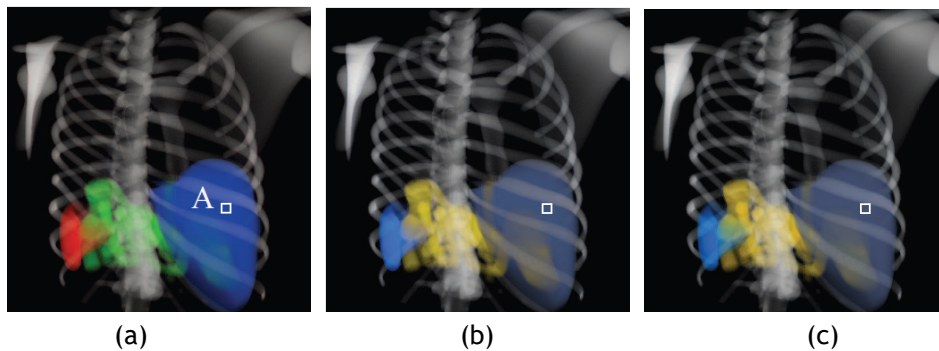


Figure 2.16: LMS-based recoloring method due to [14]: (a) original image; (b) deuteranope image view; (c) deuteranope image view after recoloring. Images courtesy of [14].

As shown in Fig. 2.15, this method does not preserves the color naturalness because the color compensation leads to map colors to other quite different colors, i.e., the contrast increases at the cost of less naturalness. Nevertheless, the color consistency is assured since the matrix \mathbf{A}_i

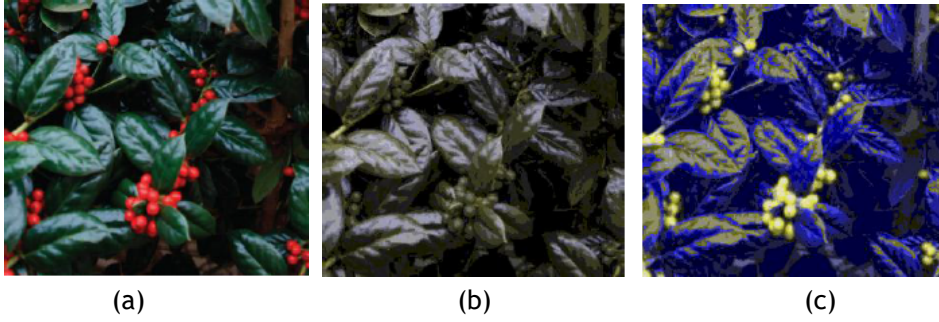


Figure 2.17: RGB-based recoloring method due to [15]: (a) original image; (b) deuteranope image view; (c) deuteranope image view after recoloring. Images courtesy of [15].

remains unchanged for each user.

Chen et al.'method [14]. In this article it is presented a LMS recoloring procedure for dichromat people in the context of volume rendering for medicine. Taking into consideration that dichromat people only possess two functional types of cones, their color space reduces to two half-planes, the first concerns blueish colors while the second concerns yellowish colors. So, the algorithm was thought of to distinguishing blues from blues and yellows from yellows, particularly when two adjacent anatomical organs are indistinguishable in terms of color. The key idea is to recolor the second organ with a color belonging to an half-plane other than the one of the first organ. This is a very simple recoloring procedure, but of great usefulness in medicine, particularly for imagiology dichromat experts. It is clear that here the color naturalness maintenance is not a concern; the important point is to be able to distinguish an anatomical organ from others in the surroundings, i.e., getting a noticeable color contrast.

2.4.2 RGB Based Methods

There are five RGB-based recoloring methods in the literature: [16] (and its follow-ups [71] [72]), [15], [73], [74], and [17]. Let us also mention that the Flatla-Gutwin method ([6]) described in Section 2.3.2 not only applies to anomalous trichromacy, but also to dichromacy.

Anagnostopoulos et al.' method [16]. The leading idea of this method is only to remap colors that are not correctly seen by protanope people. Given the homologous colors $C = (R, G, B)$ and $C_p = (R_p, G_p, B_p)$ of the original and protanope images, respectively, associated to a given pixel, Anagnostopoulos et al. assert that the color (R_p, G_p, B_p) seen by protanopes individuals is correct if the error $E = (R - R_p, G - G_p, B - B_p) \leq 0.01 (R, G, B)$. Otherwise, the pixels with incorrect colors are subject to an iterative recoloring procedure.

Such iterative recoloring procedure is performed by iteratively modifying the 3x3 discrimination matrix M , so the remapped color is given by:

$$C' = C + M \cdot E \quad (2.5)$$

where

$$M = \begin{bmatrix} m_1 & m_2 & m_3 \\ m_4 & m_5 & m_6 \\ m_7 & m_8 & m_9 \end{bmatrix} = \begin{bmatrix} -1 & 0 & 0 \\ \alpha & 1 & 0 \\ \beta & 0 & 1 \end{bmatrix} \quad (2.6)$$

with α and β taking on the initial value of 1; the value of α (resp., β) decreases (resp., increases) by 0.05 in each iteration, so that $\sum_{i=1}^9 m_i = 3$. The stopping condition of the procedure becomes true when all the remapped colors can be discriminated against each other. This recoloring procedure leads to a gradual reduction of R in favor of G and B in conformity with Eq. (2.6), which results in less saturated reds/oranges (i.e., dark grays as seen by protanope people become less dark grays), while greens get more saturated, mitigating so their red-green confusion. Therefore, this method improves the color contrast in images. However, the color consistency is not preserved because the adjustment of a given color depends on the color gamut of the image. In general, colors do not change their chromaticity in a significant manner, though the loss of chromaticity is more noticeable in the reds, so we can conclude that color naturalness is preserved as much as possible.

Deng et al.’ method [15]. This is an interesting recoloring method because it firstly maps the RGB color space (i.e. a cube) onto its inscribed rectangular dichromat color space. This dimension-reduction mapping is based on Sammon’s non-linear mapping [75]. Initially, one partitions uniformly (i.e. grid of equally-space nodes) both the 3D trichromat and 2D dichromat color spaces with the same number of nodes. Then, one uses a distance minimization procedure (e.g. steepest descent procedure) between homologous points in both spaces, in order to maintain as much as possible ratio of distances between those homologous points. This mapping between homologous colors is encoded into a unique look-up table that can be applied to any image. This unique look-up table ensures the consistency of the recoloring procedure. However, preserving distance ratios guarantees the necessary color contrast, yet at the cost of loss of naturalness, as illustrated in Fig. 2.17.

Ma et al.’ method [74]. This method is similar to the one due to Deng et al.’ method [15], but using a different device; more specifically, it uses the self-organizing map (SOM) as its nonlinear color mapping. This mapping is also known as self-organizing feature map (SOFM), and is nothing more than an artificial neural network (ANN) model, which is here used to map a feature (e.g. RGB color) from a high-dimensional space (e.g. RGB color space) onto a low-dimensional space (e.g. 2D dichromat plane); such ANN learns through unsupervised learning. Note that SOM enjoys two important properties; first, the nonlinearity allows for better compression of the color space than linear ones; second, it preserves the neighboring relationships (and, inherently, the distance ratios) between colors.

Once again, the leading idea is to perform color mapping by preserving distance ratios between homologous 3D RGB and 2D dichromat colors, as a way of improving the color discrimination in still images. However, instead of uniformly sampling the RGB color space, Ma and co-authors make a random sampling of the input image itself, in the attempt of eliminating repetitive colors and, consequently, to speed up the recoloring procedure. Thus, similar to Deng et al.’ method [15], there is a noticeable enhancement of color contrast because distance ratios hold, and a loss of color naturalness. But, unlike Deng et al.’ method, there is no longer color consistency because the color samples depend on the color gamut of the input image.

Bao et al.' method [73]. This method operates on RGB color space, and aims to improve the color discrimination of red-green dichromat people (deuteranopy and protanopy), though preserving the color naturalness. Essentially, the components R and G of a given color remain unchanged. Only the component B is changed in the recoloring procedure, depending on the location of the color in relation to the dichromat plane defined by $R = G$. If $R > G$, the new value of the blue component is given by

$$B' = B \frac{f_1}{f_1 + f_2}, \quad (2.7)$$

where f_1 is the number of pixels with $R > G$, while f_2 is the number of the remaining pixels in the image; otherwise, we have

$$B' = 255 \frac{f_1}{f_1 + f_2} + B \frac{f_2}{f_1 + f_2} \quad (2.8)$$

According to Eq. (2.7), a decrease in blue when $R > G$ and $R < B$ (i.e., violet purples) leads to a decrease of saturation and brightness; but, when $R > G$ and $R \geq B$ (i.e., magentas, reds, and oranges) leads to an increase of saturation and a decrease of brightness. Also, in conformity with Eq. (2.8), an increase in blue when $R \leq G$ and $R < B$ (i.e., cyans and blues) leads to an increase of saturation and brightness; but, when $R \leq G$ and $R \geq B$ (i.e., greens) leads to a decrease of saturation and an increase of brightness. Thus, the color discrimination improves by stressing the differences of saturation and brightness between colors behind and beyond the dichromat plane $R = G$. However, the recoloring procedure is not color consistent, since increasing/decreasing of B depends on the frequencies f_1 and f_2 in the input image. A similar recoloring procedure was proposed by the same authors for yellow-blue dichromat people (tritanopy).



Figure 2.18: RGB-based recoloring method due to [16]: (a) original image; (b) deuteranope image view; (c) deuteranope image view after recoloring. Images courtesy of [16].

Ruminski et al.' method [17]. This recoloring method mainly aims to preserve the color naturalness. For that purpose, one firstly calculates the CIE distance Δ_{CIE} between each pixel color of the original image and the homologous pixel color as seen by a dichromat individual. The recoloring procedure only takes place if the following conditions are satisfied: (i) $\Delta_{CIE} > 0.092$; (ii) the hue of the color is not blue, yellow, nor gray. Therefore, the recoloring is essentially restricted to reds and greens, and is as follows:

$$r' = r + 0.5 \Delta_{CIE}, \quad g' = g - 0.5 \Delta_{CIE}, \quad \text{and} \quad b' = r^\gamma, \quad (2.9)$$



Figure 2.19: RGB-based recoloring method due to [17]: (a) original image; (b) deuteranope image view; (c) deuteranope image view after recoloring. Images courtesy of [17].

where $\gamma = g$ represents the gamma correction; note that r , g , and b stand normalized values of R , G , and B , respectively. According to Eq. (2.9), reds become more saturated, while greens get less saturated; in addition, the gamma correction makes the reds to get closer to magentas, and magentas closer to blues. As a consequence, the gamma correction associated to blue channel aims to distinguish between original magentas and magentas introduced by red-to-blue mapping (see Fig. 2.19).

Despite the intent of Ruminski et al., this method does not preserve the color naturalness, since the original reds are all seen as saturated blues, what provokes confusion with the original blues. Thus, the contrast is not guaranteed when the image is plenty of reds and blues. Even so, Eq. (2.9) ensures the color consistency.

2.4.3 HSx Based Methods

As known, these methods build upon the HSx color spaces, which organize the color regarding hue (H), saturation (S), and brightness (i.e., intensity (I), lightness (L) or value (V)). However, because of the dichromat condition, these 3-dimensional color spaces turn into 2-dimensional color spaces. More specifically, the dichromat condition leads to a significant reduction of the image contrast, due to the projection of all colors onto the 60° (yellow) or 240° (blue) half-planes in the case of deuteranopy and protanopy; in the case of tritanopy, the projection is onto the 0° (red) or 180° (green) half-planes. This means that deuteranope and protanope people only see two hues, 60° (yellow) and 240° (blue), as shown in Fig. 2.4(b)-(c), while tritanope people see two different hues, 0° (red) and 180° (cyan), as shown in Fig. 2.4(d). Note that deuteranope and protanope people see some yellows as moss greens and some blues as grays, while tritanope people see yellows as pinks and blues as dark cyans.

As a consequence of the 2-dimensional color space of dichromat people, we observe that protanope and deuteranope people mainly confuse reddish and greenish colors, since they see these colors with the same hue 60° (yellow). In regards to tritanope people, they get confused with yellowish and blue-purplish (violet) colors, because they see these colors as reds (hue 0°). Thus, most HSx based recoloring methods focus on discriminating these confusing hues.

2.4.3.1 HSI

In the literature, we found only one recoloring method based on HSI color space; specifically, it is the one due to Yang and Ro [46].

Yang-Ro method [46]. To our best knowledge, this is the first recoloring method for CVD people (see Table 2.2). In the case of protanopy and deuteranopy, Yang and Ro tried to rid off the confusion between greens and reds by remapping reddish colors to blueish colors. Note that blueish colors are those with some amount of blue (e.g., magentas). But, this has the drawback of likely causing confusion between reddish and blueish colors. This confusion can be mitigated by decreasing the saturation of the remapped hue. Similarly, to avoid confusion between yellows and greens, one decreases the saturation of greens.

In the same paper [46], Yan and Ro also developed an algorithm for tritanope people. They avoid confusion between yellows and magentas by remapping the magentas into cyans and simultaneously decrease the saturation of the magentas to avoid confusion with the original cyans. In regards to yellows, one decreases their saturation to avoid confusion with reds.

In general terms, both recoloring algorithms can be expressed as follows:

$$H' = H + \Delta h, \quad S' = S + \Delta s, \quad \text{and} \quad I' = I, \quad (2.10)$$

where H , S , and I stand for the hue, saturation, and intensity values of the given color, Δh and Δs are the hue and saturation variations, and H' , S' , and I' are the resulting HSI values after recoloring. However, both algorithms differ in respect to the expressions of Δh and Δs , so the reader is referred to [46] for further details.

It is clear that the two methods due to Yang and Ro [46] do not maintain the color naturalness, though they increase the color contrast. In fact, reddish colors are mapped into low saturated blues for protanopy and deuteranopy, while magentas are mapped to low saturated cyans for tritanopy. But, either of these methods preserves the color consistency because each color is always mapped to a unique one, in conformity with the color mapping functions defined in Yang and Ro [46].

2.4.3.2 HSL

In the literature, we found only one recoloring method based on HSL color space, which is due to Iaccarino et al. [76].

Iaccarino et al.'s method [76]. This method aims at reducing all stimuli along the confusion lines in the color space, and only applies to red-green dichromats. Therefore, the leading idea is to mitigate the confusion between reds and greens. For that purpose, this method counts on the number of pixels (N_R) whose red component dominates both green and blue components, as well as the number of pixels (N_G) whose green component dominates both red and blue components. If $N_R > N_G$, the reference color is R (red); otherwise, it is G (green).

Then, all pixels with non-null red or green components are recolored relative to the reference color; more specifically, for pixels with colors close to the reference color, the hue is rotated 30°

(in the clockwise direction), the saturation is slightly decreased, and the lightness increased; otherwise, the hue is not subject to any change, the saturation is slightly increased, and the lightness is slightly decreased. The reader is referred to [76] for further details.

Summing up, this method promotes the contrast enhancement because the saturation increases for some pixels and decreases for others; the same applies to lightness; also, some hues change, while others do not. In turn, the color naturalness is not affected too much from the dichromat point of view, because the color components HSL are not significantly changed. However, the method does not ensure color consistency because the recoloring depends on the image. In other words, it depends on the dominant color components of pixels.

2.4.3.3 HSV

There are several recoloring methods using the HSV color spaces, namely those due to [18] [77] [19] [17].

Wong-Bishop method [18]. This recoloring method for red-green dichromat people leaves the saturation and brightness unchanged, i.e.,

$$H' = H + \Delta h, \quad S' = S, \quad \text{and} \quad V' = V, \quad (2.11)$$

where H , S , and V represent the hue, saturation, and value of a color, respectively, while Δh is the hue variation, and H' , S' , and V' are the resulting HSV values after recoloring. This method uses a non-linear hue remapping given by the following expression:

$$\Delta h = H^\theta, \quad (2.12)$$

where θ denotes the control parameter of the remapping yield by

$$\theta = \theta_{\min} + \frac{n_d}{n_u + n_d} (\theta_{\max} - \theta_{\min}) \quad (2.13)$$

whose θ_{\min} and θ_{\max} stand for the minimum and maximum values of θ , and n_d and n_u represent the number of pixels falling within the discriminating and undiscriminating hue ranges, respectively. In practical terms, this amounts to compress the discriminating hue range (i.e., blues and yellows) and to stretch the undiscriminating hue range (i.e., reds and greens) to better distinguish the confusing hues. Thus, there is a contrast improvement. But, the color naturalness is not preserved because sometimes hues are remapped to quite different hues (e.g., sometimes greens are mapped to blues). Besides, the color consistency is not preserved either because the remapping function changes dynamically, from an image to another, as expressed by Eq. (2.13).

Lai-Chang method [77]. This method operates not only on hues but also on saturation and brightness. This recoloring method comprises one of the following two alternatives. The first alternative applies to images that are neither excessively dark nor bright, so it is performed without changing the color brightness as follows:

$$H' = H + \Delta h, \quad S' = S + \Delta s, \quad \text{and} \quad V' = V, \quad (2.14)$$

where H , S , and V stand for the hue, saturation, and value of a color, Δh and Δs are the

hue and saturation variations, and H' , S' , and V' are the resulting HSV values after recoloring. However, no expression for Δh is provided in [77] because, apparently, they depend on the visual model of each, i.e., yellows and blues are left untouched for red-green dichromat people, while reds and cyans remain unchanged for yellow-blue dichromat people. Similarly, no expression for Δs is given by Lai and Chang.

The second alternative applies to images that are too light or too dark. In this case, the authors used histogram equalization over the brightness values (V) of the input image to reinforce its contrast as follows:

$$H' = H, \quad S' = S + \Delta s, \quad \text{and} \quad V' = V_{max} \sum_{i=0}^V \frac{n_i}{n} \quad (2.15)$$

where $V_{max} = 255$ is the maximum possible brightness value of a given image, n_i is the number of pixels with brightness i , and n is the total number of pixels of such image (i.e., resolution). In short, the image contrast is enhanced in the second alternative, without undermining the color consistency and naturalness. The same cannot be said on the first alternative.

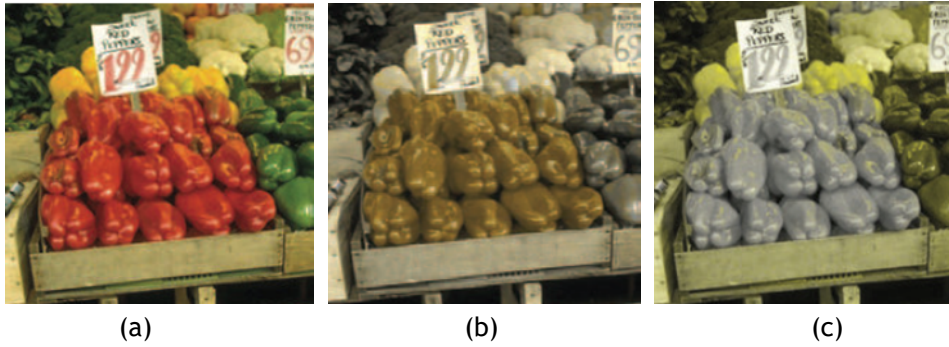


Figure 2.20: HSV-based recoloring method due to [17]: (a) original image; (b) deuteranope image view; (c) deuteranope image view after recoloring. Images courtesy of [17].



Figure 2.21: HSV-based recoloring method due to [18]: (a) original image; (b) deuteranope image view; (c) deuteranope image view after recoloring. Images courtesy of [18].

Ruminski et al.'s method [17]. Preserving color naturalness has a different meaning for red-green dichromat people because they only perceive two hues within the entire hue wheel: yellow 60° and blue 240° . With this in mind, Ruminski et al. ascertained that remapping hues

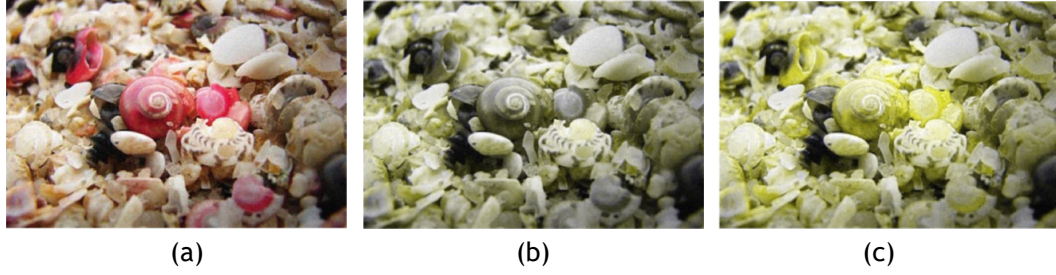


Figure 2.22: (a) HSV-based recoloring method due to [19]: (a) original image; (b) deuteranope image view; (c) deuteranope image view after recoloring. Images courtesy of [19].

is useless, so they decided to change only the values of saturation (S) and brightness (V), i.e.,

$$H' = H, \quad S' = 0.32S + 0.05, \quad \text{and} \quad V' = 0.6V + 0.01. \quad (2.16)$$

More specifically, the saturation is decreased if and only if the original hue is in the range of reds (i.e., if $H \in]300^\circ, 360^\circ \cup [0^\circ, 60^\circ[$). In turn, the brightness is decreased if and only if the original hue is in the range of greens (i.e., if $H \in]60^\circ, 180^\circ[$). Nevertheless, this recoloring procedure only takes place when the hue is not yellow, blue, and gray. Also, if the Euclidean distance between the original color and its homologous dichromat color of a given pixel is less than 0.092, the recoloring procedure is not performed either.

Fig. 2.20 illustrates how this recoloring method works, where we note that reds get less saturated and greens get darker than the original ones. This method is color consistent because the interpolation procedure outputs the same values of S' and V' for the same inputs S and V . However, the color naturalness is not preserved because in some cases reds look greens and greens look reds, as shown in Fig. 2.20(b)-(c). This is so because the method operates in both ranges of reds and greens simultaneously. In regards to contrast, the gain is not evident, mainly in images with many grays, since the method transforms reds into grays, which may originate confusion with the original grays.

Ching-Sabudin method [19]. This method applies to red-green dichromat people. It operates on the gamuts of reds and greens separately; the gamut of blues remains unchanged. Hues in the gamut of reds $H \in]300^\circ, 360^\circ \cup [0^\circ, 60^\circ[$ are all mapped to the yellow 60° while keeping the values of saturation and brightness. This is done by setting the value of G to the value of R , without the need of converting the RGB value of each pixel to HSV. In a way, this is how red-green dichromat people see reds as yellows in natural conditions, yet with higher values of saturation and brightness.

With regard to greens $H \in]60^\circ, 180^\circ[$, the confusion results from the fact that the hues of the sub-range $]60^\circ, 150^\circ[$ are also projected on the 60° yellow half-plane. In this case, one proceeds to the RGB-HSV conversion, so that the recoloring takes place in the HSV color space as follows:

$$H' = H = 180 + \frac{1}{2}(H - 60), \quad S' = S, \quad \text{and} \quad V' = V. \quad (2.17)$$

This results in a remapping of the hues $H \in]60^\circ, 180^\circ[$ into $]180^\circ, 240^\circ[$, so greens are mapped into blues, although it would be better to map hues from 150° because the red-green dichromat people already see hues in the sub-range $]150^\circ, 180^\circ[$ as blues; this is so because the red-green

dichromat people naturally see greens in the range $]150^\circ, 180^\circ[$ as the 240° blue. Recall that red-green dichromat people only see two hues: 60° yellow and 240° blue.

This method works very well for signage images because most of these images possess a small number of distinct regions, so there is an apparent increase of contrast because reds are mapped to yellows, and greens are mapped to blues. However, this method is not advantageous for real-life scenes because the Euclidean distance between the original colors and mapped colors may be far over the threshold of naturalness. But, it holds the color consistency, i.e., colors are always mapped in the same manner using Eq. (2.17).

2.4.4 CIE Based Methods

As noted in Section 2.3.4, CIE-based methods take advantage of the perceptual uniformity of the CIE color spaces. In other words, the Euclidean distance between two colors is a measure of the viewer's perceptual distance. Therefore, as described below, the color distance is also extensively explored in the CIE-based methods for dichromat people.

2.4.4.1 CIE Lab

Dichromat people perceive the values of L (brightness) and b (yellow-to-blue axis) almost correctly, but not the value of a (green-to-red axis). Therefore, they do not distinguish between two colors only varying parameter is a ; hence, the color confusion of these people.

There are many CIE Lab-based recoloring methods in the literature, namely: [26], [27], [78], [20] [79] [80], [21], [22], [23], [25] [81], [24] and [82]. The recoloring method from [9] [10] also applies to dichromacy.

Rasche et al.' method [26]. The focus of this CIE Lab-based method is on keeping the difference between colors in the recoloring process relative to trichromat color perception, no matter how different the mapped colors are far away from the original colors. The luminance L remains untouched. That is, the main goal is to preserve the color contrast between each pair of colors.

For that purpose, one computes the following error :

$$\varepsilon^2 = \sum_{i=1}^n \sum_{j=i+1}^n \left(\frac{\|c_i - c_j\|}{C_{range}} - \frac{\|T(c_i) - T(c_j)\|}{T_{range}} \right)^2, \quad (2.18)$$

where n is the number of colors, C_{range} is the maximum distance between any pair of colors in the CIE Lab color space, T_{range} is the maximum distance between any pair of colors in the 2D dichromat plane, and T is a composition of two functions: (i) a linear transformation $G : \mathbb{R}^4 \rightarrow \mathbb{R}^3$ in homogeneous CIE Lab coordinates is used to iteratively change the original color distribution; (ii) a projection of the CIE Lab image colors onto the dichromat plane (i.e., dichromat simulation).

The initial matrix G is determined using principal component analysis (PCA) of the image in the CIE Lab color space. Based on the fact that protanopes and deuteranopes (i.e., red-green dichromats) have a rather small response in the a direction (horizontal axis), G is determined

by mapping the first principal component of the image to b and the second principal component to a . For tritanopes, we swap the directions for mapping, that is, the first principal component of the image is mapped to a and the second principal component to b .

Then, the idea is applying the Fletcher-Reeves conjugate-gradient method to minimize the error given by Eq. (2.18) and, consequently, to obtain an optimal G that allows us to preserve the contrast after the image recoloring. Despite the good results in several cases, the authors point out that frequently the final images look unnatural for dichromat people. Furthermore, the method is not color-consistent because the final matrix G depends on the input image.

Rasche et al.’ method [27]. This method is based on the CIE Lab color space. Its main goal is to preserve the contrast in images for dichromat people. For that purpose, one uses a quadratic objective function that preserves the proportional distance between each pair of colors as follows:

$$S = \sum_{i=1}^{n-1} \sum_{j=i+1}^n \left(\frac{d_{ij}^D}{d_{ij}^T} - K \right)^2 \quad (2.19)$$

where $n = 256$ is the number of quantized landmark colors of a given image, d_{ij}^T and d_{ij}^D are Euclidean distances between each pair of colors as seen by trichromat and dichromat people, respectively, and the target proportionality constant $K = 100/\text{MAX}$, with MAX is the maximum d_{ij}^T in a given image. The objective function given by the non-linear equation (2.19) is subject to a minimization process known as *constrained majorization* [83]; see [27] for further details.

The focus of this method is on color contrast, not color naturalness and consistency. Preserving color naturalness is not achieved because this method forces the maximization of contrast. In regards to color consistency, it is not maintained because the color mapping depends on the specific colors existing in each image, that is, the same color present in two distinct images may be mapped to different colors.

Kovalev method [84]. This method resembles Rasche et al.’ method above [26]. In fact, its leading idea is to preserve the perceived difference between any pair of colors of the 3-dimensional CIE Lab color space of trichromat people in the 2-dimensional CIE Lab color space of dichromat people. More specifically, the error is given by the following objective function:

$$U = \sum_{i=1}^n \sum_{j=1}^n w_{ij} |d_{ij}^T - d_{ij}^D|, \quad (2.20)$$

where n is the number of colors (i.e. the standard palette of 256 colors), d_{ij}^T and d_{ij}^D are Euclidean distances between each pair of colors as seen by trichromat and dichromat people, respectively, while w_{ij} represents the estimated frequency of the joint appearance of this pair of colors (c_i and c_j) in the input images of a given dataset.

The minimization of the U follows a randomized approach that builds upon a greedy algorithm. This procedure preserves the contrast. But, putting the focus only on preserving the contrast forces the loss of naturalness. Furthermore, color consistency does not hold because it depends on the dataset of input images, from which we come out with a particular 256 color palette.

Wakita-Shimamura method [21]. This method aims to enhance the contrast (C), to improve the color distinguishability (D), and preserve the color naturalness (N) in HTML documents, with

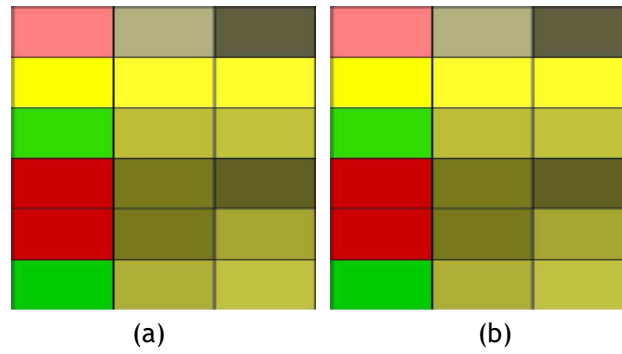


Figure 2.23: CIE Lab-based recoloring method due to [20]: (a) to deuteranope people; (b) to protanope people. 1st column: original colors; 2nd column: dichromat view of the colors; 3rd column: dichromat view of the colors after recoloring. Images courtesy of [20].

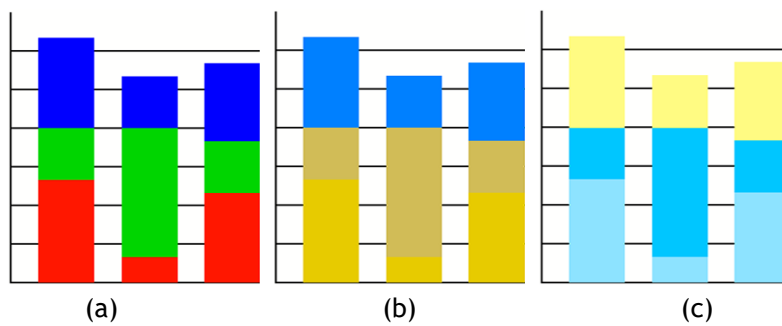


Figure 2.24: CIE Lab-based recoloring method due to [21]: (a) original image; (b) deuteranope image view; (c) deuteranope image view after recoloring. Images courtesy of [21].

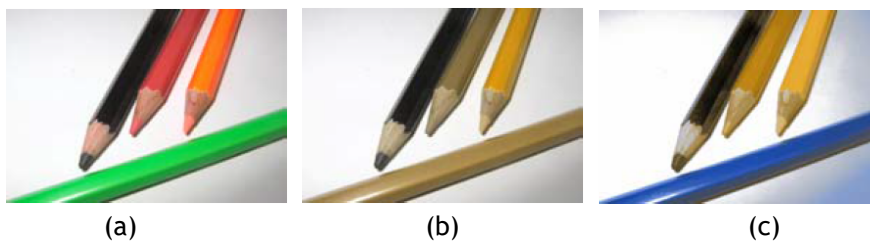


Figure 2.25: CIE Lab-based recoloring method due to [22]: (a) original image; (b) deuteranope image view; (c) deuteranope image view after recoloring. Images courtesy of [22].

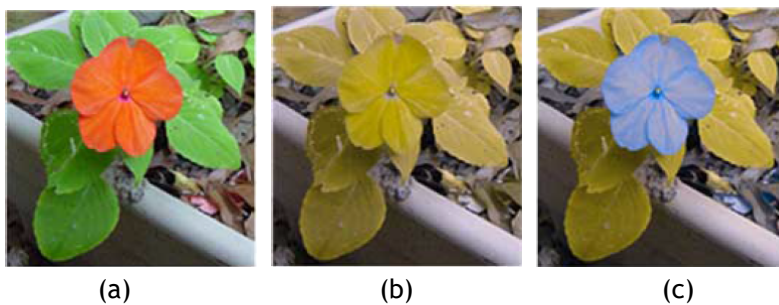


Figure 2.26: CIE Lab-based recoloring method due to [23]: (a) original image; (b) deuteranope image view; (c) deuteranope image view after recoloring. Images courtesy of [23].

the constraint that each HTML document has no more than ten colors, so that the objective function is given by:

$$f = C + D + N, \quad (2.21)$$

with

$$C = \sum_{i < j} K_C^{(i,j)} \cdot C(\mathbf{c}_i, \mathbf{c}_j), \quad (2.22)$$

$$D = \sum_{i < j} K_D^{(i,j)} \cdot D(\mathbf{c}_i, \mathbf{c}_j), \quad (2.23)$$

and

$$N = - \sum_{i < j} K_N^i \cdot \Delta(\pi(\mathbf{c}_i), \pi(\mathbf{c}'_i))^2. \quad (2.24)$$

where $(\mathbf{c}_i, \mathbf{c}_j)$ stands for any color pair; $K_{\bullet}^{(i,j)}$ are weights associated with contrast, color distinguishability, and naturalness for each pair $(\mathbf{c}_i, \mathbf{c}_j)$; $C(\mathbf{c}_i, \mathbf{c}_j)$ and $D(\mathbf{c}_i, \mathbf{c}_j)$ are the contrast and distinguishability between two colors, \mathbf{c}_i and \mathbf{c}_j ; and $\Delta(\pi(\mathbf{c}_i), \pi(\mathbf{c}'_i))$ is the distance between the original color \mathbf{c}_i and its homologous mapped color \mathbf{c}'_i as perceived by a dichromat individual. The function f is then maximized through a simulated annealing algorithm. The reader is referred to [21] for further details.

Unfortunately, despite the argument that this method preserves the naturalness and enhances the contrast and distinguishability, Fig. 2.24 seems to indicate the opposite. Furthermore, the method does not assure the color consistency because it depends on the set of colors existing in each HTML document.

Jefferson-Harvey method [22]. The idea underlying this method is to enhance the contrast and preserve the brightness and color naturalness in HTML documents. First, one extracts a set of key colors of a given HTML document using sampling of the difference histogram. Then, the recoloring procedure is formulated in terms of the minimization of the following an error function (or objective function):

$$f = \varepsilon_1 + \varepsilon_2 + \varepsilon_3, \quad (2.25)$$

with

$$\varepsilon_1 = \frac{1}{\sum_{i < j} \|\mathbf{c}_i, \mathbf{c}_j\|} \sum_{i < j} (\|\mathbf{c}_i, \mathbf{c}_j\| - \|\mathbf{c}'_i, \mathbf{c}'_j\|)^2, \quad (2.26)$$

and

$$\varepsilon_2 = \sum_{p=1}^3 \left(\sum_{i \in G_1[p]} [\mathbf{c}'_i(p)]^2 + \sum_{i \in G_2[p]} [\mathbf{c}'_i(p) - 1]^2 \right), \quad (2.27)$$

and

$$\varepsilon_3 = \sum_{i \in G_3} (\mathbf{c}'_i - \mathbf{c}_i)^2. \quad (2.28)$$

where $(\mathbf{c}_i, \mathbf{c}_j)$ and $(\mathbf{c}'_i, \mathbf{c}'_j)$ is any pair of original color and its homologous mapped color, as seen by a dichromat individual; $G_1[p]$ and $G_2[p]$ are the sets of colors having the p -th channel out of gamut, $C_i[p]$ is the mapped p -th component of the i -th representative color; G_3 is the set of colors to preserve (e.g., black and white).

In Eq. (2.25), the first error component ε_1 is formulated so that the color contrast and brightness are preserved as much as possible for the dichromatic viewer; the second error component ε_2 measures the gamut error, which has to be minimized too; the third error component ε_3 is the penalty by mapping colors that must remain unchanged. The objective function f is minimized using the Sammon algorithm [75], in order to achieve the better trade-off between the three errors above.

Considering the recoloring procedure tries to keep unchanged the distance between any pair of colors in the CIE Lab color space, we conclude that the contrast holds. But, clearly, the color consistency does not hold because the key colors vary from an image to another; consequently, the color naturalness is not maintained either.

Huang et al.' method [23]. Recall that the variations of a are not perceived by red-green dichromats, which cause loss of color discrimination in the color gamut in a given image, and, consequently, loss of visual information. Huang et al. address this problem by transferring part of a in favor of b . This is done using a color rotation as follows:

$$\begin{bmatrix} L' \\ a' \\ b' \end{bmatrix} = \begin{bmatrix} 1 & 0 & 0 \\ 0 & \cos(\phi(\theta)) & -\sin(\phi(\theta)) \\ 0 & \sin(\phi(\theta)) & \cos(\phi(\theta)) \end{bmatrix} \begin{bmatrix} L \\ a \\ b \end{bmatrix} \quad (2.29)$$

where

$$\phi(\theta) = \phi_{max} \left(1 - \left(\frac{\theta}{\pi/2} \right)^\gamma \right), \quad (2.30)$$

being $\phi(\theta)$ closer to zero as θ approaches to $\pi/2$, while ϕ_{max} represents the maximal change of θ and γ the degree of the decreasing rate that is specified through the minimization of an objective function based on the contents of the original color image. Such objective function is given by

$$E = E_{detail} + \lambda E_{naturalness}, \quad (2.31)$$

where:

$$E_{detail} = \sum_{i=1}^n \sum_{j=i+1}^n (\|C_i - C_j\| - \|\mathbf{B}(T(C_i)) - \mathbf{B}(T(C_j))\|)^2, \quad (2.32)$$

and

$$E_{naturalness} = \sum_{i=1}^n (||C_i - T(C_i)||)^2, \quad (2.33)$$

where the indexed color $C = (L, a, b)$, $T(C) = (L', a', b')$, $\mathbf{B}(T(C))$ stands for the color obtained from Brettel simulation of $T(C)$ [70], and λ is a user-specified Lagrange multiplier. The minimization of the objective function (2.31) is performed through Fletcher-Reeves conjugate-gradient method to determine the optimal solution for $\phi(\theta)$. Note that, according to Eqs. (2.29)-(2.30) yellows and blues remain unchanged because θ equals $\pi/2$ and $-\pi/2$, respectively. Moreover, the color consistency does not hold because the value of ϕ_{max} in (2.30) varies in function of the input image. Also, in conformity with Eq. (2.31), the method essentially preserves the color contrast because its authors use small values of λ (close to zero), that is, it is given more importance to contrast in detriment of naturalness.

Troiano et al.' method [20] [79] [80]. This method was designed to assist designers in the development of user interfaces based on color palettes. The leading idea is to improve the luminance contrast between contiguous colors of user interfaces, but preserving the original chromaticity of colors.

For that purpose, they adopted the following fitness function:

$$f = \left(\prod_{i=0}^n (1 - d_i) \prod_{j=1}^k r_j \right)^{\frac{1}{n+k}}, \quad (2.34)$$

where d_i is the distance between the original i -th color and its homologous mapped color, r_j refers to contrast between a given color c_i and each of its neighbor contiguous color c_j , which is calculated as follows:

$$r_j = \frac{20 + \min(R_j - T_j, 0)}{20}, \quad (2.35)$$

being R_j the contrast ratio, as defined in W3C's WCAG [85] and T_j is the threshold value (i.e., 5 or 7), In accordance with the recommendations by W3C's guidelines. The function f is then maximized through a genetic algorithm, and this involves the minimization of the distance between each original color and its homologous mapped color, as well as the maximization of the contrast between each pair of contiguous colors.

In spite of only changing the lightness (L) and preserving color chromaticity, this method does not always guarantee the color naturalness because noticeable changes in lightness may change the perceived color; for example, reducing the lightness of a pink color likely gives rise to a dark red color. The color consistency is not preserved either because it depends not only on the colors but also their adjacent colors present in a given image.

Kuhn et al.' method [24]. Similar to other methods, the leading idea of this method is to keep the distance between each pair of colors in the 2D dichromat plane equal to the distance of their homologous colors in CIE Lab color space. To this end, the method consists of three steps: (i) image color quantization; (ii) optimization of the quantized colors; and (iii) reconstruction of the final colors from the optimized ones.

The quantization step is performed using, for example, uniform quantization or any other common technique (see [86]). It is clear that this step outputs a set of quantized colors. The optimization step involves minimizing the difference between two distances; specifically, the distance between any pair of quantized colors in the CIE Lab color space and the distance between their homologous colors in the plane Lb . These colors in the plane Lb are obtained by orthographic projection onto red-green plane color space (i.e. dichromat plane), which is then followed by a rotation to align it with the plane Lb . Then, the optimization procedure based on a mass-spring system takes place in the plane Lb , where the positions of colors are iteratively updated. The final colors are obtained from the optimized ones using a symmetric rotation, i.e. from the plane Lb to dichromat plane.

As a consequence of the optimization procedure, this method increases the color contrast of the original image, but leads to significant changes in some colors (e.g. reds are sometimes mapped to blues), which undermines the color naturalness. In turn, the color consistency is not guaranteed either because it depends on the chromatic gamut of each image and quantization technique at hand.

Wang et al.' method [25] [81]. This method is a follow-up of one due to Huang et al. [23] described above. In fact, while Huang et al. use a local rotation of color to transfer part of a into b , and so to get a better discrimination between colors for red-green dichromats, Wang et al. further use a global rotation given by the angle between the axis b and the principal component axis (from principal component analysis or PCA) of the color distribution of a given image in the CIE Lab color space. This global rotation allows for an even better color discrimination along b axis. Nevertheless, as shown in Fig. 2.28, this method does not preserve the color consistency because it simply extends Huang et al.'s method, though it increases color contrast relative to Huang et al.'s method as a consequence of the global rotation of colors.

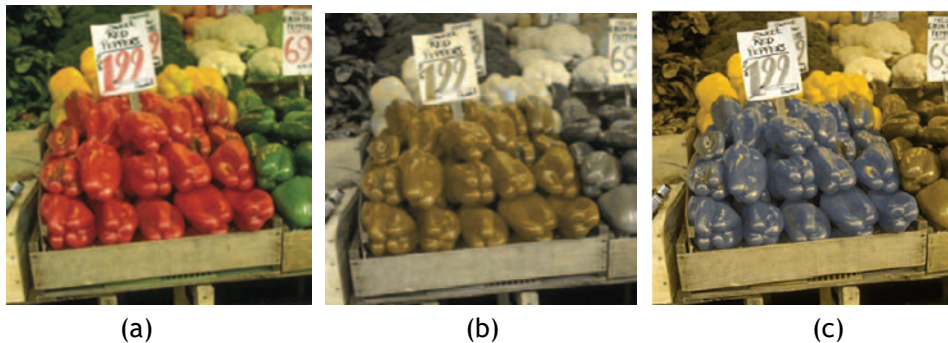


Figure 2.27: CIE Lab-based recoloring method due to [24]: (a) original image; (b) deuteranope image view; (c) deuteranope image view after recoloring. Images courtesy of [24].

Flatla et al.'s method [82]. This color adaptation method mostly applies to HTML documents (with a set of limited number of colors), not that much to photo images. It aims at improving the subjective response of CVD users by preserving both perceptual experience and subjective experience of CVD users on the Web.

Preserving the *perceptual experience* means to maintain both color naturalness and contrast as much as possible. While color naturalness concerns on minimizing the Euclidean distance between each original color and its corresponding mapped color, color contrast is meant to maximize (or recovering) the distance between each pair of mapped colors. To calculate the

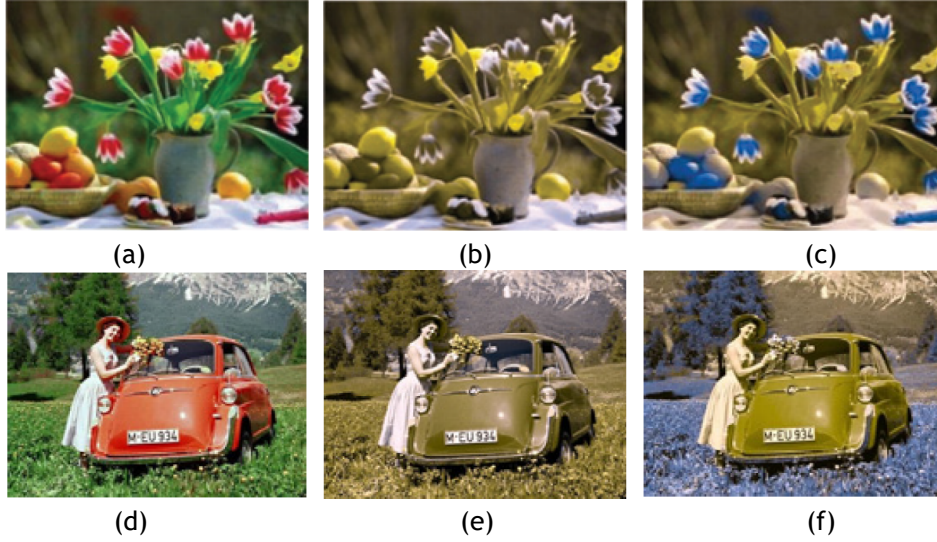


Figure 2.28: CIE Lab-based recoloring method due to [25] is not color consistent because the red colors of both original images (a) and (d) are mapped to different colors in deuteranope images (c) and (f), respectively, after recoloring. The images (b) and (e) show the original images as seen by deuteranope people. Images courtesy of [25].

perceptual naturalness and contrast (differentiability), one applies the CIE76 distance, i.e., the CIE Lab Euclidean distance.

With regards to the *subjective experience*, naturalness and contrast are computed by means of a distance concept introduced by Ou et al. [87], which measures activity, temperature and weight.

Based on these four components (i.e, perceptual color naturalness n , perceptual color contrast c , subjective color naturalness N , and subjective color contrast C), a fitness function is formulated as the weighted sum of such components as follows:

$$f = w_1 \cdot n + w_2 \cdot c + w_3 \cdot N + w_4 \cdot C \quad (2.36)$$

where the weights were determined in an empirical manner as $w_1 = w_2 = 1$ and $w_3 = w_4 = 2$. This objective function is optimized using a two-pass hill-climbing algorithm.

According to Eq. (2.36), the contrast and naturalness tends to hold. However, as for other optimization-based methods, the color consistency does not hold because the mapped colors depends on the set of colors extracted from each HTML document.

2.4.4.2 CIE Luv

We have found two color adaptation methods based on CIE Luv color space for dichromat people in the literature, namely those due to Nakauchi and Onouchi [88] and Milic et al. [63].

Nakauchi-Onouchi method [88]. This method starts with the formation of all pairs of colors in a given image, calculating then the corresponding distances ΔE_t and ΔE_d in the CIE Luv for both trichromat and dichromat people, respectively. The confusing pairs of colors are those

that satisfy the following two conditions:

$$\frac{\Delta E_d}{\Delta E_t} < r \quad (2.37)$$

and

$$\Delta E_d < \Delta E_{d_{\max}} \quad (2.38)$$

where the threshold $r = 0.9$ and $\Delta E_{d_{\max}} = 50.0$; note that the just-noticeable difference (JND) is about 9.0 in CIE Luv color space.

For each pair of confusing colors, only the one with lower frequency in image (i.e., less number of pixels) is changed. The process of changing the colors is performed by minimizing the following error function E given by the sum of confusion degrees $\varphi_{conf}(C_i)$ of all the color-confusing clusters C_i as follows:

$$E = \sum_{i \in [1, \dots, N]} \varphi_{conf}(C_i), \quad (2.39)$$

where N is the total number of clusters, including the color-confusing clusters, and

$$\varphi_{conf}(C_i) = \sum_{k=1, k \neq i}^N \frac{1}{\|C_i - C_k\| + \varepsilon} \quad (2.40)$$

where C_k represents the k -th cluster center, with $k = 1, \dots, N$, C_i is the center of i -th cluster of confusing colors, and ε is a small value to avoid divisions by zero; it is clear that $\{C_i\} \subset \{C_k\}$, the set of color-confusing clusters is a subset of the set of all color clusters. Each cluster has at least a color, but if the input image has many colors, it is quantized through LBG method (cf. [89]) to form color clusters. Note that if more than half of colors in the cluster are candidates to change (in conformity with the two conditions above), the cluster is considered as a color-confusing cluster.

In short, this method focuses on color contrast, which is improved by the error function E above. However, the method does not preserve the color consistency because the function E depends on the colors present in the input image. The color naturalness does not hold either.

Milic et al.'s method [63]. This method has been described in Section 2.3.4.3 (p.21) for anomalous trichromat people. The only difference is that the rotation about the confusion point is more accentuated for dichromats than anomalous trichromats because the severity degree is greater for the former than for the latter ones.

2.4.5 Methods for Dichromacy: a Discussion

A brief glance at Table 2.2 shows the following:

- *Dichromacy types*. Unlike the color adaptation methods for anomalous trichromat people, methods for dichromat people do not use a color compensation strategy. Instead, they use a color contrast-based strategy that mitigates the red-green confusion and yellow-magenta

Table 2.2: Recoloring methods for dichromat people.

Reference	Dichromacy type			Color space	Target medium			Color range	Perceptual requirement		
	P	D	T		N-Ph	Ph	O		CE	CC	NM
[46]	•	•	•	HSI	•	•		TC	•	•	
[78]	•	•		CIE Lab	•	•		256	•		
[21]	•	•	•	CIE Lab	•			few	•		
[26]	•	•	•	CIE Lab	•	•		~250	•		
[27]	•	•	•	CIE Lab	•	•		~250 key	•		
[76]	•	•	•	HSL	•	•		TC	•		•
[69]	•	•	•	LMS	•	•		TC			
[22]	•	•	•	CIE Lab	•	•		key	•		
[13]	•	•	•	LMS	•	•		TC	•		
[23]	•	•		CIE Lab	•	•		TC	•		
[16]	•	•	•	RGB	•	•		key	•		•
[15]	•	•	•	RGB	•			CLUT	•	•	
[73]	•	•	•	RGB	•	•		CLUT	•		•
[24]	•	•	•	CIE Lab	•	•		key	•		
[88]	•	•	•	CIE Luv	•	•		key	•		
[74]	•	•	•	RGB	•	•		key	•		
[8]	•	•	•	HSV	•	•		TC	•		
[20]	•	•	•	HSV			I	TC	•		
[18]	•	•	•	HSV	•	•		TC	•		
[71]	•	•	•	RGB	•	•		TC	•		
[25]	•	•	•	CIE Lab	•	•		TC	•		
[77]	•	•	•	HSV	•	•		TC	•		
[51]	•			RGB	•	•		TC	•		
[9]	•	•	•	CIE Lab	•	•		key	•		
[10]	•	•	•	CIE Lab	•	•		key	•		
[17]	•	•		RGB	•	•		TC	•	•	
[17]	•	•		HSV	•	•		TC	•	•	
[19]	•	•		HSV	•	•		TC	•		
[14]	•	•		LMS	•			2	•		
[7]	•	•		HSI	•			TC	•		
[6]	•	•	•	RGB	•			few	•		
[82]	•	•	•	RGB			H	few	•		•

Abbreviations:

Dichromacy type: P (protanopy); D (deutanopy); T (tritanopy).

Target medium: N-Ph (non-photo image); Ph (photo image); O (other); I (interfaces), H (HTML documents).

Color range: TC (true color); CLUT (color look-up table); few (few colors); key (key colors).

Properties: CC (color consistency); CE (contrast enhancement); NM (naturalness maintenance).

confusion inherent to deuteranope and protanope people, respectively. The compensation is not feasible because the color space of dichromat people is not 3D, but 2D. In fact, deuteranopes and protanopes only see yellows and blues, while tritanopes only see cyans and reds, with more or less brightness.

- *Color ranges.* The color range used by a given method is closely related to the color contrast enhancement technique. Basically, we have identified three main color contrast enhancement techniques: (i) objective function optimization; (ii) matrix-based color

remapping; and (iii) contrast-reinforcement compensation. The first use a small set of *key* (or representative) colors of the input image, or simply a *few* colors, so that the remaining colors are obtained by linear interpolation in the adaptation process; for example, most methods based on CIE Lab and CIE Luv color spaces use objective functions to iteratively increase distances between confusing colors, that is, to enhance the contrast.

The remaining methods use true colors (TC) to remap colors. The matrix-based methods use matrices or non-linear transformations (i.e., rotation matrix, shrinking matrix, and so forth) to remap the original colors of a given image into more contrasting colors; for example, most HSx-based methods (see, for example, [46] [76]) use a rotation matrix to color remapping. Finally, contrast-reinforcement compensation decrease one or two color components to increase the remaining color components; for example, some RGB-based methods (see, for example, [73]) take advantage of this technique.

- *Color spaces.* There is no dominant color space in color adaptation methods for dichromats, but the CIE, HSx, and RGB are the most used. Note that no method is built upon CIE XYZ, likely because this color space is not perceptually uniform. We also noted that the choice of the color space largely depends on the color adaptation strategy underlying each method. For example, the color adaptation strategy based on the objective function optimization is —as seen above— only feasible for a limited range of colors; otherwise, it would be a very time-consuming technique.
- *Target media.* With the exception of the methods due to Troiano et al. [20] and Flatla et al. [82], all the remaining methods were designed for still images. As noted above, this is largely because any color adaptation method does not depend on the medium (e.g., a still image, a HTML document, an application interface, or even a video). However, our focus was on still images.
- *Perceptual requirements.* As for anomalous trichromat people, the methods for dichromat people mainly focus on preserving or enhancing color contrast, and this is particularly important to distinguish between confusing colors in their 2D color space. Recall that confusion mainly results from the amalgamation of the 3D color space of the input image onto the 2D color color space of dichromat people. Most of these methods are not color-consistent, and are not able to preserve the color naturalness either. Moreover, there is no method that satisfies the three perceptual requirements simultaneously. Therefore, no method preserves the perceptual learning of dichromat people.

Thus, the main conclusion we can draw from the state-of-the-art methods for dichromats are the following:

- No method preserves the perceptual learning of dichromat people.

Thus, it remains to know whether or not it is feasible to design any method that preserves the perceptual learning of dichromat people.

2.5 CVD Adaptation Methods for Monochromacy

Monochromats see colors in grayscale and sometimes with slight shades of blue. That is, the color space of monochromat people is 1-dimensional. Thus, monochromacy significantly reduces the ability of discriminating objects in images, particularly when they have the same perceptual luminance. This means that two objects with the same luminance are only distinguishable if we change at least the luminance of one of them.

2.5.1 CIE Based Methods

2.5.1.1 CIE Lab

In the literature, there are only a couple methods for adapting still images for monochromat people, specifically those due to Rasche et al.'s [26] [27], which are both based on CIE Lab color space.

Rasche et al.'s method [26]. Rasche and colleagues proposed a general method in [26] that works for both monochromat and dichromat people. Such a general method takes advantage of the same error function as expressed by Eq. (2.18). In the case of monochromacy, this equation takes the following form:

$$\varepsilon^2 = \sum_{i=1}^n \sum_{j=i+1}^n \left(\frac{\| \mathbf{c}_i - \mathbf{c}_j \|}{C_{range}} - \frac{|\mathbf{g} \cdot (\mathbf{c}_i - \mathbf{c}_j)|}{T_{range}} \right)^2 \quad (2.41)$$

when \mathbf{g} stands for the luminance, whose initial value is $(1, 0, 0)$, being its optimal value determined by Fletcher-Reeves conjugate-gradient method that minimizes the error given by Eq. (2.41). Recall that the goal is to preserve the contrast between each pair of colors, \mathbf{c}_i and \mathbf{c}_j .

Rasche et al.'s method [27]. Rasche et al. proposed another general method that is valid for both monochromat and dichromat people [27], which build upon Eq. (2.19). Recall that in the case of monochromacy, the mapped colors are in grayscale so that the leading idea is to preserve both contrast and luminance consistency. These two goals are expressed as a constrained, multi-dimensional scaling problem [83]. As in [26], contrast preservation is achieved by keeping the relative distance between each pair of colors in the recoloring process. Then, one adds constraints that reinforce luminance consistency so that the desired solution can be expressed as a sequence of linear programming problems. As expected, and similar to the previous method, neither color naturalness nor color consistency are maintained by this method, because its focus is only on preserving image contrast.

2.5.2 Methods for Monochromacy: a Discussion

As shown in Table 2.3, there are only two methods developed for monochromat people, both built upon CIE Lab color space. These two methods take advantage of objective function optimization; hence, the small range of key colors. Consequently, they are not color consistent- nor

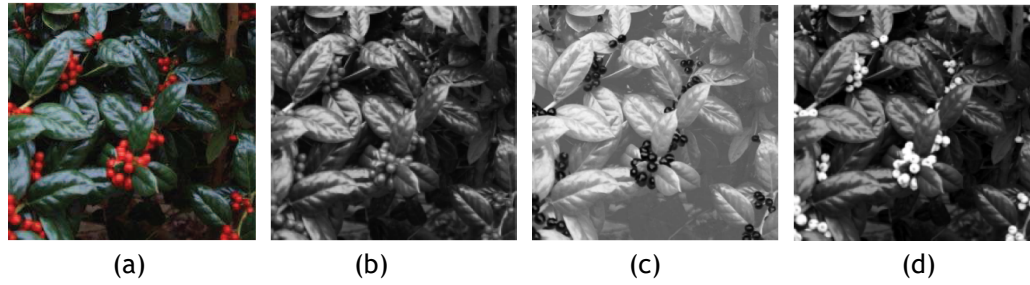


Figure 2.29: CIE Lab-based recoloring method due to [26] and [27]:(a) original image; (b) deuteranope image view; (c) deuteranope image view after recoloring by the method due to [26]; (d) deuteranope image view after recoloring by the method due to [27]. Images courtesy of [26] [27].

Table 2.3: Summary of the color adaptation methods, for monochromacy.

Reference	Monochromacy		Color space	Target medium		Color range	Perceptual requirement		
	type			N-Ph	Ph		CE	CC	NM
	blue-cone	rod							
[26]	•	•	CIE Lab	•	•	~250	•		
[27]	•	•	CIE Lab	•	•	~250 key	•		

Abbreviations:

Target medium: N-Ph (non-photos); Ph (photos).

Color range: key (key colors).

Properties: CC (color consistency); CE (contrast enhancement); NM (naturalness maintenance).

natural-compliant. That is, their focus is on ensuring the contrast between confusing colors.

2.6 Critical Analysis and Trends for the Future

Looking back to the recoloring methods described above, it is noticeable that only those designed for trichromat people preserve the perceptual learning of CVD people, because they, in general, satisfy the perceptual requirements of color contrast, color consistency, and color naturalness simultaneously.

However, these recoloring methods work in a pixelwise manner, without considering any semantics about the contents of the input image. We can even say that we are using blind methods for colorblind people. In fact, often regions featuring objects in the image do not need to be subject to recoloring at all. Note that the pixelwise nature of most recoloring methods makes contrast and naturalness conflicting requirements.

To solve this paradox in the future, we need to incorporate semantics into recoloring methods. Yet, in the literature, there already are some trends that point to this direction of semantic recoloring methods. Among them, we find the following:

- *Pattern pinning.* A way of mitigating or even eliminating confusion in the perception of color is pinning text or geometric patterns to pixels. See, for example, [90] and [91] for further details. The disadvantage of this technique is that it provokes visual noise to CVD people.

- *Selective contour enhancement.* A couple of methods are already capable of selecting confusing objects in a given image, enhancing then their contours without changing their interiors. See, for example, [92] and [93] for further details. The advantage of this technique is the improvement of the contrast (e.g., using image filters) without penalizing the color consistency and naturalness.

Let us also mention that there is also an unexplored research direction that has to do with the semantic extraction of objects from images to identify those that actually need to be subject to color adaptation. This means that we need to move from the pixel-wise to the object-wise paradigm. The advances in the *concept detection* area (see, for example, Huiskes et al. [94]) and other areas related with the extraction of semantic from images are quite promising in the CVD adaptation.

2.7 Conclusions

In the last two decades, a significant number of recoloring algorithms for CVD people have been proposed in the literature, mostly focused on still images, although there are also works whose target is other type of media (e.g., text, video, HTML documents, and so forth).

We have shown that recoloring methods must satisfy three perceptual requirements (i.e., contrast enhancement, color consistency, and color naturalness) to not disturb that much the perceptual learning of CVD people. In fact, preserving the perceptual learning is the most important to take into consideration when a recoloring method is put forward. In our opinion, this the most important contribution of the study carried out in this survey.

Chapter 3

ShrinkInverse: Creating Accessibility to Web Contents for Colorblind People

This chapter describes a recoloring algorithm that was designed and implemented to improve the color accessibility of dichromat people in the web context. It was published as a conference paper in Proceedings of the 5th International Conference on Applied Human Factors and Ergonomics (AHFE'2014), Kraków, Poland, Vol. 10, pp. 646-656, AHFE International, 2014.

3.1 Introduction

The color is an important asset when comes the time of interacting with other people and the ambient world, where the color may turn into the message itself. As known, about 5% of the people all over the world suffer from colorblindness, also formally called color vision deficit (CVD). It is clear that this visual impairment compromises the way those people see and interpret their surroundings and the visual messages they receive continuously. This is particularly relevant not only for those who need to interpret the traffic lights correctly –and recall that color blind because people see reds and greens in the same way– but also for those who use the web for leisure and professional purposes daily. With this critical problem in mind, this chapter proposes a new algorithm to adjust those colors that shed confusion on dichromat people (deuteranopes and protanopes). This algorithm takes advantage of a simple formula that operates on the HSV color space. The implementation of the algorithm was made by using web compliant languages, which confirm the appliance viability on the web, which contributes to achieving a more inclusive visual communication. The final goal is the integration of the system with the ability to perform the recoloring images and text blocks automatically, providing a better accessibility to the web pages to the CVD people, so reaching a more ergonomic design.

3.2 Background

3.2.1 RGB Color Model

The RGB color space is a cube whose axes are defined by the primary colors: red (R), green (G) and blue (B) (see Fig. 3.1(a)). In the display devices, the value of the parameters R, G, and B varies between 0 and 255. So, the represented colors are achieved by mixing different amounts of the primaries, concerning $(R, G, B) = (0, 0, 0)$ to the black color and $(R, G, B) = (255, 255, 255)$ to the white color. The other colors are obtained by specifying amount of R, G, and B, all of them in the domain $[0, 255]$. So, this means that the RGB color space is the

cube $[0, 255] \times [0, 255] \times [0, 255]$. The main disadvantage of the RGB model is that it is not intuitive enough when we intend to change the color of some element existing in an image. For example, it is not straightforward to change a saturated yellow to a lighter yellow. This lack of intuitiveness of the RGB color model originated the appearance of the called “phenomenal color spaces” [52], namely: HSL (hue, saturation, luminosity), HSV (hue, saturation, value) and the HSI (hue, saturation, intensity). These models were developed from the Munsell Color System [95], which is close to how human beings perceive colors intuitively, being each of them the result of a linear transformation of the RGB color space.

3.2.2 HSV Color Model

The HSV color space is a cone (see Fig. 3.1(b)), which can be obtained using a linear transformation of the RGB color space. Taking into account that it is a phenomenal color space, we can define colors in an intuitive manner than in RGB [96] color space. Examples of hues (H) are greens, yellows, and blues. The vividness of a color increases with its saturation (S), which varies from the less saturated hues to the most saturated hues. The value (V) has to do with the lightness or darkness of a color.

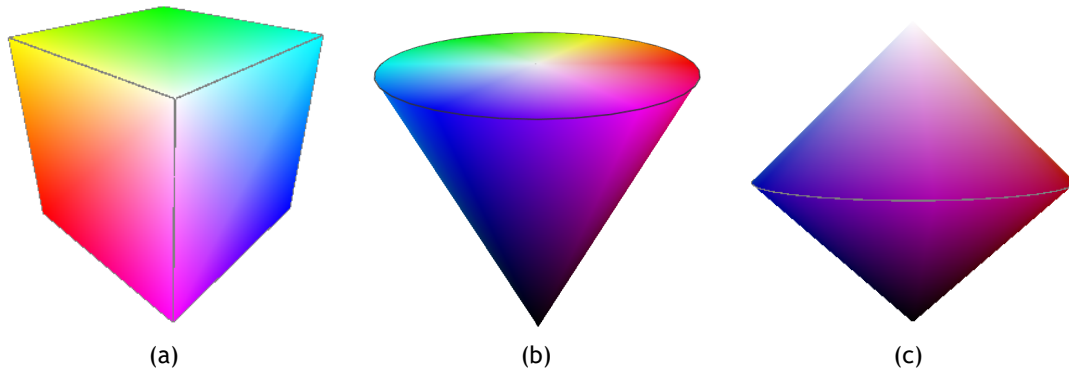


Figure 3.1: Color space models: (a) RGB; (b) HSV; c) HSL.

3.2.3 HSL Color Model

Similar to the HSV color space, every color is represented as a triplet (H, S, L) , where $H \in [0^\circ, 360^\circ]$, $S \in [0, 1]$ and $L \in [0, 1]$. However, unlike HSV, the HSL color space attains the chromatic maximum at the midpoint of the grayscale $L = 1/2$, not when $L = 1$. As a consequence, the HSL color space is a double cone with coincident bases (see Fig. 3.1(c)), so the white color is at the first apex and the black color is at the second apex. Note that there is another color space, called HSI, which is congruent with the HSL color space [97], but they are obtained from RGB using distinct linear transformations.

3.3 The ShrinkInverse Algorithm

The ShrinkInverse algorithm has been designed for the major two families of dichromats, that is, deuteranopes and protanopes, mainly because of the following:

- deuteranopia and protanopia are the most common visual impairments in dichromats;
- unlike tritanopes, deuteranopes and protanopes see colors in a very similar way;
- the dichromacy is quite disabling.

ShrinkInverse algorithm proposed in this chapter makes use of the HSV color space to carry out the recoloring procedure. So, firstly, the color of the pixel is converted from RGB to HSV. Then, too dark colors (light less than 20%) and little-saturated colors (less than 30%) become darker. As a consequence, we end up getting more contrast in the recolored image because the remaining colors (i.e. whose hues are in the interval $[50^\circ, 160^\circ]$) in the original image are not changed in the recolored image. These unchanged colors are the yellows and greens. The yellows are seen correctly, and the greens are seen in a more faint, but without too much away from its original green (as seen by a trichromat).

The colors which hues are not in the interval $[50^\circ, 160^\circ]$ are mapped as follows:

1. To map the interval $[160^\circ, 410^\circ]$ into the interval $[160^\circ, 300^\circ]$;
2. To invert the hues, by symmetry, relative to the center of the interval.

The first step is performed so that the colors closer to 160° become more compact than the ones near 410° . The compression factor starts at the value 0.2 and is gradually increased until to reach the value 0.35. Consequently, the blues becomes more compact than reds, because reds include pinks, magentas, reds, and oranges, that is, the reds have more color diversity, which leads to the need for more differentiation. To strike on such differentiation between the colors in the gamut of reds (pinks, magentas, reds, and oranges), we need the second step listed above, which performs an inversion of the distribution of the hues in the new target hue interval $[160^\circ, 300^\circ]$.

After the first step, the blues are distributed from 160° onwards, then appears the mapped violets, magentas, reds and, at last, the oranges near 300° . However, the deuteranopes and protanopes perceives much better the differentiation in hues in $[160^\circ, 240^\circ]$ than in $[240^\circ, 300^\circ]$. So, by inverting the position of the mapped hues, the discrimination between the reddish colors is improved. Besides, the colors near 300° are seen (by dichromat people) as strong blues, while the blues are seen more lightly.

This recoloring is applied not only to colors like pinks, magentas, reds, and oranges (i.e. colors that are normally mistaken by greens) but also to blues. This is achieved by compressing the blues into a sub-interval of the interval of blues, leaving the remaining sub-interval of blues to mapping reds (i.e. pinks, magentas, reds, and oranges).

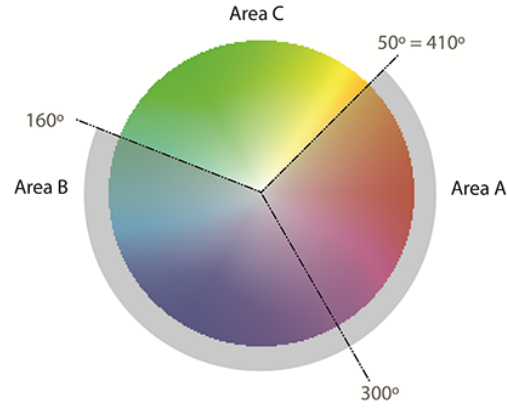


Figure 3.2: The first step of the ShrinkInverse recoloring algorithm: Area A concerns the interval of colors that are shrunk and pushed to the right sub-interval of Area B; the original colors of Area B are shrunk and pushed to its left sub-interval; the colors in the interval of Area C remain unchanged.

The recoloring is done by only re-mapping the hue (H) for some colors and the value (V) for other colors; the saturation (S) remains always unchanged. That is, we end up having the following trivariate recoloring functions:

$$H' = \rho(H), \quad S' = S, \quad \text{and} \quad V' = \mu(V) \quad (3.1)$$

The hue remapping function $\rho(H)$ is as follows:

$$\rho(H) = \begin{cases} \varphi(\beta(H)) & \text{if } H \in [160^\circ, 410^\circ \equiv 50^\circ] \\ & \text{if } H \in [50^\circ, 160^\circ] \end{cases} \quad (3.2)$$

where

$$\beta(H) = 160 + 0.2 \cdot H + 0.1415 \cdot \frac{|160 - H|}{250} \cdot H \quad (3.3)$$

and

$$\varphi(H) = \begin{cases} 230 - |H - 230| & \text{if } H \geq 230 \\ 230 + |H - 230| & \text{if } H \leq 230 \end{cases} \quad (3.4)$$

The value of value (V) is changed through the function $\mu(H)$, expressed by Eq. 3.5.

$$\mu(H) = \begin{cases} 0.5 \cdot V & \text{if } (V < 50) \vee (S < 30) \\ V & \text{if } (V \geq 50) \wedge (S \geq 30) \end{cases} \quad (3.5)$$

ALGORITHM 1: ShrinkInverse

Input: pixel (R, G, B) .

Output: pixel (R', G', B') .

```
1 Convert  $(R, G, B)$  to  $(H, S, V)$ ; if  $(V < 50)$  or  $(S < 30)$  then
2   |  $V \leftarrow 0.5 \cdot V$ ;
3 end
4 else
5   | if  $H \leq 50$  then
6     |  $H \leftarrow H + 360$ ;
7   end
8   | if  $H \in [160, 410]$  then
9     |  $H \leftarrow H + 0.2 \cdot H + 0.1415 \cdot (|160 - H|/250) \cdot H$ ;
10    | if  $H < 232$  then
11      |  $H \leftarrow 230 + |H - 232|$ ;
12    end
13    else
14      |  $H \leftarrow 230 - |H - 232|$ ;
15    end
16  end
17 end
18 Convert  $(H, S, V)$  to  $(R', G', B')$ ;
```

ALGORITHM 2: Image recoloring algorithm

Input: *image*: the image to adapt.

Input: *width*: the image width.

Input: *height*: the image height.

```
1 for  $i=0$  to  $width-1$  do
2   | for  $j=0$  to  $height-1$  do
3     | ShrinkInverse( $image[i][j].R, image[i][j].G, image[i][j].B$ );
4   end
5 end
```

The hue remapping function of Eq. 3.2 works as inversion operation after a shrink process for the angular interval $[160^\circ, 410^\circ]$. The shrink process is performed by Eq. 3.3, and the inversion operation is done by Eq. 3.4.

3.4 The Recoloring Algorithm

The recoloring algorithm here proposed is based on two operations: *shrink* and *inversion*; hence, the term “ShrinkInverse” used to name our algorithm. The shrink is expressed in line 10 of Alg. 1, while the inversion of hues performed by the symmetry relative to 230° (cf. lines 12 and 14 of Alg. 1). Alg. 2 iterates on all pixels of an image, calling then Alg. 1 to remap every single pixel color. To remap the hue, one needs to convert previously (R, G, B) values to their corresponding (H, S, V) values, and vice-versa (cf. lines 1 and 13 of Alg. 1).

3.5 Experimental Results

3.5.1 Setup

Regarding hardware and software, all experiments and testing were carried out using a laptop with an Intel Core 2 Quad CPU Q9550 of 4G RAM, equipped with the 64-bit Microsoft Windows operating system. The algorithm was implemented in Javascript programming language, to run in HTML5 compliant web browsers.

In particular, the ShrinkInverse algorithm has been designed and implemented for deuteranope and protanope people. As argued above, this was so because deuteranopia and protanopia are not only the most frequent cases of dichromacy but also because they see all the colors similarly. It is also worth noting that our experiments and testing have focused only on still images.

3.5.2 Comparative Analysis

To compare our algorithm with others in the literature, we found reasonable only compare it with those two due to laccarino et al. [76] and Ching-Sabudin [19] for the following reasons:

- They apply to deuteranope and protanope people;
- They use a phenomenal color space to remap hues;
- They are the two most recent recoloring algorithms built upon a phenomenal color space.

3.5.3 Time Performance

In addition to the ShrinkInverse algorithm, we also implemented those algorithms due to laccarino et al. [76] and Ching-Sabudin [19] within the setup described above. We have used a dataset of about one hundred 250×180 and 580×434 images to measure the average times taken those three algorithms, as shown in Table 3.1. As shown, our algorithm is approximately 30% slower than the Ching-Sabudin algorithm, but 30% faster than the algorithm due to laccarino and colleagues. In a way, this is so because ShrinkInverse does not perform any pre-processing step as happens in laccarino et al. algorithm to calculate the number of “red pixels” and “green pixels” of each image, before starting the recoloring procedure itself. The algorithm due to Ching-Sabudin is faster because pixels whose colors own a red value greater than green and blue values are not subject to RGB-to-HSV conversion, and vice-versa. Specifically, about one-third of the total of pixels are not RGB-to-HSV converted.

3.5.4 Comparative Recoloring

Before proceeding any further, let us say that we also had to implement the simulation algorithms proposed Brettel et al. [70]. This is a very important requirement to realize how deuteranopes and protanopes see colors in images. This understanding of how deuteranopes

Table 3.1: Average time spent by the image recoloring algorithms.

Algorithm	250 x 180 images	580 x 434 images
laccarino et al.	0.136 sec.	0.823 sec.
Ching-Sabudin	0.076 sec.	0.387 sec.
ShrinkInverse	0.110 sec.	0.611 sec.

and protanopes see colors also led us to use images with high chromatic diversity, like those shown in Fig. 3.3, during our experiments and testing.

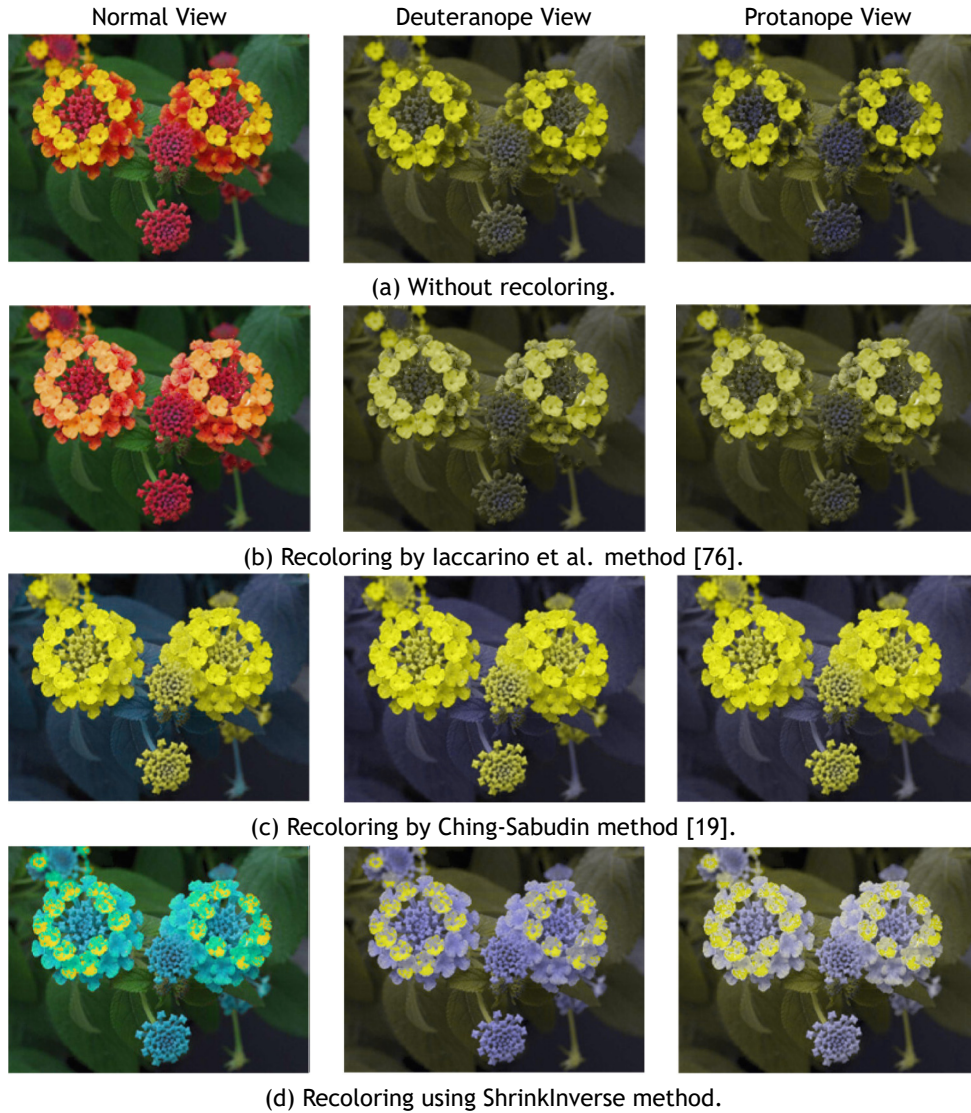


Figure 3.3: Lantana flowers recolored by laccarino et al. [76], Ching-Sabudin [19] and ShrinkInverse methods.

As known, deuteranopes and protanopes see yellows and blues in a correct manner and the greens in a weak way. This is illustrated in Fig. 3.3(a) and means that these colors must remain unchanged after the recoloring a given image, yet deuteranopes and protanopes see greens with less saturation and lightness. Note that these dichromats do mistake reddish colors, including pinks and oranges, with greenish colors.



Figure 3.4: Strawberries recolored by laccarino et al. [76], Ching-Sabudin [19] and ShrinkInverse methods.

Fig. 3.3(b) depicts the images recolored by the algorithm due to laccarino et al. [76]. As observed, in respect to deuteranopes and protanopes, this recoloring technique does not enhance that much the chromatic diversity of recolored images relative to images without recoloring, as can be observed by comparing Fig. 3.3(a) and (b).

Fig. 3.3(c) shows images recolored by the Ching-Sabudin algorithm [19]. Unlike laccarino et al. [76], this algorithm retains the vivid yellows, but the images recolored in this manner look too yellowish and the details cannot be distinguished very well, since the reddish colors were mapped to yellows, and yellows are confined to a small range of colors (i.e. low color diversity). Besides, most greens are now mapped to blues, what implies that deuteranopes and protanopes can no longer see greens, which is a color that they see, although in faint or less saturated manner.

Visual results produced by the ShrinkInverse algorithm are shown in Fig. 3.3(d). Although the

original image has no blue, we can guarantee that this color remains unchanged as well the yellows and greens. Taking into consideration that deuteranope and protanope people are red-green dichromats, our algorithm maps reds to a sub-interval of the range of blues. As observed in Figs. 3.3 and 3.4, the flowers and the strawberries as seen by deuteranopes and protanopes seem to have an enhanced visual appearance. It is noticeable the improvement in the discrimination of the details of the images. As a margin note, the images of flowers shown in Fig. 3.3 and the images of strawberries depicted in Fig. 3.4 were produced within an HTML5-compliant browser.

3.6 Further Remarks

We have described a recoloring algorithm, called *ShrinkInverse*, to improve the color perception of deuteranope and protanope people on still images. The main concern in the design and development of this algorithm was to improve the contrast in recolored images. However, it is clear that the color naturalness is not preserved at all; for example, looking at Fig. 3.4, we observe that red strawberries are seen as a light blue, which is opposed to the perceptual learning of colorblind people. Even so, it is color consistent, because colors are always mapped in the same manner. Thus, this shows us how difficult it is to design a recoloring algorithm for the colorblind, simply because it is necessary to combine the clashing parameters of naturalness, consistency, and contrast to maintain the perceptual learning untouchable as much as possible.

Chapter 4

RGBeat: A Recoloring Algorithm for Deutan and Protan Dichromats

This chapter describes a new recoloring algorithm that was designed for dichromat people, here called RGBeat. Unlike most recoloring algorithms, RGBeat preserves color naturalness, contrast, and consistency. See Chapter 2 for further details about these three important parameters. Furthermore, it maps colors from RGB to RGB directly, although this RGB-RGB mapping has been accomplished with the help of the RGB-HSV and HSV-RGB mappings. It was submitted to IEEE Transactions on Visualization and Computer Graphics and is currently under revision.

4.1 Introduction

It is widely accepted that people with deutan and protan dichromats only see blues and yellows so that they cannot distinguish reds from greens very well. In fact, we will see that deutan and protan dichromats only see exactly two hues in the HSV color space, 240-blue (240°) and 60-yellow (60°). Thus, their color space is limited to a color triangle that cuts off the HSV color cone into two identical parts. With this in mind, we propose here a novel recoloring algorithm for deutan and protan dichromats to enhance their color perception, particularly in HTML5-compliant web environments. This is accomplished by enhancing color contrast of text and imaging in web pages, while keeping the naturalness of color as much as possible. Also, as far as we know, this is the first web recoloring approach for dichromat people that takes into consideration both text and image recoloring in an integrated manner. Moreover, it is also one of the first color adaptation methods that increase the visual perception of deutan and protan dichromats relative to original images.

4.2 Recoloring Algorithm

Our recoloring algorithm was designed for deuteranopia and protanopia, simply because they are the most common types of dichromacy, and their color perception is quite similar.

4.2.1 Leading Idea

As shown further ahead, deutan or protan dichromats only perceive two hues, yellow (60°) and blue (240°), yet with more or less luminance and saturation, as illustrated in Fig. 4.1. These people see greens as yellows, but they are perceived as unsaturated greens, i.e., greens are

perceived faintly. On the other hand, reds are seen as dark unsaturated yellows. As a consequence, deutan and protan dichromats confuse reddish and greenish colors, though they can distinguish some reds from greens, which stems from their color perceptual learning throughout life.

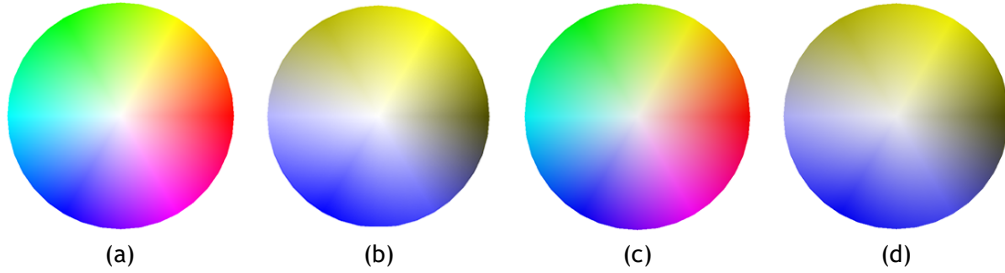


Figure 4.1: HSV cone sections: (a) a section with $value = 100\%$, as seen by trichromat people; (b) a section with $value = 100\%$, as seen by deuteranope people; (c) a section with $value = 75\%$, as seen by trichromat people; and (d) a section with $value = 75\%$, as seen by deuteranope people. Deuteranope simulation based on Vienot et al.'s algorithm [2].

Thus, the leading idea of our algorithm is to reduce the confusion between reds and greens, even more, so that only reds will be subject to a recoloring procedure. For that purpose, as explained in the previous section, it is crucial to preserve the color perceptual consistency, and to slightly increase the color contrast for reds to preserve the color naturalness as much as possible.

4.2.2 HSV Color Domain of Deuteranopy and Protanopy

In comparison to the color range seen by trichromat people, the range of colors seen by deutan or protan dichromats is quite limited. This turns up more evident when we consider HSV colors, as illustrated in Fig. 4.2. The HSV color space is a cone such that $H \in [0^\circ, 360^\circ[$ stands for the hues (or color wheel), $S \in [0, 100]$ denotes the saturation range, which increases from and perpendicular to cone axis, and $V \in [0, 255]$ the brightness values, which increases from the apex to base of the cone [96]. In Fig. 4.2(a), we have the entire cone of colors seen by trichromat people, while the colors seen by deutan and protan dichromats are mapped onto colors in the $60^\circ/240^\circ$ plane, which cuts the cone into two parts (cf. Fig. 4.2(b)).

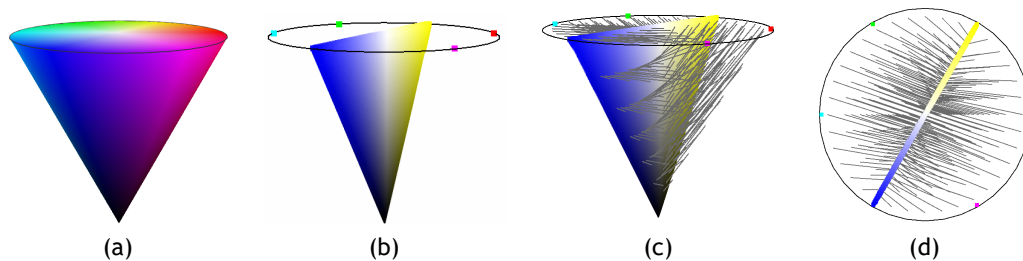


Figure 4.2: The HSV color space when seen by: (a) trichromat people; (b) deuteranope people (deuteranope half planes); (c) and (d) deuteranope people, with the color projection lines, joining colors seen by trichromat and deuteranope people, being (c) a lateral view and (d) the top view. Deuteranope simulation based on Vienot et al.'s algorithm [2].

Roughly speaking, the deutan or protan dichromats only see yellows and blues. But, contrary

to the widespread idea that such blues and yellows include multiple hues, we can say that they only see the yellow hue of 60° and the blue hue of 240° , with the saturation increasing outwards the cone axis, and the value (or brightness) increasing from cone apex to its base. This has been confirmed by our experiments, using the simulation algorithm due to Vienot et al.'s algorithm [2], converting then the color to the HVS color space [98]. In fact, by varying R , G and B in the range $[0, 255]$, and converting RGB to $\text{RGB}_{\text{deuteranope}}$ (i.e., the deuteranope simulation through the method proposed by Vienot et al. [2]), and then $\text{RGB}_{\text{deuteranope}}$ to HSV, we constructed the deuteranope color gamut in the HSV color space. This deuteranope color gamut reduces to two coplanar triangles, which can be seen as resulting from the intersection between a plane and the HSV cone (see Fig. 4.2). Note that a similar planar color gamut for deuteranope people has been obtained for LMS color space [70] and CIE XYZ color space [99].

As shown in Fig. 4.2(c), the visual system of a deutan dichromat transforms the conical HVS color space (Fig. 4.2(a)) into a triangular color space (Fig. 4.2(b)), which amounts to project each hue of the HSV cone into a triangle that belongs to the plane defined by the apex, 60° -hue point and 240° -hue point. As illustrated in Fig. 4.2, such color projection entails a change of saturation and brightness (usually a loss). It is clear that colors projected onto the yellow part of the triangle $]150^\circ, 330^\circ[$ noticeably loses value (brightness), while colors projected onto the blue part tend to keep value (brightness) unchanged. With regard to saturation, no major changes occur (see Fig. 4.2(d)). When there is a change, the saturation may increase or decrease (although slightly). The behavior of the protan dichromat's projection is similar, though shades are slightly different.

4.2.3 Recoloring Procedure

A brief glance at Fig. 4.1 shows us that deutan or protan dichromats tend to see reds as dark unsaturated greens, so that a pure red is seen as dark green, not to say black. As shown in Fig. 4.2, greens, and reds are often seen in a similar way by deutan or protan dichromats; hence, their well-known confusion between reds and greens, also known as colorblindness. With this problem in mind, we took the decision of not changing the saturation $S \in [0, 100]$, neither the brightness (value) $V \in [0, 255]$ in the HSV model; only hues were changed as follows:

- Hues in the range $]0^\circ, 60^\circ[$ (range of reds and oranges) are squeezed into the range $]30^\circ, 60^\circ[$.
- Hues in the range $]300^\circ, 360^\circ[$ (range of reds, pinks, and magentas) are squeezed into the range $]300^\circ, 330^\circ[$.

The remaining hues in the range $[60^\circ, 300^\circ]$ remain unchanged. This way, those deutan or protan dichromats end up having less dark hues (yellows and blues) in the range of reds (for trichromats). This ensures that the requirements of consistency and naturalness of colors are fulfilled. But, despite the soundness of this recoloring approach, we can ask ourselves about its actual help for colorblind. Indeed, it is convenient here to recall that:

- Reducing the hue range seems to us a good decision because what we are just eliminating is the subrange of confusing hues, i.e., the reds in this case. For example, looking at Figs. 4.3 and 4.4, we see that a deutan cannot distinguish a green flower from a red flower, but with

our recoloring technique, deuterans can distinguish them very easily. In short, the question is not reducing the hue range, but cutting off the subrange of reds, after mapping reds to close hues as much as possible. The purpose is thus to be able to discriminate confusing hues.

- Mapping hues must be done reducing the impact on the perceptual learning of the deuterans as much as possible, i.e., without affecting the naturalness of the color that much. So, it makes sense to remap hues according to our technique, which keeps the color consistency while increases the contrast.

Before proceeding any further, let us recall that the hue compression of $]0^\circ, 60^\circ[$ into $]30^\circ, 60^\circ[$ corresponds to the following linear interpolation formula of equation 4.1.

$$H' = 30 + \frac{1}{2} \cdot H \quad (4.1)$$

The hue compression of $]300^\circ, 360^\circ[$ into $]300^\circ, 330^\circ[$ is given by equation 4.2.

$$H'' = 300 + \frac{1}{2} \cdot (H - 300) \quad (4.2)$$

4.2.3.1 Mapping hues from $]0^\circ, 60^\circ[$ into $]30^\circ, 60^\circ[$

Let us consider the color (R, G, B) , with $R, G, B \in [0, 255]$, with the corresponding normalized color (r, g, b) given by equation 4.3.

$$r = R/255 \quad g = G/255 \quad b = B/255 \quad (4.3)$$

Let us also assume that the values of S and V remain unchanged. We know that by only changing the value of H in the range $]0^\circ, 60^\circ[$, we only change the value of G in the RGB color space. Indeed, considering $H \in]0^\circ, 60^\circ[$, the HSV-RGB conversion formula due to Smith [98] sets that

$$R = V \quad G = V(1 - S(1 - 6H)) \quad B = V(1 - S) \quad (4.4)$$

Since we stated that S and V remain unchanged in the HSV model, we conclude that G is the only RGB parameter that changes as a consequence of changing the parameter H in the HSV color space.

In these circumstances, we have $R = \max(R, B, G)$, $B = \min(R, B, G)$, and $G \in [B, R]$, being these equalities also valid for the (normalized) rgb colors. In other words, the values of R and B (resp., r and b) remain unchanged for $H \in]0^\circ, 60^\circ[$.

ALGORITHM 3: MappingColor

Input: R, G, B .

Output: R, G, B .

```
1 if ( $R > G$ ) AND ( $R > B$ ) then
2   if ( $G > B$ ) then
3      $G \leftarrow 0.5 \cdot (R + G)$ ;
4   end
5   else
6      $B \leftarrow 0.5 \cdot (R + B)$ ;
7   end
8 end
```

Now, recalling the RGB-HSV conversion formula due to Smith [98], and considering $]0^\circ, 60^\circ[$ the domain of H , we get

$$H = 60 \cdot \left(\frac{g - b}{r - b} \right) \quad (4.5)$$

But, we know that varying H in $]0^\circ, 60^\circ[$ only provokes changes in the value of g . So, replacing the value of H given by Eq. (4.5) into Eq. (4.1), we have

$$60 \cdot \left(\frac{g' - b}{r - b} \right) = 30 + \frac{60 \cdot \left(\frac{g - b}{r - b} \right)}{2} \quad (4.6)$$

or, equivalently,

$$g' = \frac{r + g}{2} \quad (4.7)$$

The novelty about the hue mapping from $]0^\circ, 60^\circ[$ into $]30^\circ, 60^\circ[$ translates itself into a color mapping in the RGB color space given by Eq. (4.7). That is, there is no need to convert from RGB into HSV and vice-versa. In short, we have only to remap the rgb reddish colors in conformity with Eq. (4.7), since $r' = r$ and $b' = b$.

4.2.3.2 Mapping hues from $]300^\circ, 360^\circ[$ into $]300^\circ, 330^\circ[$

Once again, let us also assume that the values of S and V remain unchanged. By only changing the value of $H \in]300^\circ, 360^\circ]$, we end up only change the value of B in the RGB color space. Accordingly, we have $R = \max(R, B, G)$, $G = \min(R, B, G)$, and $B \in [G, R]$, and the same applies to (normalized) RGB colors. Therefore, the values of R and G (resp., r and g) remain unchanged for $H \in [300^\circ, 360^\circ]$.

Now, taking into the account that the RGB-HSV conversion formula due to [98], with $H \in [0^\circ, 360^\circ[$, we get

$$H = 60 \cdot \left(\frac{g - b}{r - g} \right) + 360 \quad (4.8)$$

But, we know that varying $H \in [300^\circ, 360^\circ]$ only provokes changes in the value of B . So, replacing the value of H given by Eq. (4.8) into Eq. (4.2), we have

$$60 \cdot \left(\frac{g - b'}{r - g} \right) + 360 = 300 + \frac{(60 \cdot \left(\frac{g - b}{r - g} \right) + 360) - 300}{2} \quad (4.9)$$

or, equivalently,

$$b' = \frac{r + b}{2} \quad (4.10)$$

In short, the recoloring procedure based on Eqs. (4.7) and (4.10) translates itself into a color remapping in the RGB color space, as shown in Alg. 3, not being necessary to make the RGB-HSV conversion, and vice-versa, explicitly. It is clear that this simplification constitutes an enormous gain in processing time.

4.2.3.3 Changes in Perceived Chroma and Luminance

The algorithm relies on –though it does not explicitly use– the HSV color space. It maintains each color's saturation S and value V during recoloring. However, this does not mean that perceived chroma and perceived luminance hold. In fact, as explained below, maintaining S and/or V in HSV space during recoloring does not maintain the perceived chroma nor perceived luminance of the color.

In respect to perceived chroma, its change is a result of changing the hues to close hues according to Eqs. (4.1) and (4.2); for example, an orange is mapped to a yellowish orange. Recall that we tried to reduce the color mapping to a minimum to not provoke significant perceived changes in the perceptual learning of deutan and protan dichromats.

As regards to changing the perceived luminance, it is not so obvious because the values of S and V remain unchanged. According to Poynton [100], the perceived luminance is given by equation 4.11.

$$L = 0.299 \cdot R + 0.587 \cdot G + 0.114 \cdot B \quad (4.11)$$

so that, taking also into consideration Eq. (4.4), one concludes that changes in G provoke changes in L ; the values of R and B remain unchanged because the values of S and V do not change in the recoloring procedure. Thus, increasing the value of G results in an increase in the value of L ; as a consequence, the contrast also increases, eliminating the confusion between reds and greens.

ALGORITHM 4: TextRecoloring

Input: *HTMLdocument*.

```
1 css[] = style sheets of HTMLdocument;
2 n = number of style sheets in css[] ;
3 for i=1 to n do
4   css[i] = i-th style sheet;
5   m = number of CSS rules of css[i];
6   for j=1 to m do
7     cssrule[j] = j-th CSS rule;
8     if cssrule.color then
9       [R,G,B] = cssrule.color;
10      cssrule.color = MappingColor([R,G,B]);
11    end
12    if cssrule.backgroundColor then
13      [R,G,B] = cssrule.backgroundColor;
14      cssrule.backgroundColor = MappingColor([R,G,B]);
15    end
16  end
17 end
```

ALGORITHM 5: ImageRecoloring

Input: *Image*, *width*, *height*.

```
1 for i=0 to width-1 do
2   for j=0 to height-1 do
3     R ← Image[i][j].R;
4     G ← Image[i][j].G;
5     B ← Image[i][j].B;
6     MappingColor(R, G, B);
7     Image[i][j].R ← R;
8     Image[i][j].G ← G;
9     Image[i][j].B ← B;
10  end
11 end
```

4.3 Text Recoloring Algorithm for HTML Documents

Alg. 4 was designed for recoloring text in HTML documents, which involve three major procedures, namely:

1. Accessing to all cascading style sheets (CSSs) associated to such web page, and to all CSS rules associated to each style sheet.
2. Recoloring each text block by changing its corresponding CSS rules, whenever necessary. This is done by changing the `color` and `background-color` properties associated to each CSS rule.
3. Render the HTML web page with the modified CSS rules, which is an automatic process provided by any web browser.

Note that Alg. 3 applies to images, but it is also used in Alg. 4 to change both text and background. To dynamically access and update the content, structure, and style of an HTML doc-

ALGORITHM 6: RecoloringDocumentImages

Input: *HTMLdoc*.

```
1 Images ← retrieve set of images associated to HTMLdoc;  
2 n = number of images in Images[] ;  
3 for i=0 to n-1 do  
4   width ← Images[i].width;  
5   height ← Images[i]. height;  
6   RecoloringImage(Images[i],width,height);  
7 end
```

ument, we use the HTML Document Object Model (DOM) as the programming interface for Javascript. In fact, tasks like accessing to each style sheet, each rule defined in a style sheet, each value of the rule properties, as well as determining the number of style sheets associated with an HTML document, and the number of rules defined in each style sheet, are all done using DOM object methods.

Thus, the recoloring of text blocks of a web page is done by changing the CSS rule objects associated with text blocks of an HTML document. This recoloring procedure operates on the CSS rules instead of being on the text blocks themselves. The recoloring procedure of all text blocks of a HTML document is described in Alg. 4. Recall that a HTML document usually is tied to a set of CSSs, so that we need to retrieve this set of CSSs using the Javascript statement `var css = document.styleSheets;` (cf. line 1 in Alg. 4).

Each style sheet consists of a set of CSS style rules; hence the two ‘for’ loops in Alg. 4. The procedure `MappingColor` (i.e., Alg. 3) is called at the end of each iteration of the inner ‘for’ loop to change the CSS style rule whenever is appropriate, that is, when the `color` and `background-color` properties are specified by the CSS style rule.

4.4 Image Recoloring Algorithm for HTML Documents

Recoloring a single $M \times N$ image is described in Alg. 5. This algorithm calls the `MappingColor` algorithm (cf. Alg. 3) for every single pixel of the image. It is clear that Alg. 5 can be applied to all images associated with a given web page, as described in Alg. 6.

Recoloring starts with the retrieval of images from the HTML document (cf. line 1 in Alg. 6). The recoloring takes place in the line 6, where one calls the procedure `RecoloringImage` (i.e., Alg. 5), which in turn, calls the the procedure `MappingColor` (i.e., Alg. 3) to adapt the color of each individual pixel. This is the same procedure applied to adapt the color of text and backgrounds, from the CSS style sheet rules. Note that the HTML5 specification provides a 2D context (or even a 3D context, when necessary) for a canvas in such a way that an image can be organized pixel-wise.

4.5 Results

As argued above, our recoloring algorithm (Alg. 3) was designed for deutan and protan dichromat people, because they are the most common dichromat people, and because they see colors in a similar manner. Our algorithm applies to text, still images, and video, no matter whether they are in web pages or not.

4.5.1 Setup

Before proceeding any further, let us say that all experimental results were obtained using a laptop equipped with a 32-bit Microsoft Windows operating system running on an Intel Pentium Dual CPU T2330 1.60GHz, with 3G RAM. Besides, the algorithms described in this chapter were coded in Javascript programming language for HTML5 web browsers, in particular for Chrome.

4.5.2 Methodology

To compare our algorithm with others found in the literature, we selected the ones due to Iaccarino et al. [76] and Ching-Sabudin [19], because they share some features, namely:

- They are dedicated to deuteranopia and protanopia.
- They use a phenomenal color space. Recall that “A phenomenal color space is a color space which uses as classifying descriptors hue, saturation, and brightness.” [101]. In fact, HSV, HSI and HSL are all phenomenal color spaces [96] [52].
- They likely are some of the fastest color mapping methods based on phenomenal color spaces.
- Iaccarino et al.’s method [76] tends to preserve color naturalness, at the cost of not reinforcing too much contrast. On the other hand, Ching-Sabudin [19] reinforces the contrast, but not preserves color naturalness.

We also implemented the algorithms proposed by Vienot et al. [2] that simulate how deuteranope and protanope people see the colors (see Fig. 4.3(b) to (d)). Also, we have carried out two sorts of evaluation of the methods: qualitative and quantitative. The qualitative evaluation is visual and subjective, in the attempt of grasping which is the more suited method in recoloring process. The quantitative evaluation is objective because it is based on mathematical metrics or formulas, and works here as a way of confirming our subjective, visual evaluation.

4.5.3 Qualitative Evaluation

As known, deuteranope and protanope individuals only see some yellows and blues, with variable saturation and brightness. Thus, yellows and blues must remain unchanged after the recoloring a given image. Interestingly, greens look unsaturated greens, but, in fact, they are little-saturated

yellows. As shown in Fig. 4.3, the three algorithms leave the yellows unchanged somehow; the same applies to blues, as illustrated in Fig. 4.4. Note that the original image in Fig. 4.4 exhibits the primary colors: red, green, and blue.

The differences between those three algorithms become noticeable when one has to re-coloring colors that people with dichromacy perceive as similar, the so-called confusing colors. The main problem is that deuteranope and protanope people mistake reddish colors (including pinks and oranges) with greenish colors, as shown in Figs. 4.3-4.4.

4.5.3.1 Iaccarino et al.'s

As shown in Figs. 4.3 and 4.4, Iaccarino et al.'s recoloring technique [76] does not produce a significant improvement relative to the original images, when seen by deuteranope or protanope people, though the yellows seem even less vivid.

4.5.3.2 Ching-Sabudin's

On the other hand, Ching-Sabudin's technique [19] maps reds into yellows (Figs. 4.3-4.4), what results in loss of contrast between reds and yellows, i.e., between a primary color and a secondary color. Even worse it is the fact that greens are mapped into weak blues so that deuteranope and protanope people can no longer see greens (yet in the form of little-saturated yellows).

4.5.3.3 RGBeat

Our recoloring technique preserves the colors correctly seen by people with deuteranopia and protanopia, i.e., yellows and blues. Reds concerning hues (via RGB-HSV conversion) greater than zero (i.e., those reds more close to oranges and yellows) are mapped to darkish yellows, while reds concerning hues less than 360 (i.e., reds close to pinks and magentas) are mapped to greyish blues, as illustrated in Figs. 4.3-4.4.

4.5.4 Quantitative Evaluation

The quantitative evaluation was focused on three properties: consistency, naturalness, and contrast.

4.5.4.1 Consistency-Based Evaluation

The three algorithms here compared are all consistent in terms of recoloring. This means that the equally-colored pixels of an image will exhibit the same color after applying the same recoloring procedure.

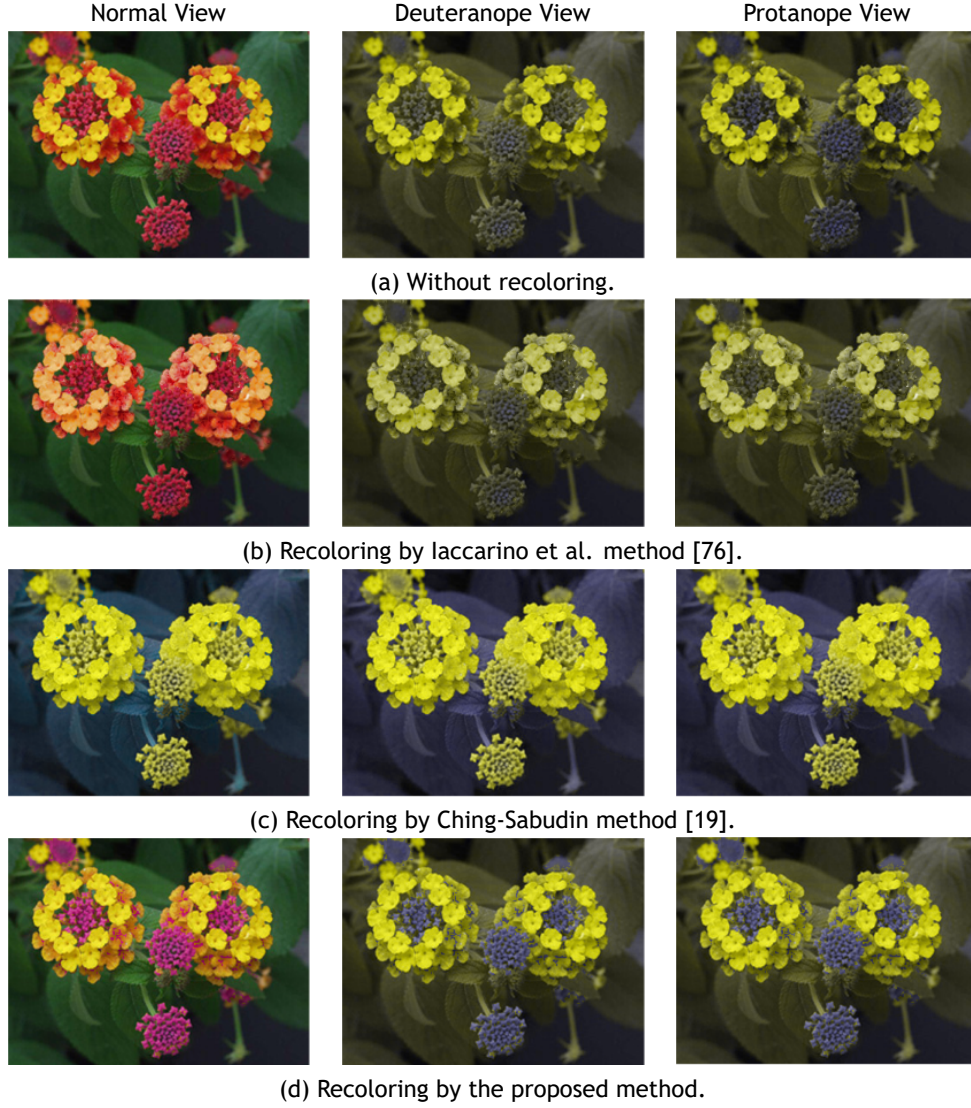


Figure 4.3: Lantana flowers recoloring by Iaccarino et al. [76], Ching-Sabudin [19] and CEA method.

4.5.4.2 Naturalness-Based Evaluation

As seen before in Section 4.2, the color naturalness assures that a mapped color will be close to the original color, as perceived by deutan and protan dichromats. According to Flatla et al. [82], the naturalness of an image is given by the following formula:

$$\nu = \frac{1}{n} \sum_{i=1}^n \Delta(P_i, P_i^*) \quad (4.12)$$

where n stands for the number of pixels (or resolution) of the image, P_i is the color of the i -th pixel and P_i^* is the color of the i -th pixel after the recoloring, while $\Delta(P_i, P_i^*)$ denotes the color difference between P_i and P_i^* in conformity with the CIE76 color-difference formula expressed in CIE Lab space coordinates, i.e., $\Delta = \sqrt{(L_i^* - L_i)^2 + (a_i^* - a_i)^2 + (b_i^* - b_i)^2}$, where (L_i, a_i, b_i) and (L_i^*, a_i^*, b_i^*) represent the Lab colors of P_i and P_i^* , respectively. The smaller the value of ν ,

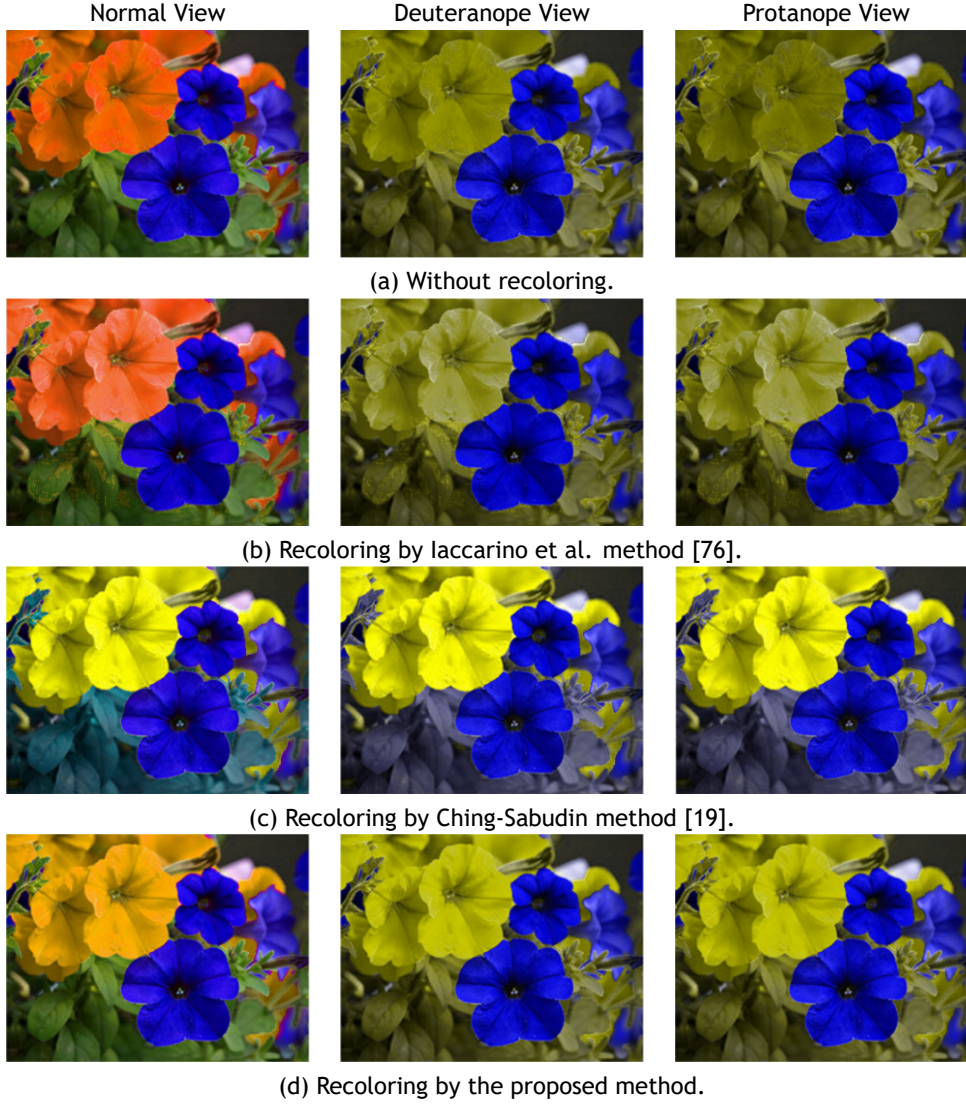


Figure 4.4: Petunia flowers recolored by laccarino et al. [76], Ching-Sabudin [19] and CEA methods.

more natural is the recoloring procedure of each image.

Eq. (5.8) applies to thricromats. However, it also applies to deutan and protan dichromats, since we consider that P_i and P_i^* are the colors seen by them before and after the recoloring procedure, respectively. The naturalness benchmarking of the three algorithms was carried out regarding a dataset of 100 still images possessing reddish colors, which are confusing colors for deutan and protan dichromats; 15 of such images are depicted in Fig. 4.5.

laccarino et al.'s. In regards to naturalness, laccarino et al.'s recoloring technique [76] ranks second, with a mean score of $\bar{\nu} = 8.6$ for the entire image dataset. This relatively high score can be explained by the following. First, despite the fact that almost all colors are changed, only a few of them change noticeably. Second, the hue rotation resulting from recoloring does not exceed the 45° (albeit the cumulative adjustments in saturation and light), while the remaining colors suffer a less noticeable change (about 10% in saturation and light).

Ching-Sabudin's. The algorithm proposed in [19] ranks third regarding naturalness, with a mean score of $\bar{\nu} = 20.76$ for the entire image dataset. The reasons behind this high score are twofold.

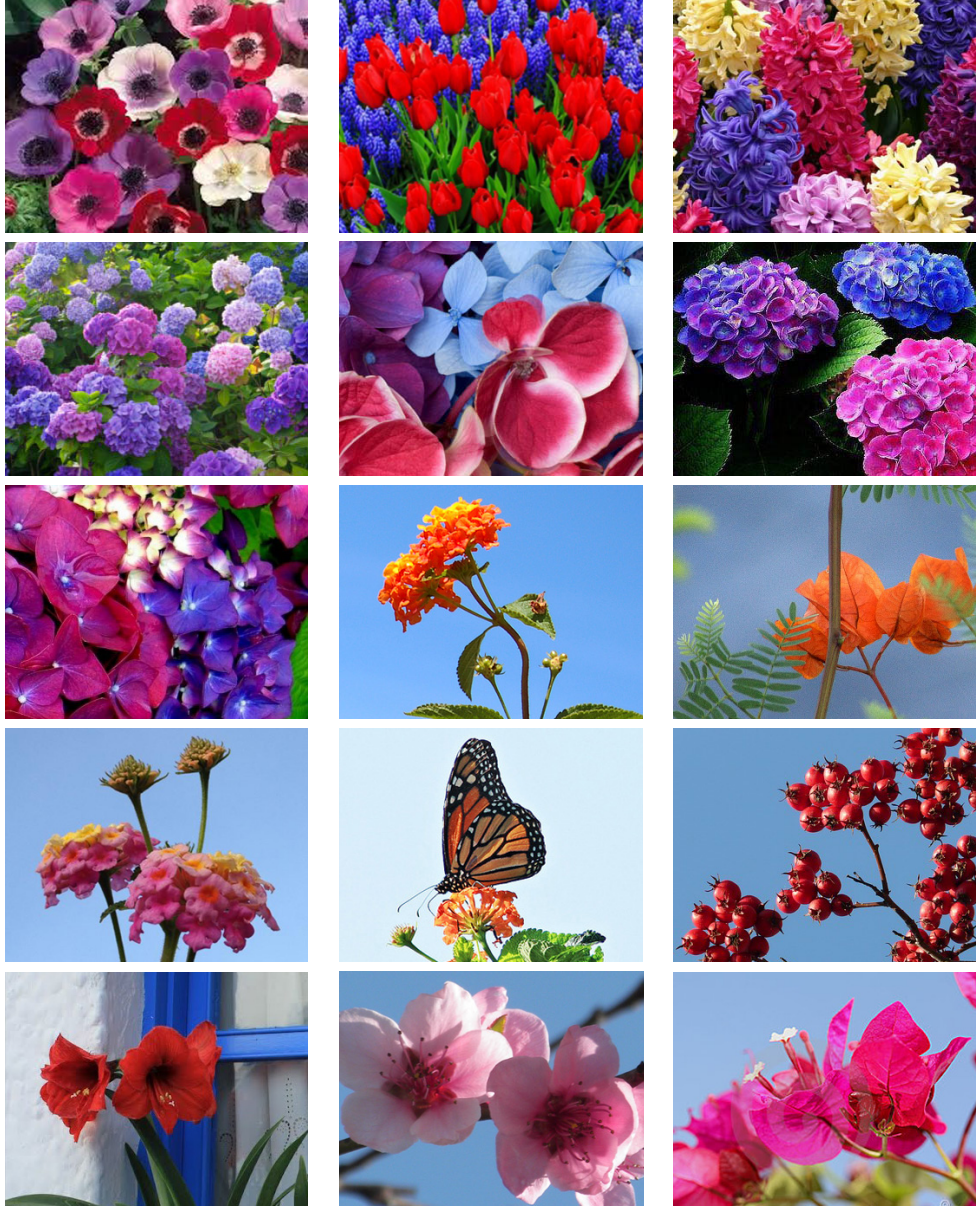


Figure 4.5: Still images of a dataset with 100 images (350x270 resolution) that we used to study and benchmark algorithms in respect to the following properties: naturalness, contrast, and performance. All images possess reddish colors (i.e., confusing colors for deuteranope e protanope people), whose hues are in the range $[-60^\circ, +60^\circ]$.

First, this happens because $2/3$ of colors are subject to recoloring. Second, the reddish hues in the range $[-60^\circ, 60^\circ]$ suffer a rotation that may attain 120° , and the same applies to greenish colors.

RGBeat. Our technique ranks first in respect to naturalness, with a mean score of $\bar{v} = 3.8$ for the entire image dataset. This is so because $2/3$ of colors remain unchanged, in largely because only those satisfying the condition $R > G, B$ end up being changed. Furthermore, the remapped colors are subject to a rotation with the maximum amplitude of 30° .

4.5.4.3 Contrast-Based Evaluation

The contrast benchmarking of the three techniques was accomplished using the squared Laplacian (cf. [?]) as follows:

$$C = \frac{1}{W \cdot H} \sum_{x=1}^W \sum_{y=1}^H G(x, y)^2 \quad (4.13)$$

where $W \times H$ denotes the image resolution, while $G(x, y)$ is given by:

$$G(x, y) = \sum_{i=x-1}^{x+1} |I(x, y) - I(i, y)| + \sum_{j=y-1}^{y+1} |I(x, y) - I(x, j)| \quad (4.14)$$

where $I(x, y)$ is intensity of the pixel (x, y) , which in turn is given by (cf. [100]):

$$I(x, y) = 0.299 \cdot R/255 + 0.587 \cdot G/255 + 0.114 \cdot B/255 \quad (4.15)$$

It is clear that the computation of contrast C through Eq. (5.5) applies to any color space. Because we are working in the deuteranope (and, also, protanope) color space, we used the deuteranope simulation algorithm due to Vienot et al. [2] before computing the contrast C of each image as seen by deuteranope people, before and after recoloring. Besides, our quantitative evaluation of contrast took place in the deuteranope color space. More specifically, in the deuteranope color space, we obtained a mean contrast value of $\bar{C} = 0.0418$ for the entire dataset of testing images, before applying any recoloring procedure.

Iaccarino et al.'s. Based on our testing, the algorithm due to Iaccarino et al. [76] does not show any contrast improvement because the mean contrast after recoloring all images of the dataset is 0.0417, i.e., slightly lower than the mean contrast before recoloring. This is explained by the small changes in hue, saturation, and brightness inherent to the recoloring procedure of the Iaccarino et al. algorithm.

Ching-Sabudin's. In regards to Ching-Sabudin technique [19], we noted its ability to enhance the contrast, since the entire dataset of images scored 0.047 in mean contrast, featuring an increase of 12.4% in respect to the mean contrast before recoloring. However, this contrast increase is made at the cost of some loss of naturalness. In fact, 2/3 of colors are remapped by the recoloring procedure; but, more importantly, it is the fact that reddish hues in the range $[-60^\circ, 60^\circ]$ are all mapped to yellows when it would be more natural to remap hues in the subrange $[-60^\circ, 0^\circ[$ to blues and hues in the subrange $[0^\circ, 60^\circ[$ to yellows.

RGBeat. Our technique also improves the contrast, but not so much as Ching-Sabudin's technique; it scored 0.045 in mean contrast, featuring an increase of 7.7% relative to the original images before recoloring. Recall that our recoloring technique only operates on the hue range $[-60^\circ, 60^\circ]$ (i.e., confusing hue range), so that hues in the subrange $[-60^\circ, 0^\circ[$ are mapped to

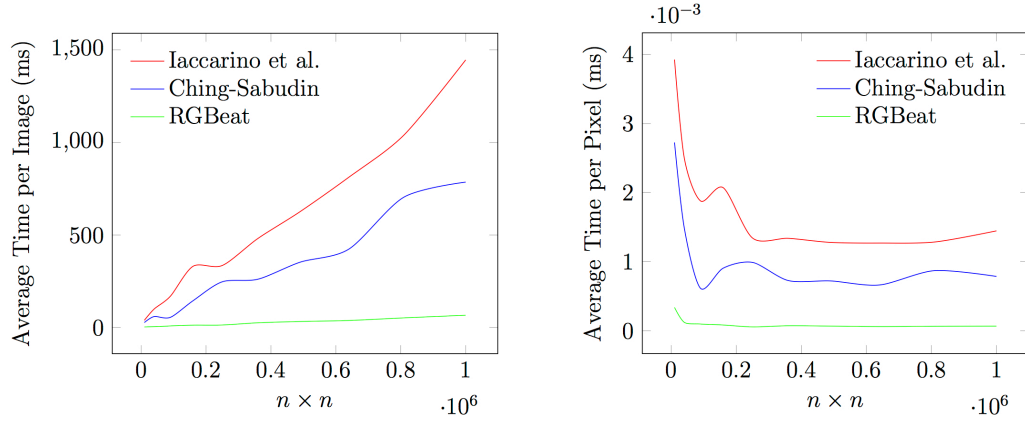


Figure 4.6: Time performance of Iaccarino et al. [76], Ching-Sabudin [19] and CEA methods: (left) average image recoloring time for images with different resolutions; (right) average pixel recoloring time for images with different resolutions.

blues, while hues in the subrange $[0^\circ, 60^\circ]$ are mapped to yellows.

In short, in spite of Ching-Sabudin's technique scores higher than our technique regarding contrast, our technique is capable of enhancing the contrast with a negligible loss of naturalness.

4.5.5 Time Performance-Based Evaluation

To assess the time performance of the three algorithms coded in JavaScript programming language, we used ten offline web pages containing a total of 160 images. Each page incorporates 16 images with the same resolution $n \times n$, but the resolution increases 100 pixels wide and 100 pixels high from page to page, i.e., we have images with resolutions of $n \times n$, with $n = 100, 200, \dots, 1000$.

Fig. 4.6 shows how the algorithms behave over images with increasingly higher resolutions. More specifically, Fig. 4.6(left) shows how much the average time spent by those algorithms depends on the resolution of the images, while Fig. 4.6(right) features the average time per pixel for each collection of images with the same resolution.

As expected, for those three algorithms, the average time to recoloring images increases with the resolution (Fig. 4.6(left)), but the average time per pixel decreases with the resolution, converging to a minimum that keeps constant when $n \rightarrow \infty$ (Fig. 4.6(right)). This indicates that the time complexity of the three algorithms is linear. This is so because not all the pixels are recolored. Nevertheless, RGBeat is faster than the two algorithms mentioned above because it takes less time per pixel. In fact, the average time per pixel is about $1.4 \mu s$, $0.8 \mu s$, and $0.06675 \mu s$ for the algorithms of Iaccarino et al., Ching-Sabudin, and RGBeat, respectively, when $n \rightarrow \infty$.

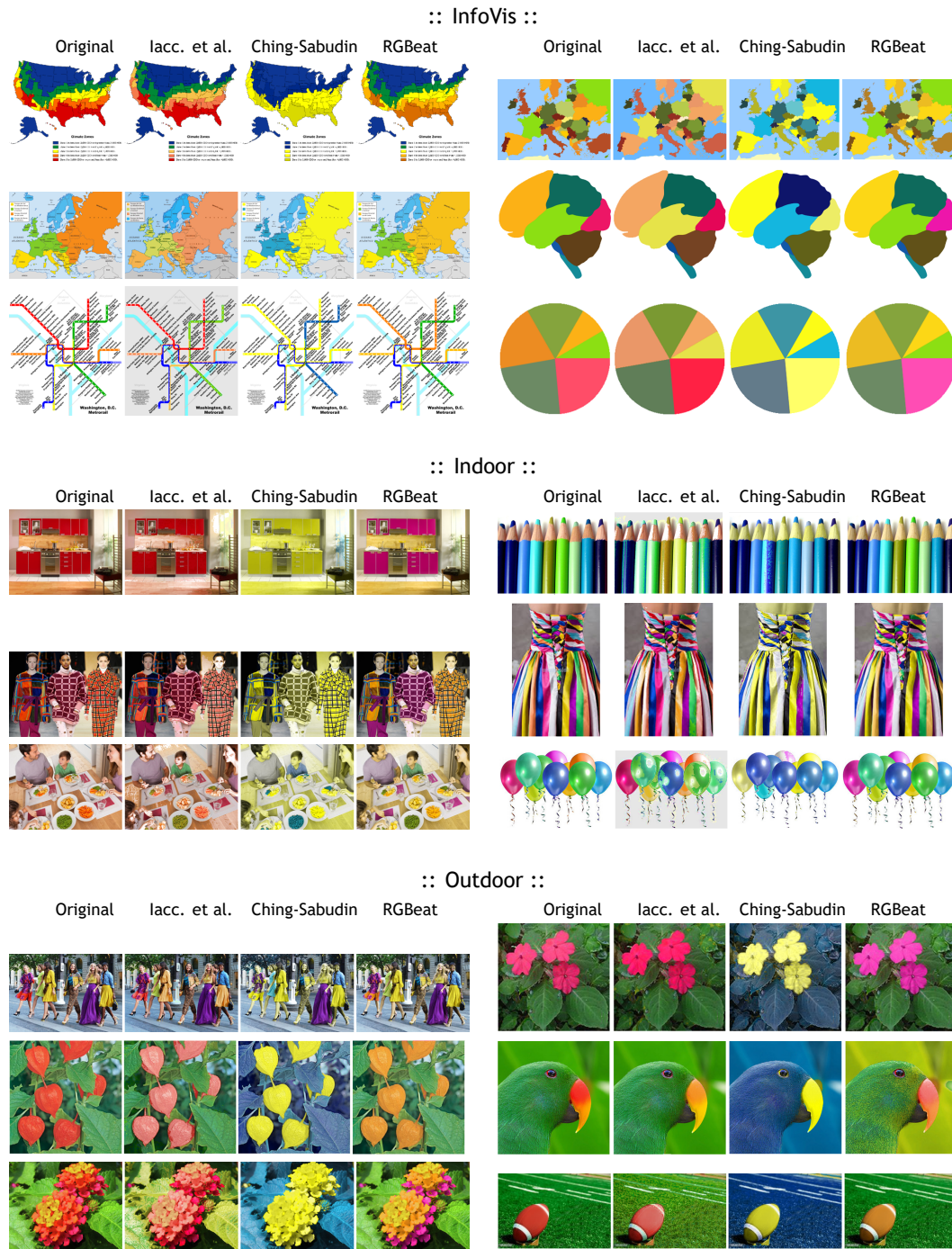
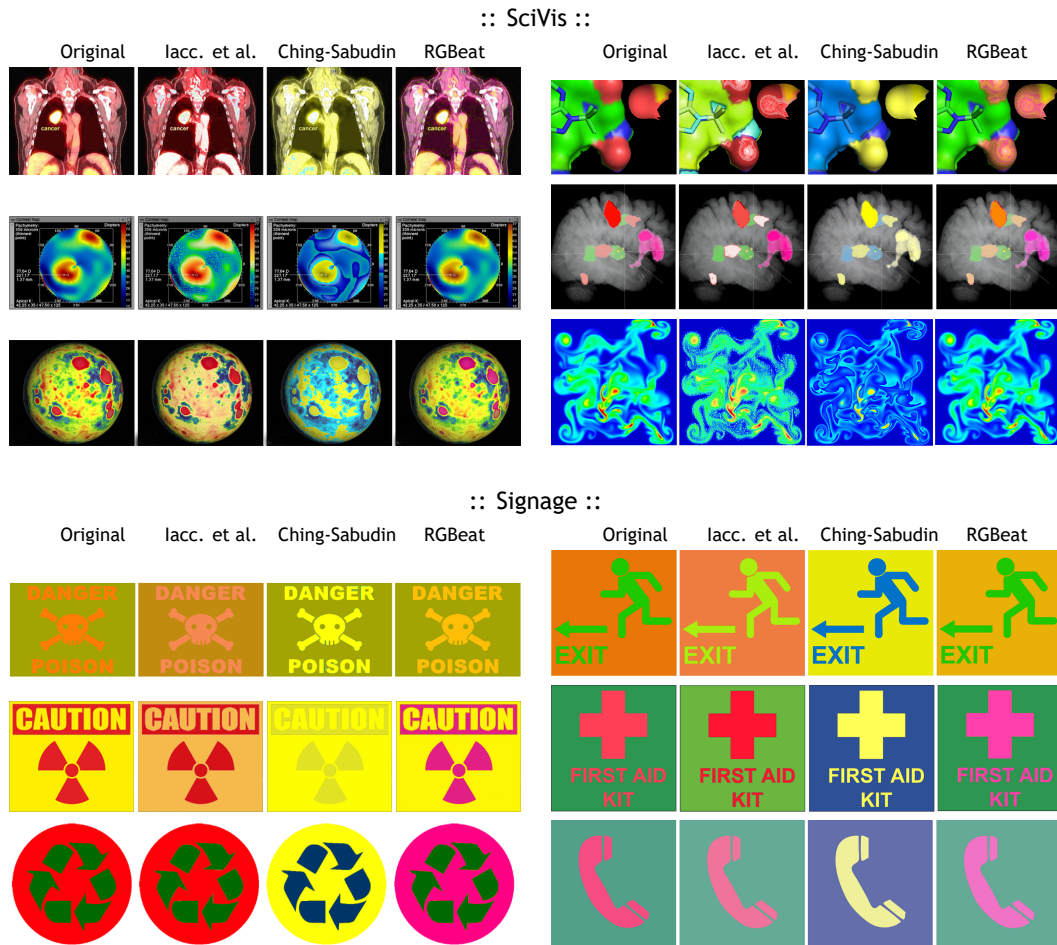


Figure 4.7: Dataset of images belonging to the categories *InfoVis*, *Indoor*, and *Outdoor*.

4.6 Subjective Evaluation

To make sure about the quality of the results produced by the RGBeat algorithm, we proceeded with its subjective evaluation.



4.6.2 The Questionnaire

Although some authors have adopted the Law of Comparative Judgment (LCJ) of L.L. Thurstone for statistical studies [23][24], we do not follow that pathway, because LCJ does not allow the comparison of four alternatives simultaneously. Instead, we use descriptive statistics techniques to compare more than two methods simultaneously [103] [104]. More specifically, we have used questionnaires as one of such descriptive statistics techniques.

In the makeup of the web questionnaire (see <http://rgbeat.ipcb.pt/>), and as shown in Figs. 5.7 and 5.8, we considered 5 categories of images: visualization of information (*InfoVis*), indoor scenes (*Indoor*), outdoor scenes (*Outdoor*), visualization of scientific information (*SciVis*), and signage (*Signage*). We elected 6 images for each category making up a total of 30, which are exactly those depicted in Figs. 5.7 and 5.8. These images were chosen regarding the importance of using a representative set of images (see Shaffer and Zhang [104]), in order to reduce the sampling error and, consequently, getting a significant statistical confidence interval.

The questionnaire was designed for web browsers (via Google Forms) so that each category of images corresponds to a separate web page of the questionnaire. Each one of these five pages displays 6×4 images, i.e., 6 rows of 4 optional images placed randomly in a horizontal manner. Each row includes the original image and more three recolored images produced by above recoloring algorithms (Iaccarino et al., Ching-Sabudin and RGBeat); these four images concerning the same scene are randomly placed in each row. The user is asked for his/her preference order (i.e., *ranking* from 1st to 4th) of four images of each row regarding naturalness and legibility/contrast (discrimination of objects in images). Note that this ranking scale is adequate to situations where the ranking involves a maximum of five alternatives [105]. Then, the image ranked first is assigned the score 4, the second the score 3, the third the score 2, and the fourth the score 1 (see [106] for further details about the design of questionnaires). The questionnaire was validated by four specialists on visual representation and color vision deficiency researchers.

4.6.3 Data Collecting

The raw quantitative results of the questionnaires are shown in Fig. 4.9, where the CVD people's preferences are expressed in relation to five categories of images mentioned in Section 5.4.2 (see Figs. 5.7 and 5.8). Taking into consideration that we have a universe of 13 respondents and 6 images per category, the size of the data sample for each category is 78 responses ($= 6 \times 13$); for example, for the InfoVis category in Fig. 4.9, the data sample of the RGBeat is 78, as a result of summing up 16 responses with score 1, 30 responses with score 2, 27 responses with score 3, and 5 responses with score 4. That is, we used scoring in the range [1, 4], which has to do with the number of recoloring methods under benchmarking.

4.6.4 Data Analysis

The descriptive statistics-based analysis of the data collected from the questionnaire was carried in two steps: (i) box-and-whisker diagrams; (ii) coefficient of variation. The box-and-whisker

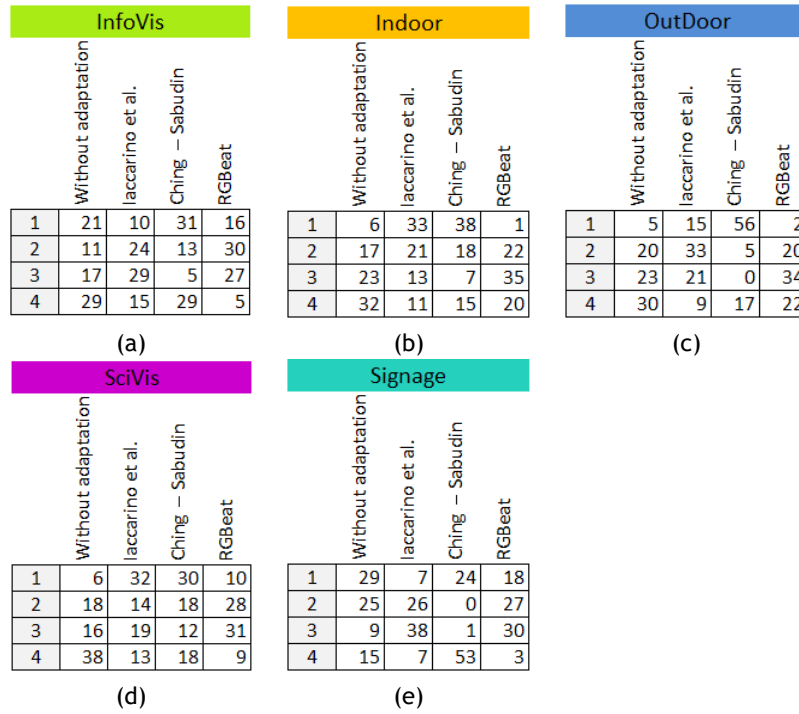


Figure 4.9: Distribution of the preference scores of color adaptation methods per category.

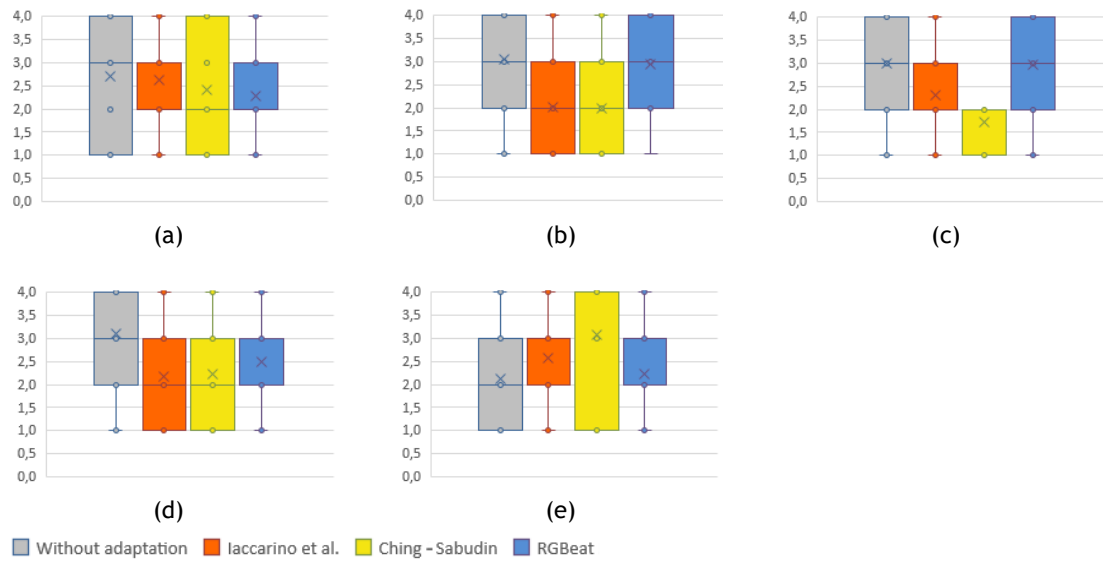


Figure 4.10: Box-and-whisker diagrams of preferences of color adaptation methods per category: (a) InfoVis; (b) Indoor; (c) Outdoor; (d) SciVis; and (e) Signage. The *mean* is represented by a cross and *median* by an horizontal line.

diagram is a type of visual data tool that allows us to display the distribution (and, inherently, the concentration) of preferences of the CVD people, while the coefficient of variation is a metric that quantifies such dispersion/concentration of preferences.

4.6.4.1 Box-and-Whisker Diagrams

The box-and-whisker diagram is a visual data tool to quickly examine datasets graphically. Its central box at least features 50% of the preferences of the respondents relative to each method. This box consists of the second and third quartiles, which are separated by the median of the data sample (78 responses), which is represented by a horizontal straight line segment; the arithmetic mean is represented by a cross.

A brief glance at the diagrams depicted in Figure 5.10, which represent the data listed in Fig. 4.9, shows us the following in respect to each category of images:

- *Infovis*: The method without adaptation (MWA, for brevity) (i.e., original images without adaptation) and laccarino et al.'s method gathered more than 56% of preferences with the top scores 4 or 3 (see Fig. 4.9(a) and Fig. 5.10(a)). Looking at box-and-whisker diagrams of these methods, we observe that their averages are similar (cf. Table 5.1) but the preferences of laccarino et al.'s method are much less dispersed, as its box is smaller. In fact, laccarino et al.'s standard deviation is smaller than the one of the MWA (cf. Table 5.1), and the same applies to the coefficient of variation. Thus, for infovis-type images, the best solution is to use laccarino et al.'s method.
- *Indoor*: In this case, either MWA or RGBeat reunites 70% of the preferences with the scores 4 and 3. Besides, their arithmetic averages are similar (see Fig. 4.9(b) and Fig. 5.10(b)). As a consequence, even looking at their box-and-whisker diagrams, it is difficult to say which is the top-ranked method of those two for indoor-type images, because they have similar visual dispersion (i.e., boxes with the same size). However, we see in Table 5.1 that RGBeat has a smaller standard deviation than the method without recoloring. Additionally, RGBeat's coefficient of variation is also less than the one of the method without recoloring. Thus, we conclude that RGBeat ranks first for indoor-type images.
- *Outdoor*: The visual results for this category are similar to those obtained for the indoor category. In fact, the MWA and the RGBeat were scored with 4s and 3s in more than 68% of the preferences (see Fig. 4.9(c) and Fig. 5.10(c)). Note that their arithmetic averages and dispersion boxes are visually indistinguishable in their box-and-whisker diagrams, so we cannot draw any conclusion about the top-ranked method of those two for outdoor-type images. However, looking at Table 5.1, we observe that RGBeat's coefficient of variation, as well as the standard deviation, is smaller than MWA's one. Thus, RGBeat ranks first in this category.
- *SciVis*: MWA got the higher scored preferences, with approximately 50% of preferences scored as 4 (see Fig. 4.9(d) and Fig. 5.10(d)). Besides, its arithmetic mean is much higher than for the other methods, and this agrees with the fact that its coefficient of variation is smaller than for any other method (cf. Table 5.1). Thus, in the case of scivis-type images, the best solution is to leave them as they stand, i.e., without color adaptation.
- *Signage*: Ching-Sabudin method reached 68% of responses scored as 4, so that its arithmetic mean is higher than for other methods (see Fig. 4.9(e) and Fig. 5.10(e)). Despite its significant dispersion, it is due to an accumulation of frequencies at the upper side of the rank scale, i.e., 53 of the 78 responses are scored as 4, while the frequencies accumulated

in the bottom of the scale of scores are less than half. Therefore, this method ranks first for the signage-type images.

Table 4.1: Statistical results for different adaptation color methods.

Category	Metric	MWA	<i>laccarino et al.</i>	<i>Ching-Sabudin</i>	<i>RGBeat</i>
<i>InfoVis</i>	\bar{x}	2.69	2.63	2.41	2.27
	σ	1.231	0.941	1.343	0.863
	v	46%	36%	56%	38%
<i>Indoor</i>	\bar{x}	3.04	2.03	1.99	2.95
	σ	0.973	1.081	1.168	0.771
	v	32%	53%	59%	26%
<i>Outdoor</i>	\bar{x}	3.00	2.31	1.72	2.97
	σ	0.953	0.916	1.237	0.805
	v	32%	40%	72%	27%
<i>SciVis</i>	\bar{x}	3.10	2.17	2.23	2.50
	σ	1.014	1.144	1.194	0.864
	v	33%	53%	54%	35%
<i>Signage</i>	\bar{x}	2.13	2.58	3.06	2.23
	σ	1.121	0.782	1.390	0.852
	v	53%	30%	45%	38%
	\bar{x}	2.79	2.34	2.28	2.58

Statistical metrics:

\bar{x} : arithmetic mean; σ : standard deviation; v : coefficient of variation.

Summing up, the RGBeat method ranks first in two categories, indoors and outdoors. This agrees with the fact that it preserves the naturalness more than any other method (see Section 4.5.4). On the other hand, laccarino et al.’s method gets on top in two other categories, infovis and signage, although it ranks second regarding naturalness. However, its contrast varies only -0.24% relative to the contrast of original images, while RGBeat’s contrast is +7.7% (see Section 4.5.4).

Interestingly, the MWA ranks first in the scivis category, i.e., there is no variation in naturalness and contrast for obvious reasons. These results lead us to conclude that the recoloring process must not change the colors in a noticeable manner to preserve the individual’s perceptual learning as much as possible. Recall that RGBeat only changes the red hues to close hues, whereas laccarino et al.’s method changes all hues, but to close hues as well. In contrast, Ching-Sabudin method provokes significant color changes, i.e., the distance between an original hue and the resulting hue is greater than for the other two adaptation methods.

Overall, RGBeat ranks first because it ranks first in two categories (indoors and outdoors) and second in three categories (infovis, scivis, and signage), what explains why its coefficient of variation (34%) is lower than in any other method, as shown in Table 5.1. Moreover, it is the only method that outperforms the MWA, i.e., RGBeat images are perceptually better than original images.

4.7 Contributions

Now, we are in a position of listing the main contributions of this work, namely:

- *Color perceptual enhancement.* Adaptation methods are worthy being investigated, because they may enhance the perception of CVD people. Recall that RGBeat makes a noticeable enhancement in relation the original images (MWA). To preserve the perceptual learning of each person, we have also learned we cannot change the colors too much; otherwise, the naturalness and contrast may change significantly. We have demonstrated that it is possible to increase the color contrast without compromising the image naturalness and perceptual learning of CVD people, henceforth resulting an augmented perception of CVD people. In fact, as shown in Table 5.1, RGBeat is the only method that performs better than MWA, because its coefficient of variation (34%) is less than the one of the MWA (40%).
- *Mathematical formulation.* RGBeat’s mathematical formulation is based on RGB and HSV color models, from which we have derived recoloring formulas that exclusively operate on the RGB color model (cf. Eqs. (4.7) and (4.10)).
- *Deuteranope and protanope’s color space.* By applying Vienot et al.’s algorithm [2], we have shown that the deuteranope and protanope’s color space consists of two coplanar half planes (see Fig. 4.2). In fact, deuteranope and protanope people only see two different hues: 60° (yellow) and 240° (blue). A similar result was achieved by Brettel et al. [70] themselves for LMS color space, as well as by Meyer and Greenberg [99] for CIE XYZ color space.
- *Generality.* We have shown that RGBeat also applies to images and text in HTML documents. Supposedly, it also applies to video because a video is a sequence of frames. Taking into consideration that RGBeat spends $0.06675 \mu\text{s}$ per pixel (see Section 4.5.5) on average, we conclude that recoloring video in real-time is feasible for images with 623,220 pixels; for example, youtube videos in the format 16:9 with resolutions 854×480 at most can be recolored in real-time.
- *Time performance.* In regards to time performance, RGBeat attains real-time performance, and thus outperforms the other two adaptation methods, largely because it avoids the explicit conversion between the RGB and HSV color spaces.

Summing up, our method guarantees a balanced trade-off of four requirements, color consistency, naturalness maintenance, contrast improvement and speed, and at the same time it is capable of augmenting the perception of CVD people.

4.8 Further Remarks

We have introduced a recoloring method, called RGBeat, that applies to HTML documents, including their images, videos, and text. The main novelty of this method is that it is the only one that produces images that are perceptually richer than the original images. This was accomplished by stressing on naturalness maintenance, which imposes limits to the increase of contrast. Furthermore, RGBeat has revealed quite fast because it only operates on the range of reds, making it feasible to re-colorize video in real time.

Let us also mention that we have developed an extension for the Chrome browser that allows for online adaptation of web pages and their contents (e.g., text, still images and video) au-

tomatically. Shortly, we intend to use some multi-threading or parallel processing tools (e.g., Web Workers API) in order to even further speed up color-adaptive browsers in real-time.

Chapter 5

Contour Enhancement Algorithm for Improving Visual Perception of Deutan and Protan Dichromats

This chapter describes an innovative contour-enhancement algorithm that was designed for dichromat people, here called CEA. Unlike the majority of color adaptation algorithms, its leading idea is not recoloring by remapping colors, but to enhance contours of indistinguishable neighboring image regions. Similar to RGBeat described in the previous chapter, it also preserves color naturalness, contrast, and consistency. This chapter corresponds to a paper also submitted to IEEE Transactions on Visualization and Computer Graphics, and is currently under revision.

5.1 Introduction

A variety of recoloring methods has been proposed in the literature to remedy the problem of confusing red-green colors faced by dichromat people (as well by other color-blinded people). The common strategy to mitigate this problem is to remap colors to other colors. But, this does not guarantee the necessary contrast to distinguish the elements of an image, nor the naturalness of colors learned from the experience of each person. In other words, the individual's perceptual learning may not hold under color remapping. With this in mind, we introduce the first algorithm primarily focused on the enhancement of object contours in still images, instead of recoloring the pixels of the regions bounded by such contours. This is particularly adequate to increase contrast in images where we find adjacent regions that are color indistinguishable from the dichromacy's point of view.

5.2 Contour Enhancement Algorithm

The individuals with dichromacy see only two distinct hues; more specifically, blues and yellows for deutan and protan dichromats, and reds and greenish blue for tritan dichromats, although with different values of saturation and brightness. For example, a deutan dichromat perceives a weakly saturated yellow as a moss green. The reduced chromatic range as perceived by dichromat people may lead to the lack of discrimination between neighbor regions in an image, resulting in confusion about what is being seen in the image.

To mitigate this problem, we propose an approach that enhances contours between adjacent image regions, which are indistinguishable for dichromat individuals. The idea is to highlight the

contours that separate contiguous regions represented with different colors but seen as similar or identical by dichromat people.

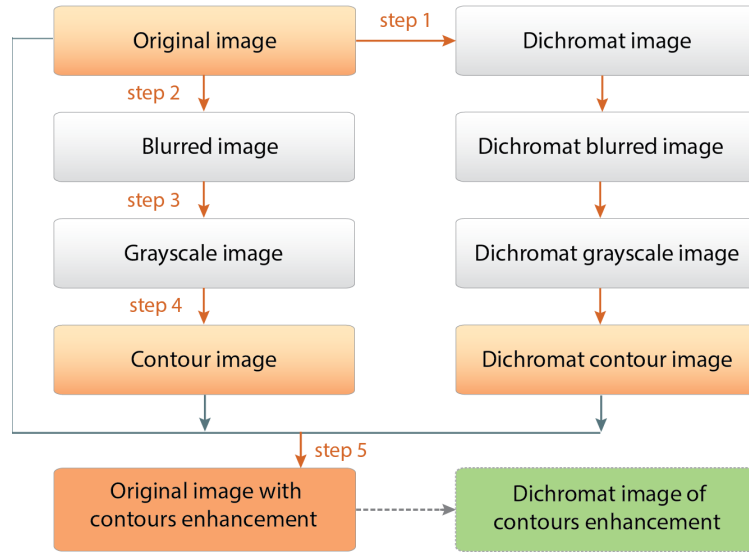


Figure 5.1: Global schema of the contours enhancement process.

This contour enhancement procedure is illustrated in Figs. 5.1 and 5.2, and comprises the following steps:

1. Generate the image as seen by (deutan and protan) dichromat individuals from the original image.
2. Apply a Gaussian blur filter to both original and dichromat images.
3. Convert both original and dichromat images to grayscale.
4. Compute contours in both original and dichromat images.
5. Highlight those contours of the original image that are absent in the respective dichromat image.

5.2.1 Dichromat Image Generation

Taking the original image as input data, the first step of our algorithm consists in generating the corresponding image as seen by a dichromat individual. This is accomplished using the simulation algorithm due to Vienot et al. [2]. Essentially, this algorithm comprises three steps: (i) the RGB→LMS conversion [107] [108]; (ii) the dichromat simulation (e.g. deuteranope) in the LMS color space, as proposed by Vienot et al. [2]; (iii) the LMS→RGB conversion. Each step is associated with a particular matrix, so the entire process reduces to a product of three matrices, resulting in the following overall matrix:

$$M = \begin{bmatrix} 0.2928 & 0.7072 & 0 \\ 0.2928 & 0.7072 & 0 \\ 0.02234 & 0.02234 & 1 \end{bmatrix} \quad (5.1)$$



Figure 5.2: The contour enhancement process applied to an hibiscus flower.

Summing up, we generate the image as seen by a dichromat individual by multiplying the matrix M above by the vector $[RGB]^T$ associated to each pixel. It is clear that this step may be adjusted to any CVD using a different overall simulation matrix M .

Interestingly, as shown in Figs. 5.2(a)-(b), a deutan dichromat individual cannot see the hibiscus flower at all because he/she cannot distinguish the green background from the red flower.

5.2.2 Gaussian Blur Filter

Both images, the original image and dichromat image, are subject to a noise reducing procedure through a gaussian blur filter (see [97] for further details). This is a pre-processing step, and is performed using the Gaussian 3×3 kernel matrix:

$$B = \begin{bmatrix} 0.077847 & 0.123317 & 0.077847 \\ 0.123317 & 0.195346 & 0.123317 \\ 0.077847 & 0.123317 & 0.077847 \end{bmatrix} \quad (5.2)$$

Recall that this sort of image-blurring filters is commonly used in image analysis and processing, particularly when they coupled with contour detectors, which are sensitive to noise.

5.2.3 Grayscale Conversion

The conversion to a grayscale representation is performed by computing the luminance of each pixel [100], in conformity with the following expression:

$$I = 0.2989 R + 0.5866 G + 0.1145 B \quad (5.3)$$

where, R , G , and B are color components of the pixel. This conversion is justified by the fact that the human eye can perceive brightness changes better than color changes [97]. This fact is valid not only for trichromat but also for dichromat people. Figs. 5.2(e) and (f) show the images that result from converting the images in Figs. 5.2(c) and (d) to grayscale, respectively.

5.2.4 Contour Detection

The core of our method lies in the detection of contours of regions within the grayscale images of both original and dichromat images. Its leading idea is to identify contours (or part of them) in the original grayscale image that do not exist in grayscale dichromat image. This is illustrated in Figs. 5.2(e) and (f)), where the contours of the flower are completely absent in the grayscale dichromat image (Fig. 5.2(f)). This is so because a deutan dichromat individual cannot perceive the difference between the green background from the red flower at all.

Such contours are determined by applying the Sobel gradient masks in the x and y directions to each pixel [97]. As a result, we obtain two Sobelized images G_x and G_y in the x and y directions,

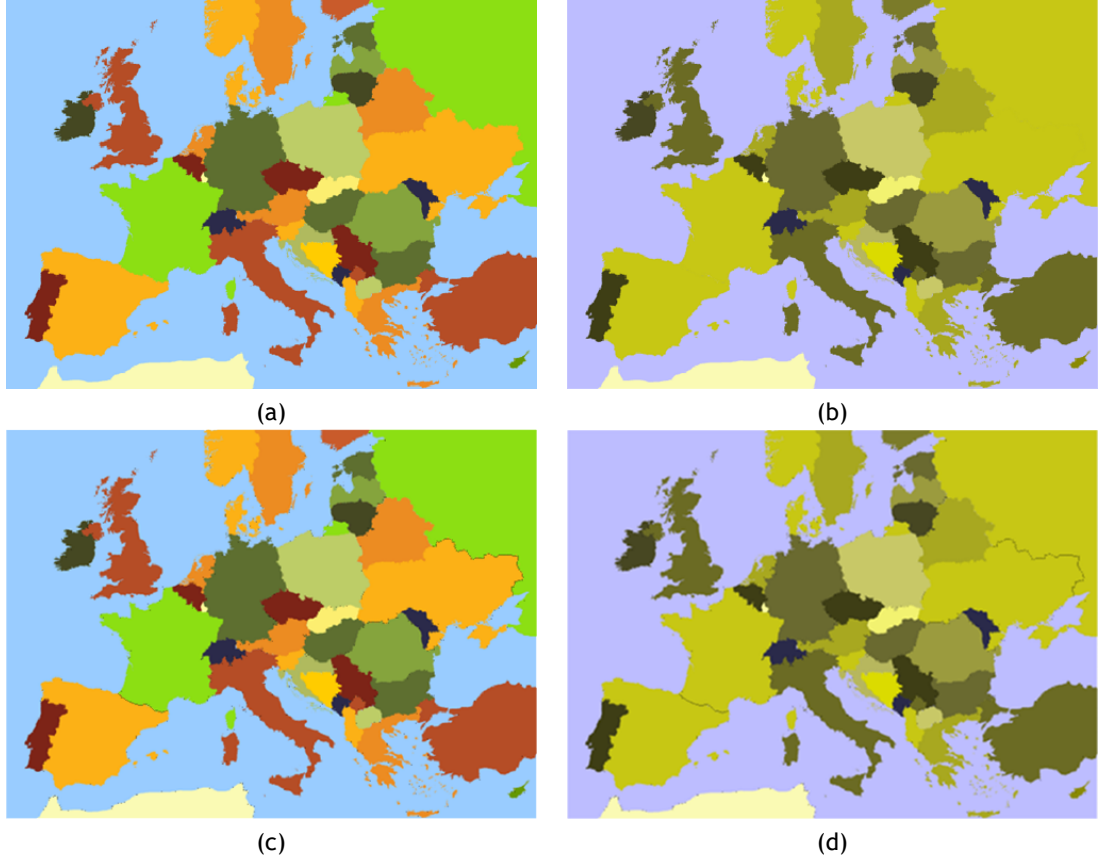


Figure 5.3: Image adaptation of an Europe map through the CEA algorithm: (a) original image; (b) original image as seen by deuteranope people; (c) adapted image; and (d) adapted image as seen by deuteranope people (deuteranope simulation was performed using Vienot et al.’ method [2]).

respectively, which are then merged into a Sobelized image through the following expression:

$$S = \sqrt{G_x^2 + G_y^2}. \quad (5.4)$$

Note that this process must be applied to both grayscale counterparts (Figs. 5.2(e) and (f)) of the original image and dichromat image. The resulting images are shown in Figs. 5.2(g) and (h).

5.2.5 Contour Highlighting

The contour enhancement step in subtracting the contours of the grayscale dichromat image to those contours of the original grayscale image. In this way, we obtain the missing contours in the dichromat image, which are then highlighted with more or less luminance, depending on the current luminance of each pixel in the dichromat image, as illustrated in Figs. 5.2(i) and (j).

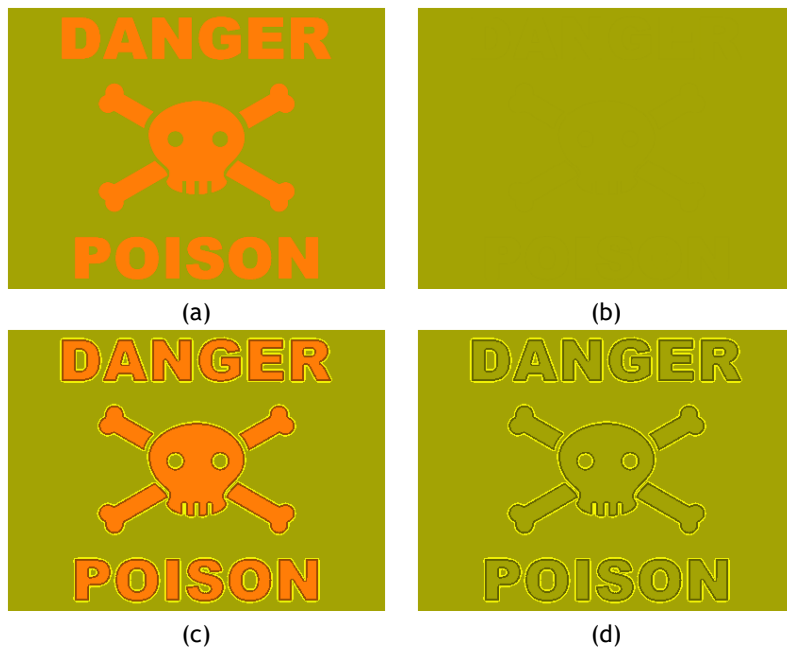


Figure 5.4: Image adaptation of a danger nameplate through the CEA algorithm: (a) original image; (b) original image as seen by deuteranope people; (c) adapted image; and (d) adapted image as seen by deuteranope people (deuteranope simulation was performed using Vienot et al.' method [2]).

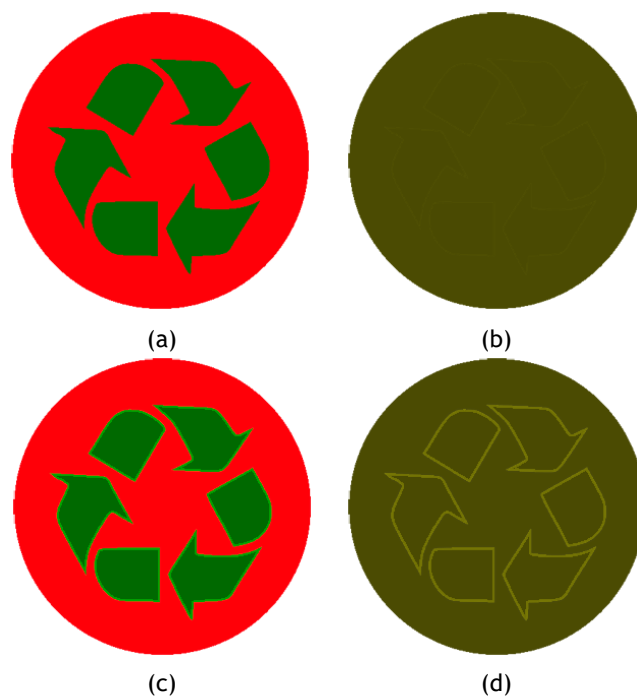


Figure 5.5: Image adaptation of a recycling sign through the CEA algorithm: (a) original image; (b) original image as seen by deuteranope people; (c) adapted image; and (d) adapted image as seen by deuteranope people (deuteranope simulation was performed using Vienot et al.' method [2]).

5.3 Results

To our best knowledge, CEA is the first contour-based color adaptation algorithm for CVD people. However, our testing was focused exclusively only on deutan and protan dichromat people, largely because their color perception is quite similar, in addition to the fact that deuteranopia and protanopia are the most common types of dichromacy we find in world male population.

5.3.1 Setup

Testing was performed using a 64-bit Microsoft Windows laptop equipped with an Intel Core i7-4750HQ CPU 2.0GHz, with 8G RAM. CEA algorithm and its competitors (Ching-Sabudin method [19] and Iaccarino et al.'s method [76]) were coded in Javascript programming language for HTML5 web compliant browsers, including Firefox and Chrome. Note that we also implemented in Javascript the Vienot et al.'s algorithm [2] which simulates how deuteranopes see colors, and yet an algorithm to count regions in images.

Those two competitor algorithms (Ching-Sabudin method and Iaccarino et al.'s method) were chosen because they also apply to deutan and protan dichromat people. Besides, these algorithms have the further advantage of their codes are publically available.

In methodological terms, as explained further below, we used three metrics to evaluate the efficiency of CEA: perceived region rate (ρ), naturalness (ν), and contrast (C).

5.3.2 Perceived Region Rate

By definition, the perceived region rate (ρ) is the ratio of the number of regions (or objects) seen by the CVD individual to the number of regions as seen by a trichromat individual. For example, the image depicted in Fig. 5.5(a) has seven regions seen by a trichromat individual, but the same image as seen by a deutan dichromat individual has only one region; therefore, the value of $\rho = 1/7$. That is, there are 6 out of 7 regions that not seen by the deutan dichromat individual. But, after applying our CEA algorithm, every single deutan dichromat individual was capable of seeing those six unseen regions. This was accomplished without changing the color of pixels inside each region; only region contour pixels were changed where needed to avoid color confusion. This made it possible to distinguish between Spain and France in Fig. 5.3 along their common border.

In Fig. 5.6, we show the overall results for perceived region rate for a dataset of 100 images divided into five categories, namely: infovis (information visualization), indoor, outdoor, scivis (scientific visualization), and signage. Examples of these images are shown in Figs. 5.7-5.8. As observed from Fig. 5.6, the perceived region rate of our algorithm has significant gains for infovis-, scivis-, and signage-type images, when compared to the corresponding images as seen by deutan and protan dichromats before adaptation. That is, these CVD people see more image regions after adaptation than before adaptation, resulting in an increase of their visual perception.

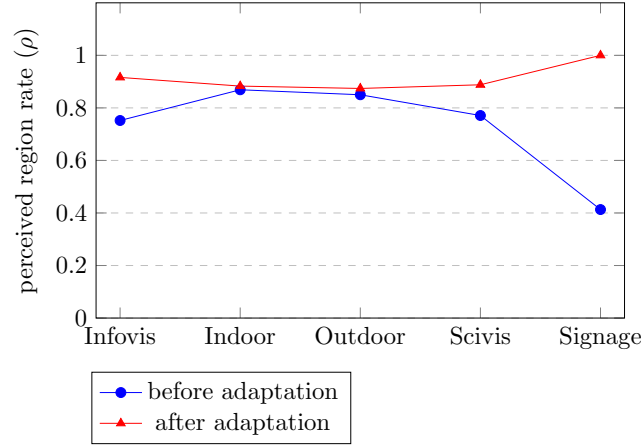


Figure 5.6: Perceived region rate before (in blue) and after (in red) CEA-based image adaptation for five categories of images.

5.3.3 Contrast

In the literature, there are various ways for contrast measuring of images. Our contrast metric C is based on Squared Laplacian [?], and is as follows:

$$C = \frac{1}{W \cdot H} \sum_{x=1}^W \sum_{y=1}^H G(x, y)^2 \quad (5.5)$$

being $G(x, y)$ given by:

$$G(x, y) = \sum_{i=x-1}^{x+1} |I(x, y) - I(i, y)| + \sum_{j=y-1}^{y+1} |I(x, y) - I(x, j)| \quad (5.6)$$

where $I(x, y)$ is the value of the intensity of the pixel at position (x, y) . W and H are the width and height of the image.

For the computation of the pixel intensity, we use the formula from equation 5.7, derived from by Poynton [100]:

$$I(x, y) = 0.299 \frac{R}{255} + 0.587 \frac{G}{255} + 0.114 \frac{B}{255} \quad (5.7)$$

After applying the simulation algorithm for deuteranopes described in [2], the mean average value of the contrast of the original dataset as seen by deuteranope people was $\bar{C} = 0.0418$. After applying our contour enhancement procedure, the average contrast increased to $\bar{C} = 0.054$, representing a gain of 28.5%. In respect to laccarino et al.'s method [76], the average contrast for the same dataset of 100 images was $\bar{C} = 0.0417$, so there was no gain in contrast. Finally, we obtained an average contrast of about 0.047 for Ching-Sabudin method [19], featuring an increase of 12.4% relative to the average contrast before the color adaptation process.

Notice that the contrast computation is achieved only after the deuteranope view simulation (which comes after the contour enhancement), since our goal is to improve the perception of images for deutan and protan dichromat people.

5.3.4 Naturalness

According to Flatla et al. [82], the color naturalness of an image can be expressed as follows:

$$\nu = \frac{1}{W \times H} \sum_{i=1}^{W \times H} \Delta(P_i, P_i^*) \quad (5.8)$$

where $W \times H$ denotes the image resolution, P_i is the color of the i -th pixel and P_i^* is the color of the i -th pixel after the color adaptation, while $\Delta(P_i, P_i^*)$ denotes the color difference between P_i and P_i^* in conformity with the CIE76 color-difference formula expressed in CIE Lab space coordinates given by

$$\Delta = \sqrt{(L_i^* - L_i)^2 + (a_i^* - a_i)^2 + (b_i^* - b_i)^2} \quad (5.9)$$

where (L_i, a_i, b_i) and (L_i^*, a_i^*, b_i^*) represent the Lab colors of P_i and P_i^* , respectively. The smaller the value of ν , more natural is the recoloring procedure of each image.

Considering the reference dataset of 100 still images, we achieved an average value for the naturalness of about $\bar{\nu} = 2.0$ for the deuteranope people. For the methods in comparison, Iaccarino et al. [76] and Ching & Sabudin [19], we got the naturalness scores of $\bar{\nu} = 8.6$ and $\bar{\nu} = 20.76$, respectively. These values are expectable since our method only changes the contour pixels, not interior pixels of regions; Iaccarino's et al.'s method changes colors to close colors, while Ching-Sabudin method changes colors too far away colors. Summing up, CEA method outperforms those two competitor algorithms in respect to color naturalness maintenance.

5.4 Subjective Evaluation

To assess the CEA algorithm in the perceptual augmentation of CVD users, we carried a statistical study based on a questionnaire as described below.

5.4.1 The Universe of CVD People

The subjective evaluation involved 13 CVD male volunteers. Initially, they performed the D-15 Color Arrangement Test [102] for a more accurate characterization of the universe of CVD users. The following results were obtained:

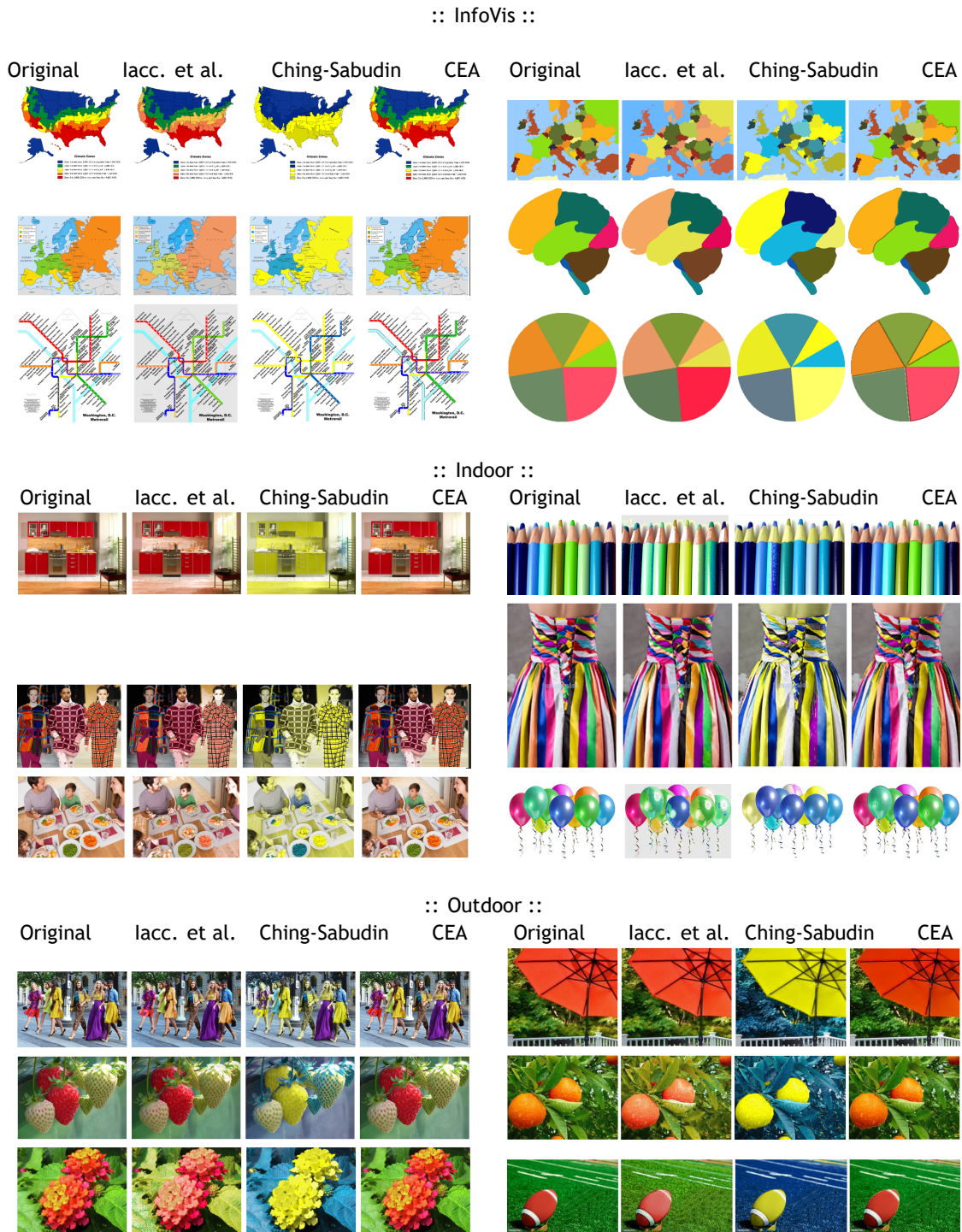


Figure 5.7: Dataset of images belonging to the categories *InfoVis*, *Indoor* and *Outdoor* used in the usability tests.

- 2 people with strong protanomaly (ages 32 and 49),
- 1 person with moderate protanomaly (age 27),
- 5 people with strong deuteranomaly (ages 49, 51, 57 and 69),
- 4 people with moderate deuteranomaly (ages 17, 21, 26 and 46), and

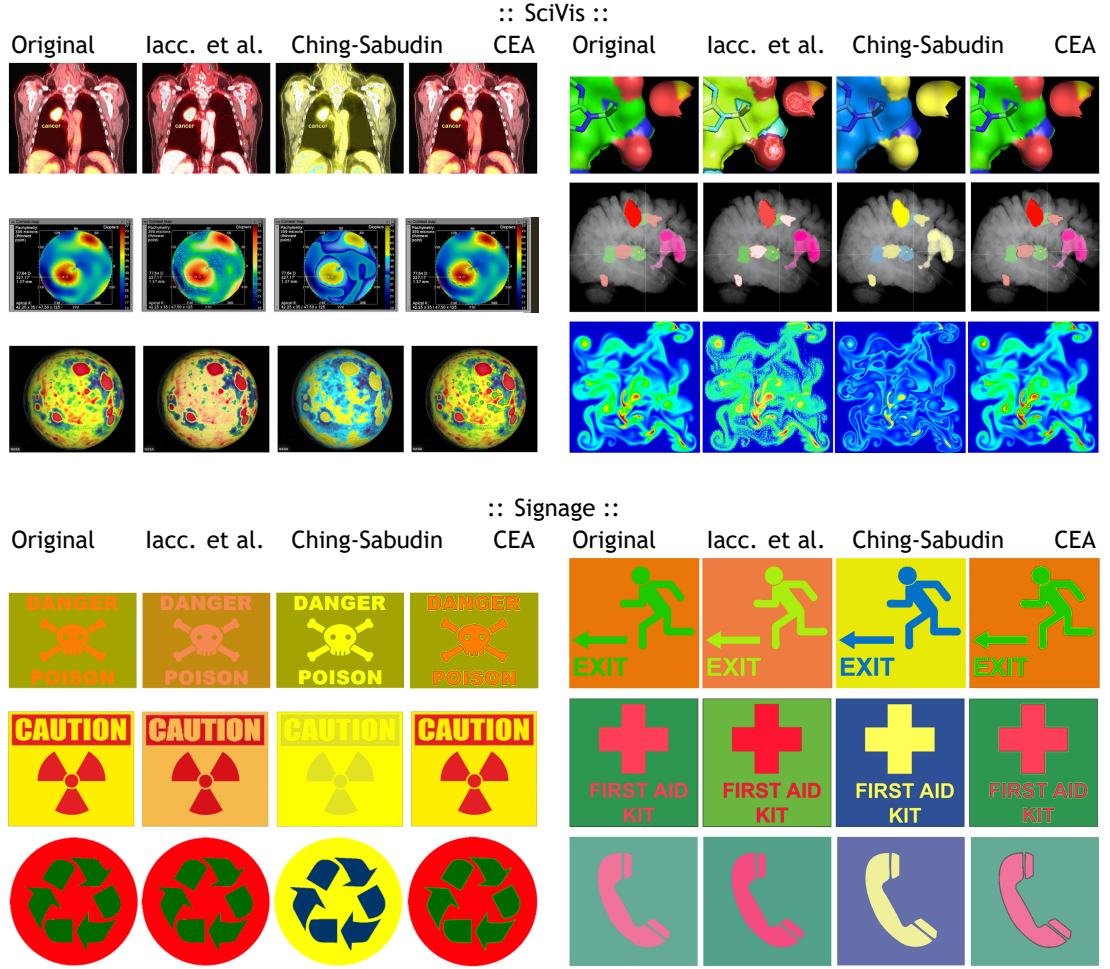


Figure 5.8: Dataset of images belonging to the categories *SciVis* and *Signage* used in the subjective evaluation tests.

- 1 person with deuteranopia (age 35).

In spite of the fact that the CEA algorithm has been designed for deuteranope and protanope people, we also considered deuteranomalous and protanomalous people in our study because of their high degree of CVD severity, i.e., they see in a similar way to deutan and protan dichromats [30].

5.4.2 The Questionnaire

5.4.2.1 Methodology

Unlike most color adaption subjective evaluation studies based on questionnaires [23] [24], we have not adopted the Law of Comparative Judgment (LCJ) of L.L.Thurstone [109], because this law only allows us to compare two alternatives or algorithms. In our study, we compare four alternatives: the original image without color adaptation (WCA), laccarino et al.'s method [76], Ching-Sabudin method [19], and our CEA method. Consequently, we decided to use descriptive statistics techniques [103] [104], in particular the following metrics: arithmetic mean (\bar{x}),

standard deviation (σ), and coefficient of variation ($v = \sigma/\bar{x}$), also called relative standard deviation. For each questionnaire image, those four alternatives are presented randomly to each CVD individual to not influence the choice of the respondents somehow.

5.4.2.2 Dataset of images

In our subjective evaluation study, we considered five categories of images (see Figs. 5.7 and 5.8): *InfoVis*, concerning visualization of information; *Indoor*, concerning indoor scenes, *Outdoor*, concerning outdoor scenes, *SciVis*, concerning scientific visualization; and *Signage*, concerning traffic and warning signs. More specifically, we selected six images by category, in a total of thirty images. Therefore, each CVD individual had to score thirty images times four alternatives, in a total of 120 images; the scores were thus 1 (highest score), 2, 3, and 4 (lowest score).

It is worth noting that the dataset of images was selected in conformity with the principles of representativeness and diversity suggested by Shaffer and Zhang [104]), to reduce the sampling error and, consequently, getting a significant statistical confidence interval.

5.4.2.3 Implementation

For the implementation of the questionnaire available at <http://cea.ipcb.pt/>, we used the Google Forms from the Google Docs application package to collect data from each CVD individual. The questionnaire consists of six web pages, one page per category of images. These images are disposed in the questionnaire in the same order as they are in Figs. 5.7 and 5.8.

In the questionnaire, each CVD volunteer expresses his/her satisfaction degree (or preference) by scoring the four alternatives of each image, regarding the discrimination of the contents (contrast) and naturalness. Scoring is performed using a (discrete) qualitative ordinal scale [110], from the more (highest score 1) to less (lowest score 4) preferred alternative. Note that this scoring scale is adequate up to five items [105].

5.4.2.4 Validation

For the validation of the questionnaire, we benefited from the contribution of 2 statisticians and 2 CVD researchers. The statistics experts were critical to adopt descriptive statistics techniques, as adequate for multiple options up to 5, as well as to design the questionnaire itself. In respect to CVD researchers, one of whom is also a dichromat individual, they played an important role in the formulation of the questions focused on color contrast and naturalness, as selected for the questionnaire.

5.4.3 Data Scoring and Collecting

Fig. 5.9 shows the raw quantitative results obtained from the questionnaire. These results express the CVD people's preferences relative to five image categories depicted in Figs. 5.7 and

5.8, namely: InfoVis, Indoor, Outdoor, SciVis, and Signage. Recalling that we have 6 images per category and a universe of 13 respondents, we see the data sample consists of 78 responses ($= 6 \times 13$) per category; for example, considering the CEA method, the data sample for the SciVis category (see Fig. 5.9(d)), comprises 1 response with score 1, 16 responses with score 2, 22 responses with score 3, and 18 responses with score 4. Summing the number of responses for any other method, we always obtain 78 responses with the scores ranging in $[1, 4]$. It is clear that the number of scores is equal to the number of methods under analysis.

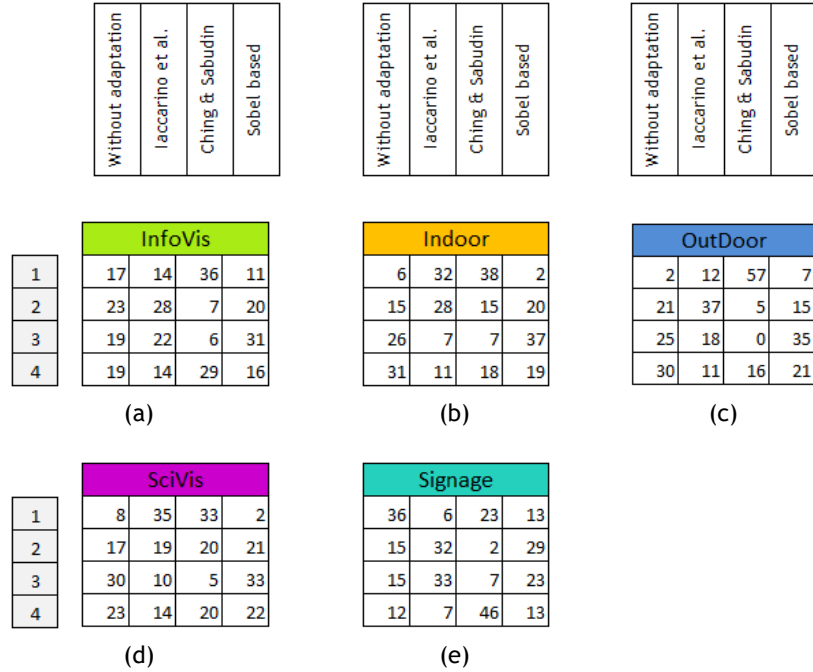


Figure 5.9: Distribution of the preference scores of color adaptation methods per category.

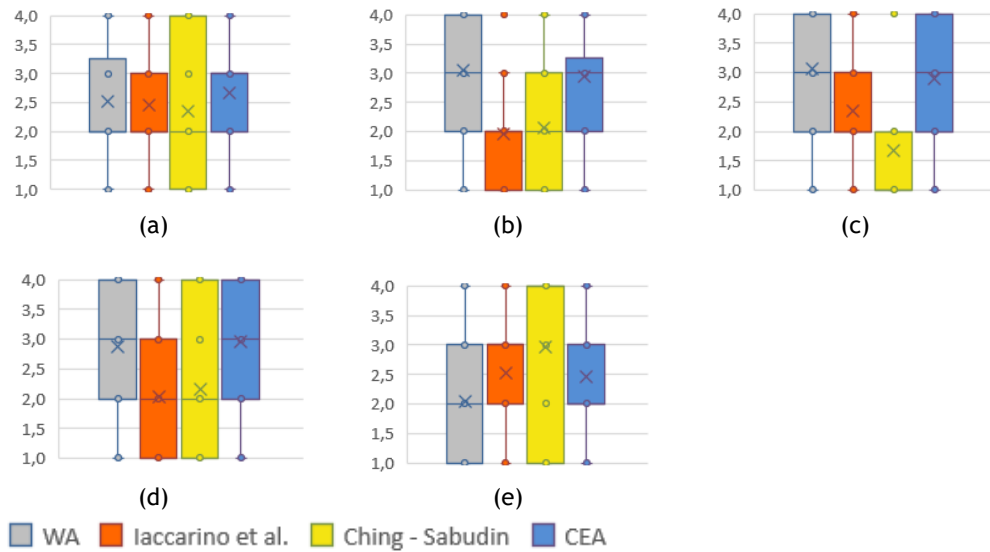


Figure 5.10: Box-and-whisker diagrams of the distribution of preferences of color adaptation methods per category: (a) InfoVis; (b) Indoor; (c) Outdoor; (d) SciVis; and (e) Signage. The *mean* is represented by a cross and *median* by the horizontal line.

5.4.4 Data Analysis

We based data analysis on two descriptive statistical tools: (i) box-and-whisker diagrams (see Fig. 5.10); (ii) coefficient of variation (see Table 5.1). Such diagrams and statistical data were produced from raw data presented in Fig. 5.9. The box-and-whisker diagrams constitute a visual tool that helps us to observe the distribution of preferences of CVD respondents rapidly [111]. As its name says, a box-and-whisker diagram has one box and two whiskers (see Fig. 5.10). The box represents the consensus of preferences and includes at least 50% of the preferences of each method. More specifically, such box represents the preferences of the second and third quartiles, which are put apart through the median (cf. horizontal straight line segment inside the box). The arithmetic mean shows off as a cross inside the box.

On the other hand, the coefficient of variation (CV, for brevity) measures the dispersion/concentration of the distribution of such preferences [103], as shown in Table 5.1. Recall that the coefficient of variation v is given by the ratio \bar{x}/σ , where \bar{x} stands for the mean, and σ the standard deviation. Sometimes, the coefficient of variation is also called relative standard deviation.

Therefore, a brief glance at Figs. 5.9-5.10 and statistical data listed in Table 5.1 shows us the following:

- *Infovis*: When compared to other methods, CEA method is the one with the highest mean (2.67). Furthermore, it presents the lowest coefficient of variation (36%). So, in respect to infovis-type images, CEA method performs better than any other testing method, including the WA approach.
- *Indoor*: Taking into consideration the diagram (b) in Fig. 5.10, we again see that both WA and CEA methods are better than the other two methods, but their arithmetic means are similar, 3.04 and 2.94, respectively. In spite of its higher dispersion (31%) face to the CEA method (26%), the WA method tends to count with higher scores (31 out of 78 preferences with score 4) than CEA method. Therefore, the WA method ranks first for the indoor-type images.
- *Outdoor*: In respect to outdoor-type images, the WA alternative reaches the higher mean (3.06) and the smaller dispersion (29%), so it ranks first for the outdoor-type images. Thus, the best color adaptation method for outdoor-type images seems to be not using any recoloring procedure at all.
- *SciVis*: In regards to scivis-type images, the best adaptation method is the CEA method, since it has the higher mean (2.96) and the smaller dispersion (27%), i.e., it is more consensual than any other method.
- *Signage*: Ching-Sabudin method ranks first in this image category because it has the higher mean (2.97), despite its high coefficient of variation (45%). In fact, the coefficient of variation is not relevant in this case because most scores (46 out of 78) accumulate at bin 4. Note that the CEA method is also a good solution for signage-type images because it also allows for the identification of unseen image regions, as shown in Fig. 5.6.

Summing up, CEA method is better than WA method in three categories of images, namely infovis-, scivis- and signage-type images. In regards to indoor- and outdoor-type images, the

best option is to leave them as they are, i.e., the WA method, according which there is no need performing any computational recoloring procedure. These results are in agreement with those shown in Fig. 5.6.

Table 5.1: Statistical results for different adaptation color methods.

Category	Metric	MWA	<i>laccarino et al.</i>	<i>Ching-Sabudin</i>	CEA
<i>InfoVis</i>	\bar{x}	2.51	2.49	2.36	2.67
	σ	1.090	0.989	1.386	0.963
	v	43%	40%	59%	36%
<i>Indoor</i>	\bar{x}	3.04	1.96	2.06	2.94
	σ	0.946	1.038	1.231	0.779
	v	31%	53%	60%	26%
<i>Outdoor</i>	\bar{x}	3.06	2.36	1.68	2.90
	σ	0.873	0.911	1.211	0.906
	v	29%	39%	67%	31%
<i>SciVis</i>	\bar{x}	2.87	2.04	2.15	2.96
	σ	0.958	1.145	1.228	0.813
	v	33%	56%	57%	27%
<i>Signage</i>	\bar{x}	2.04	2.53	2.97	2.46
	σ	1.133	0.768	1.348	0.963
	v	56%	30%	45%	39%
Statistical metrics:					
\bar{x} : arithmetic mean; σ : standard deviation; v : coefficient of variation.					

5.5 Conclusions

In contrast to the state-of-the-art of the color adaptation methods, which use a pixel-wise recoloring procedure in an attempt of improving the color perception of deutan and protan dichromats, the focus of the CEA method is on the detection and highlighting of region contours where necessary, so the region interiors are left untouched. In other words, the CEA method is a contour-wise recoloring procedure. Thus, the CEA method is a disruptive technique when compared to the current state-of-the-art of color adaptation methods. This opens new perspectives for a new family of color adaptation methods based on image analysis and processing.

In fact, to discriminate between confusing neighbor regions of a given image, we have introduced a contour highlighting or enhancement algorithm that increases the image contrast, while keeping the naturalness of image color, since there are no color changes in the region interiors and most contours do not need to be highlighted. As a consequence, deutan and protan dichromats can see more images regions than usual, i.e., their image perception increases to a rate close to trichromats' perception, but without disturbing their perceptual learning about the surrounding world.

Chapter 6

Conclusions

This thesis introduces a few contributions to the fields of accessible computing and computer-human interaction, particularly in respect to color adaptation methods/algorithms. In fact, their most important shortcomings of such algorithms were revealed, mainly in methodological terms. For example, the most important requirement to proceed to recoloring of an image at the convenience of a colorblind individual is to know *a priori* his/her color gamut. This is the basis for any procedure that aims at enhancing the visual perception of an individual.

6.1 The Revisited Problem

The color vision deficiency (CVD) is a visual impairment that affects the color perception of about 5% of the world population. The colorblind people are used to look for additional clues to resolve ambiguities in situations of their daily lives (e.g. positions, smells, shapes, textures, etc). However, in computational environments, it is not possible to exploit these clues, what necessarily leads to difficulties in the interpretation of some colored data or objects in imaging, largely because such data or objects are mistaken with others when there is not enough contrast among them; for example, green foliage on a red background may originate confusion in the perception of a dichromat because he/she sees this scene as green foliage on a green background.

As shown throughout this thesis, we found that the methodology followed by most color adaptation methods basically consists in mapping a color of each pixel of a given image into another color, i.e., the color mapping. This thesis shows that this pixel-based recoloring methodology is inadequate when we need only to discriminate neighbor objects from each other along their boundaries. Otherwise, we risk to jeopardize the experience-based perceptual learning of any colorblind individual.

6.2 Contributions

This section synthesizes the most significant empirical findings to answer the research questions put forward in Chapter 1:

Is it possible to increase the visual perception of a color-blind individual by applying a recoloring process to an image without undermining his/her perceptual learning?

We saw through the usability studies performed in the Chapter 4 and Chapter 5 that each re-

coloring method is more or less adequate to the CVD adaptation, depending on the category of images. The commitment with the naturalness preservation is crucial for the adaptation of photo-images representing real world scenes, due to the experience-based perceptual learning of colorblind people, throughout their lives. In the other hand, in the adaptation for images corresponding to signage plates, the high contrast foreground/background is more appreciated. The reader is referred to Chapter 4 and Chapter 5 for further details.

Is it possible for a CVD individual to see objects that are not distinguishable from others in a given image without undermining his/her perceptual learning?

The answer is positive. Object-sensitive recoloring methods constitute a new category of color adaptation methods as the one described in Chapter 5. To our best knowledge, this is the first object-sensitive method we may find in the literature. The selective recoloring of objects along their boundaries can be done in a manner that the visual perception of colorblind people increases without compromising their perceptual learning. It is even possible making visible an object that usually a colorblind individual does not see.

Are image CVD adaptation algorithms useful for colorblind people?

Yes, it was shown in Chapter 4 and Chapter 5 the real usefulness of the CVD adaptation algorithms. However, the CVD adaptation may be improved since one changes the adaptation paradigm, by replacing the pixel-sensitive approaches by the object-sensitive approaches. Moreover, this paradigm must be sustained on a methodology that privileges the color space of each color-blind individual in detriment of general color space for which all colorblind people have the same CVD degree of severity.

6.3 Research Limitations

During the course of our research work, we have identified a number of limitations, namely:

Customized color space? In the development of our algorithms, we have not used personalized color spaces for colorblind people. Truly speaking, this is not taken into account in other algorithms found in the literature either. This is important because the severity degree of CVD varies from an individual to another. This must be the basis of any color adaptation method.

Usability assessment and testing? Most recoloring methods found in the literature lack usability assessment and testing. This prevents any validation of such methods in practice. We have adopted the usability-based validation in the last stage of our doctoral program, including the algorithms described in this thesis.

Contour-adaptation metric? There is necessary to come up with a contour-adaptation metric capable of guaranteeing an increase of visual perception of colorblind people, without com-

promising their experience-based perceptual learning. This metric was proposed in this work - the perception region rate (see Chapter 5) - , which indicates readily what is really seen on an image, before and after the CVD adaptation.

6.4 Future Work

Given the limitations listed in the previous section, we would say that in the future we need to further deal with the following issues:

Customized color space?

To elaborate an algorithm capable of delineating the color space of each colorblind individual, possibly using the principles behind optics.

Usability assessment and testing?

To define a standard methodology to construct usability testing and assessment in conformity with the principles of computer-human interaction.

Contour-adaptation metric?

It is necessary to change the way of recoloring images and text, no matter the medium (e.g., imaging, web, etc.). In particular, the recoloring procedure must be applied to where it is needed. It is clear that this requires some sort of metric other than the metrics of color contrast, color naturalness, and color consistency we have used in this thesis.

But, above all, we need to further explore the possibilities offered by the contour-based methods, known as edge-based methods in image analysis and processing. This shall take us to the development of a new category of methods, which are object-sensitive. In addition, we can eventually take advantage of image semantics that identifies the nature or category of a given image before proceeding to its color adaptation.

6.5 Closure of the Research Work

At this point, it is necessary to recalling the thesis statement as expressed in Chapter 1, which is as follows:

It is feasible to achieve a computational adaptive method for color-blind people that is capable of increasing their visual perception (i.e. to enable them to see more image objects/elements than in adaptation-free circumstances) without undermining their perceptual learning.

As shown in the previous chapters, color adaptation methods are only useful if they preserve the perceptual learning of CVD people. This can be achieved since such methods satisfy three color perceptual requirements: naturalness, consistency, and contrast. Note that most adaptation methods are based on pixel-wise recoloring strategy, that is, a local recoloring strategy that is devoid of any semantic information associated to imaging. This opens a window for future research using region-based and contour-based techniques for color adaptation, in a way as done in image analysis and processing. Our contour enhancement algorithm described in Chapter 5 goes in this direction.

Bibliography

- [1] G. M. Machado and M. M. Oliveira, "A model for simulation of color vision deficiency and a color contrast enhancement technique for dichromats," 2011. xxiii, 12, 13
- [2] F. Vienot, H. Brettel, and J. D. Mollon, "Digital video colourmaps for checking the legibility of displays by dichromats," *Color Research and Application*, vol. 24, no. 4, pp. 243-252, 1999. xxiii, 13, 14, 15, 25, 60, 61, 67, 72, 80, 84, 87, 88, 89, 90
- [3] L. Petrich, "My science and math stuff," p. Simulation of the Dichromacy, 2012. xxiii, 13, 14
- [4] S. Yang, Y. M. Ro, J. Nam, J. Hong, S. Y. Choi, and J.-H. Lee, "Improving visual accessibility for color vision deficiency based on mpeg-21," *Etri Journal*, vol. 26, no. 3, pp. 195-202, 2004. xxiii, 11, 14, 15, 23
- [5] J. Lee and W. Santos, "An adaptative fuzzy-based system to evaluate color blindness," in *Proceedings of the 17th International Conference on Systems, Signals and Image Processing (IWSSIP '10)*, Rio de Janeiro, Brazil, June 17-19. IOS Press, 2010, pp. 211-214. xxiii, 14, 15, 23
- [6] D. Flatla and C. Gutwin, "Ssmrecolor: Improving recoloring tools with situation-specific models of color differentiation," in *Proceedings of the 30th International conference on Human factors in computing systems (CHI '12)*, Austin, Texas, USA, May 5-10. ACM SIGCHI, 2012, pp. 2297-2306. xxiii, 15, 16, 23, 26, 43
- [7] Y.-C. Chen and T.-S. Liao, "Hardware digital color enhancement for color vision deficiencies," *Etri Journal*, vol. 33, no. 1, pp. 71-77, 2011. xxiii, 16, 17, 23, 43
- [8] J.-B. Huang, S.-Y. Wu, and C.-S. Chen, "Enhancing color representation for the color vision impaired," in *Proceedings of the Workshop on Computer Vision Applications for the Visually Impaired - 10th European Conference on Computer Vision (ECCV'2008)*, Marseille, France, October 12-18. IEEE Computer Society, 2008. xxiii, 17, 23, 43
- [9] J.-B. Huang, C.-S. Chen, T.-C. Jen, and S.-J. Wang, "Image recolorization for the color-blind," in *Proceedings of the International Conference on Acoustics, Speech, and Signal Processing (ICASSP'2009)*, Taipei, Taiwan, April 19-24. IEEE Computer Society, 2009, pp. 1161-1164. xxiii, 18, 19, 23, 34, 43
- [10] C.-R. Huang, K.-C. Chiu, and C.-S. Chen, "Key color priority based image recoloring for dichromats," in *Proceedings of the Advances in Multimedia Information Processing - 11th Pacific Rim Conference on Multimedia PCM'2010*, Shanghai, China, September 21-24. Springer-Verlag, 2010, pp. 637-647. xxiii, 18, 19, 23, 34, 43
- [11] M. Ichikawa, K. Tanaka, S. Kondo, K. Hiroshima, K. Ichikawa, S. Tanabe, and K. Fukami, "Web-page color modification for barrier-free color vision with genetic algorithm," in *Proceedings of the Genetic and Evolutionary Computation Conference (GECCO'2003)*, Chicago, USA, July 12-16. Springer-Verlag, 2003, pp. 2134-2146. xxiii, 20, 23

- [12] R. Mochizuki, T. Nakamura, J. Chao, and R. Lenz, "Color-weak correction by discrimination threshold matching," in *Proceedings of the 5th Conference on Colour in Graphics, Imaging and Vision (CGIV'2008)*, Penang, Malaysia, August 26-28. Society for Imaging Science and Technology, 2008, pp. 208-213. xxiii, 18, 19, 20, 21, 23
- [13] L. Jefferson and R. Harvey, "An interface to support color blind computer users," in *Proceedings of the Conference on Human Factors in Computing Systems (SIGCHI'2007)*, San Jose, California, USA, April 28-May 3. ACM Press, 2007, pp. 1535-1538. xxiv, 24, 25, 43
- [14] W. Chen, W. Chen, and H. Bao, "An efficient direct volume rendering approach for dichromats," *IEEE Transactions on Visualization and Computer Graphics*, vol. 17, no. 12, pp. 2144-2152, 2011. xxiv, 24, 25, 26, 43
- [15] Y. Deng, Y. Wang, Y. Ma, J. Bao, and X. Gu, "A fixed transformation of color images for dichromats based on similarity matrices," in *Proceedings of the Advanced Intelligent Computing Theories and Applications. With Aspects of Theoretical and Methodological Issues: 3rd International Conference on Intelligent Computing (ICIC'2007)*, Qingdao, China, August 21-24. Springer Berlin Heidelberg, 2007, pp. 1018-1028. xxiv, 26, 27, 43
- [16] C.-N. Anagnostopoulos, G. Tsekouras, I. Anagnostopoulos, and C. Kalloniatis, "Intelligent modification for the daltonization process of digitized paintings," in *Proceedings of the 5th International Conference on Computer Vision Systems (ICVS'2007)*, Bielefeld, Germany, March 21-24. Applied Computer Science Group, 2007. xxiv, 26, 28, 43
- [17] J. Ruminski, J. Wtorek, Rumin, x, J. ska, M. Kaczmarek, A. Bujnowski, T. Kocejko, and A. Polinski, "Color transformation methods for dichromats," in *Proceedings of the 3rd Conference on Human System Interactions (HSI'2010)*, Rzeszow, Poland, May 13-15. IEEE Computer Society, 2010, pp. 634-641. xxiv, 26, 28, 29, 31, 32, 43
- [18] A. Wong and W. Bishop, "Perceptually-adaptive color enhancement of still images for individuals with dichromacy," in *Proceedings of the Canadian Conference on Electrical and Computer Engineering (CCECE'2008)*, Niagara Falls, ON, Canada, May 4-7. IEEE Computer Society, 2008, pp. 2027-2032. xxiv, 31, 32, 43
- [19] S.-L. Ching and M. Sabudin, "Website image colour transformation for the colour blind," in *Proceedings of the 2nd International Conference on Computer Technology and Development (ICCTD'2010)*, Cairo, Egypt, November 2-4. IEEE Computer Society, 2010, pp. 255-259. xxiv, 31, 33, 43, 54, 55, 56, 67, 68, 69, 70, 72, 73, 89, 90, 91, 93
- [20] L. Troiano, C. Birtolo, and M. Miranda, "Adapting palettes to color vision deficiencies by genetic algorithm," in *Proceedings of the 10th Annual Conference on Genetic and Evolutionary Computation (GECCO'08)*, Atlanta, Georgia, USA, July 12-16. xxiv, 34, 36, 39, 43, 44
- [21] K. Wakita and K. Shimamura, "Smartcolor: Disambiguation framework for the colorblind," in *Proceedings of the 19th International ACM SIGACCESS Conference on Computers and Accessibility (ASSETS'05)*, Baltimore, Maryland, USA, October 30-November 1. ACM Press, 2005, pp. 158-165. xxiv, 34, 35, 36, 37, 43
- [22] L. Jefferson and R. Harvey, "Accommodating color blind computer users," in *Proceedings of the 8th International ACM SIGACCESS Conference on Computers and Accessibility (ASSETS'2006)*, Portland, Oregon, USA, October 23-25. ACM Press, 2006, pp. 40-47. xxiv, 34, 36, 37, 43

- [23] J.-B. Huang, Y.-C. Tseng, S.-I. Wu, and S.-J. Wang, "Information preserving color transformation for protanopia and deuteranopia," *Signal Processing Letters*, vol. 14, no. 10, pp. 711-714, 2007. xxiv, 34, 36, 38, 40, 43, 76, 93
- [24] G. Kuhn, M. Oliveira, and L. Fernandes, "An efficient naturalness-preserving image-recoloring method for dichromats," *Transactions on Visualization and Computer Graphics*, vol. 14, no. 6, pp. 1747-1754, 2008. xxiv, 34, 39, 40, 43, 76, 93
- [25] M. Wang, B. Liu, and X.-S. Hua, "Accessible image search," in *Proceedings of the 17th International Conference on Multimedia (MM'09), Beijing, China, October 19-23*. xxiv, 34, 40, 41, 43
- [26] K. Rasche, R. Geist, and J. Westall, "Detail preserving reproduction of color images for monochromats and dichromats," *IEEE Computer Graphics and Applications*, vol. 25, no. 3, pp. 22-30, 2005. xxiv, 34, 35, 43, 45, 46
- [27] —, "Re-coloring images for gamuts of lower dimension," *Computer Graphics Forum*, vol. 24, no. 3, pp. 423-432, 2005. xxiv, 34, 35, 43, 45, 46
- [28] M. A. Barbara Astle, *Enfermagem Médico-Cirúrgica: Conceitos e Prática Clínica*, 6th ed. Lusociencia - Edições Técnicas e Científicas, Lda, 2003, vol. 4. 10
- [29] E. Marieb, *Anatomy & Physiology*, 1st ed. Addison Wesley Longman, 2001. 10
- [30] L. Sharpe, A. Stockman, H. Jagle, and J. Nathans, "Opsin genes, cone photopigments, color vision and color blindness," *Color vision: From genes to perception*, vol. 351, 1999. 10, 11, 12, 75, 93
- [31] J. M. B. Lopes, *Cor e Luz*. Lisboa: IST-UTL, 2008. 10
- [32] R.-L. Rousseau, *Le Language des Couleurs*. St. Jean de Braye: édition Dangles, 1980. 10
- [33] A. Damasio, T. Yamada, M.D, H. Damasio, J. Corbett, and J. McKee, "Central achromatopsia: Behavioral, anatomic, and physiologic aspects," in *Neurology*. American Academy of Neurology, 1980, pp. 1064-1071. 10
- [34] L. Rüttinger, D. Braun, K. Gegenfurtner, D. Petersen, P. Schonle, and L. T. Sharpe, "Selective color constancy deficits after circumscribed unilateral brain lesions," *Journal of Neuroscience*, vol. 19, pp. 3094-3106, 1999. 10
- [35] J. D. Mollon, F. Newcombe, P. G. Polden, and G. Ratcliff, "On the presence of three cone mechanisms in a case of total achromatopsia," in *Color Vision Deficiencies V, Chapter 3*, G. Verriest, Ed. Bristol: Adam Hilger, 1980, pp. 130-135. 10
- [36] J. Birch, I. Chisholm, P. Kinnear, M. Marré, A. Pinckers, J. Pokorny, and G. Verriest, "Acquired color vision defects," in *Congetinal and Acquired Color Vision Defects*. Grune and Stratton, 1979. 11
- [37] J. Birch, *Diagnosis of Defective Colour Vision*, 2nd ed. Edimburgh: Elsevier Science, 2001. 11
- [38] B. Case, "Color blindness," Tech. Rep., 2003. 11
- [39] H. Kolb, E. Fernandez, and R. Nelson, Eds., *WebVision: The Organization of the Retina and Visual System*. John Moran Eye Center - University of Utah, 2011. 11

- [40] A. Byrne and D. Hilbert, "How do things look to the color-blind?" in *Color Ontology and Color Science*, M. Cohen, Jonathan Metthen, Ed. MIT Press, 2010. 12
- [41] J. C. Gardner, M. Michaelides, G. E. Holder, N. Kanuga, T. R. Webb, J. D. Mollon, A. T. Moore, and A. J. Hardcastle, "Blue cone monochromacy: causative mutations and associated phenotypes," *Molecular Vision*, vol. 15, pp. 876-884, 2009. 12
- [42] Y. Miyake, *Electrodiagnosis of Retinal Diseases*. Springer Tokyo, 2006, ch. Rod Monochromacy, pp. 136-137. 12
- [43] J. H. University, "An online catalog of human genes and genetic disorders - online mendelian inheritance in man (OMIM)," 2015-07-21 1966. 12
- [44] A. Reitner, L. T. Sharpe, and E. Zrenner, "Is colour vision possible with only rods and blue-sensitive cones?" *Nature*, vol. 352, no. 6338, pp. 798-800, 1991. 12
- [45] S. Yang, Y. M. Ro, E. K. Wong, and J.-H. Lee, "Quantification and standardized description of color vision deficiency caused by anomalous trichromats - part i: Simulation and measurement," *EURASIP Journal on Image and Video Processing*, vol. 2008, pp. 1-9, 2008. 13, 15
- [46] S. Yang and Y. M. Ro, "Visual contents adaptation for color vision deficiency," in *Proceedings of the International Conference on Image Processing (ICIP'2003)*, Barcelona, Spain, September 4-17, vol. 1. IEEE Computer Society, 2003, pp. 453-456. 15, 23, 30, 43, 44
- [47] S. Yang, Y. M. Ro, E. K. Wong, and J.-H. Lee, "Color compensation for anomalous trichromats based on error score of fm-100 hue test," in *Proceedings of the 27th Annual International Conference of the Engineering in Medicine and Biology Society*, Shanghai, China. IEEE Computer Society, 2005, pp. 6571-6574. 15, 23
- [48] J. Nam, Y. M. Ro, Y. Huh, and M. Kim, "Visual content adaptation according to user perception characteristics," *IEEE Transactions on Multimedia*, vol. 7, no. 3, pp. 435-445, 2005. 15
- [49] J. Lee, "Uma ferramenta adaptativa para facilitar a visualização de imagens para pessoas portadoras de daltonismo," Ph.D. dissertation, 2008. 15, 23
- [50] J. Lee and W. Santos, "An adaptive fuzzy-based system to simulate, quantify and compensate color blindness," *Integrated Computer-Aided Engineering*, vol. 18, no. 1, pp. 29-40, 2011. 15, 23
- [51] S. Poret, R. D. Dony, and S. Gregori, "Image processing for colour blindness correction," in *Proceedings of the International Conference on Science and Technology for Humanity (TIC-STH'2009)*, Toronto, Canada, September 28-29. IEEE Computer Society, 2009, pp. 539-544. 15, 23, 43
- [52] M. Tkalcic and J. F. Tasic, "Colour spaces: perceptual, historical and applicational background," in *Proceedings of the Computer as a Tool - region 8 (EUROCON'2003)*, Ljubljana, Slovenia, September 22-24, vol. 1. IEEE Computer Society, 2003, pp. 304-308. 16, 50, 67
- [53] C. I. de L'éclairage, "Colorimetry," Commission Internationale de L'éclairage, Vienna: Central Bureau of the CIE, Tech. Rep. CIE-15:2004, 2004. 17

- [54] B. Fraser, C. Murphy, and F. Bunting, *Real World Color Management*, 2nd ed. Peachpit Press, 2005. 17
- [55] T. Yanagida, K. Okajima, and H. Mimura, *Color Research & Application*. WILEY, 2014, vol. 40, no. 5, ch. Color scheme adjustment by fuzzy constraint satisfaction for color vision deficiencies, pp. 446-464. 18
- [56] J. Rissanen, "Stochastic complexity in learning," *Journal of Computer and System Sciences*, vol. 55, no. 1, pp. 89-95, 1997. 18
- [57] P. Whitfield and W. Stiles, *Color science : concepts and methods, quantitative data and formulae*, 2nd ed., 1982. 18
- [58] M. Fairchild, *Color Appearance Models*, 3rd ed. WILEY, 2013. 18
- [59] S. Oshima, R. Mochizuki, J. Chao, and R. Lenz, "Color reproduction using riemann normal coordinates," in *Proceedings of the Computational Color Imaging: Second International Workshop (CCIW'2009)*, Saint-Etienne, France, March 26-27. *Revised Selected Papers*, vol. 5646. Springer Berlin Heidelberg, 2009, pp. 140-149. 19, 23
- [60] R. Mochizuki, S. Oshima, and J. Chao, "Fast color-weakness compensation with discrimination threshold matching," in *Proceedings of the 3rd International Workshop on Computational Color Imaging (CCIW'2011)*, Milan, Italy, April 20-21. Springer Berlin Heidelberg, 2011, pp. 176-187. 19, 23
- [61] R. Mochizuki, S. Oshima, R. Lenz, and J. Chao, "Exact compensation of color-weakness with discrimination threshold matching," in *Proceedings of the 6th International Conference on Universal Access in Human-Computer Interaction. Applications and Services (UAHCI'2011)*, Orlando, Florida, USA, July 9-14, vol. 6768. Springer Berlin Heidelberg, 2011, pp. 155-164. 19, 23
- [62] S. Oshima, R. Mochizuki, R. Lenz, and J. Chao, "Color-weakness compensation using riemann normal coordinates," in *IEEE International Symposium on Multimedia (ISM'2012)*, Irvine, California, USA, December 10-12. IEEE Computer Society, 2012, pp. 175-178. 20, 21, 23
- [63] N. Milic, M. Hoffmann, T. Tomacs, D. Novakovic, and B. Milosavljevic, "A content-dependent naturalness-preserving daltonization method for dichromatic and anomalous trichromatic color vision deficiencies," *Journal of Imaging Science and Technology*, vol. 59, no. 1, p. 010504, 2015. 20, 21, 23, 41, 42
- [64] M. Ichikawa, K. Tanaka, S. Kondo, K. Hiroshima, K. Ichikawa, S. Tanabe, and K. Fukami, "Preliminary study on color modification for still images to realize barrier-free color vision," in *Proceedings of the International Conference on Systems, Man and Cybernetics* The Hague, Netherland, October 10-13, vol. 1. IEEE Computer Society, 2004, pp. 36-41. 20, 21, 23
- [65] T. Kojima, R. Mochizuki, R. Lenz, and J. Chao, "Riemann geometric color-weak compensation for individual observers," in *Proceedings of the Universal Access in Human-Computer Interaction, in the Universal Access to Information and Knowledge (UAHCI'2014)*, Heraklion, Crete, Greece, June 22-27, vol. 8514. Springer International Publishing, 2014, pp. 121-131. 21, 23

- [66] S. Oshima, R. Mochizuki, R. Lenz, and J. Chao, "Modeling, measuring, and compensating color weak vision," *Transactions on Image Processing*, vol. 25, no. 6, pp. 2587-2600, 2016. 21, 23
- [67] J. D. Mollon and J. P. Reffin, *Handbook of the Cambridge Colour Tests*, ser. Cambridge Research Systems. Cambridge University Press, 2000. 22
- [68] Y. M. Ro and S. Yang, "Color adaptation for anomalous trichromats," *International Journal of Imaging Systems and Technology*, vol. 14, no. 1, pp. 16-20, 2004. 23
- [69] Y. Ma, X.-D. Gu, and Y.-Y. Wang, "A new color blindness cure model based on bp neural network," in *Proceedings of the Advances in Neural Networks - Third International Symposium on Neural Networks (ISNN'2006)*, Chengdu, China, May 28-June 1, vol. 3973. Springer-Verlag Berlin, 2006, pp. 740-745. 24, 25, 43
- [70] H. Brettel, F. c. Vienot, and J. D. Mollon, "Computerized simulation of color appearance for dichromats," *Journal of the Optical Society of America a-Optics Image Science and Vision*, vol. 14, no. 10, pp. 2647-2655, 1997. 25, 39, 54, 61, 80
- [71] P. Doliotis, G. Tsekouras, C.-N. Anagnostopoulos, and V. Athitsos, "Intelligent modification of colors in digitized paintings for enhancing the visual perception of color-blind viewers," in *Proceedings of the Advances in Information and Communication Technology - International Conference on Artificial Intelligence Applications and Innovations (IAI'2009)*, Thessaloniki, Greece, September 16-18, vol. 296. Springer USA, 2009, pp. 293-301. 26, 43
- [72] J.-Y. Jeong, H.-J. Kim, T.-S. Wang, Y.-J. Yoon, and S.-J. Ko, "An efficient re-coloring method with information preserving for the color-blind," *Transactions on Consumer Electronics*, vol. 57, no. 4, pp. 1953-1960, 2011. 26
- [73] J. Bao, Y. Wang, Y. Ma, and X. Gu, "Re-coloring images for dichromats based on an improved adaptive mapping algorithm," in *Proceedings of the International Conference on Audio, Language and Image Processing (ICALIP'2008)*, Shanghai, China, July 7-9, 2008, pp. 152-156. 26, 28, 43, 44
- [74] Y. Ma, X. Gu, and Y. Wang, "Color discrimination enhancement for dichromats using self-organizing color transformation," *Information Sciences*, vol. 179, no. 6, pp. 830-843, 2008. 26, 27, 43
- [75] J. Sammon, "A nonlinear mapping for data structure analysis," *Transactions on Computers*, vol. C-18, no. 5, pp. 401-409, May 1969. 27, 38
- [76] G. Iaccarino, D. Malandrino, M. Del Percio, and V. Scarano, "Efficient edge-services for colorblind users," in *Proceedings of the 15th International Conference on World Wide Web (WWW'2006)*, Edinburgh, Scotland, May 23-26, ser. Lecture Notes in Computer Science. ACM Press, 2006, pp. 919-920. 30, 31, 43, 44, 54, 55, 56, 67, 68, 69, 70, 72, 73, 89, 90, 91, 93
- [77] C. L. Lai, S. W. Chang, and Ieee, "An image processing based visual compensation system for vision defects," in *Proceedings of the 13th International Symposium on Consumer Electronics (ISCE'2009)*, Kyoto, Japan, 25-28 May. IEEE Computer Society, 2009. 31, 32, 43

- [78] V. A. Kovalev, "Towards image retrieval for eight percent of color-blind men," in *Proceedings of the 17th International Conference on Pattern Recognition (ICPR'2004)*, Cambridge, United Kingdom, August 23-26, vol. 2. IEEE Computer Society, 2004, pp. 943-946. 34, 43
- [79] C. Birtolo, P. Pagano, and L. Troiano, "Evolving colors in user interfaces by interactive genetic algorithm," in *Proceedings of the World Congress on Nature and Biologically Inspired Computing (NaBIC'2009)*, Coimbatore, India, December 9-11. IEEE Computer Society, 2009, pp. 349-355. 34, 39
- [80] L. Troiano, C. Birtolo, and G. Cirillo, "Interactive genetic algorithm for choosing suitable colors in user interface," University of Sannio, Tech. Rep., 2010. 34, 39
- [81] M. Wang, B. Liu, and X.-S. Hua, "Accessible image search for colorblindness," *Transactions on Intelligent Systems and Technologies*, vol. 1, no. 1, pp. 1-26, 2010. 34, 40
- [82] D. R. Flatla, K. Reinecke, C. Gutwin, and K. Z. Gajos, "Sprweb: preserving subjective responses to website colour schemes through automatic recolouring," in *Proceedings of the Conference on Human Factors in Computing Systems (SIGCHI'2013)*, Paris, France, April 27-May 2. ACM Press, 2013, pp. 2069-2078. 34, 40, 43, 44, 69, 91
- [83] T. Cox, *Multidimensional Scaling*, 1st ed. Chapman & Hall, 1994. 35, 45
- [84] V. Kovalev and M. Petrou, "Optimising the choice of colours of an image database for dichromats," in *Proceedings of the Machine Learning and Data Mining in Pattern Recognition: 4th International Conference (MLDM'2005)*, Leipzig, Germany, July 9-11. Springer Berlin Heidelberg, 2005, pp. 456-465. 35
- [85] B. Caldwell, M. Cooper, L. Reid, and G. Vanderheidenl, "Web content accessibility guidelines (wcag) 2.0," December 2008. 39
- [86] L. Velho, A. Frery, and J. Gomes, *Image Processing for Computer Graphics and Vision*, ser. Texts in Computer Science. Springer-Verlag London, England, 2008. 40
- [87] L.-C. Ou, M. R. Luo, A. Woodcock, and A. Wright, "A study of colour emotion and colour preference. part i: Colour emotions for single colours," *Color Research & Application*, vol. 29, no. 3, pp. 232-240, 2004. 41
- [88] S. Nakauchi and T. Onouchi, "Detection and modification of confusing color combinations for red-green dichromats to achieve a color universal design," *Color Research & Application*, vol. 33, no. 3, pp. 203-211, 2008. 41, 43
- [89] R. Gray, J. Kieffer, and Y. Linde, "Locally optimal block quantizer design," *Information and Control*, vol. 45, no. 2, pp. 178-198, 1980. 42
- [90] B. Sajadi, A. Majumder, M. M. Oliveira, R. G. Schneider, and R. Raskar, "Using patterns to encode color information for dichromats," *IEEE Transactions on Visualization and Computer Graphics*, vol. 19, no. 1, pp. 118-129, 2013. 46
- [91] D. R. Flatla, A. R. Andrade, R. D. Teviotdale, D. L. Knowles, and C. Stewart, "Colourid: Improving colour identification for people with impaired colour vision," in *Proceedings of the 33rd Annual ACM Conference on Human Factors in Computing Systems* Seoul, Republic of Korea, April 18-23. ACM Press, 2015, pp. 3543-3552. 46

- [92] N. Suetake, G. Tanaka, H. Hashii, and E. Uchino, "Simple lightness modification for color vision impaired based on craik-o'brien effect," *Journal of the Franklin Institute*, vol. 349, no. 6, pp. 2093-2107, 2012. 47
- [93] S. Bao, G. Tanaka, H. Tamukoh, and N. Suetake, "Lightness modification method considering craik-o'brien effect for protanopia and deuteranopia," *IEICE Transactions on Fundamentals of Electronics, Communications and Computer Sciences*, vol. E99.A, no. 11, pp. 2008-2011, 2016. 47
- [94] M. J. Huiskes, B. Thomee, and M. S. Lew, "New trends and ideas in visual concept detection: The mir flickr retrieval evaluation initiative," in *Proceedings of the International Conference on Multimedia Information Retrieval (MIR'10)*, Philadelphia, Pennsylvania, USA. ACM Press, 2010, pp. 527-536. 47
- [95] A. H. Munsell, *A Color Notation - A Measured Color System, based on the Three Qualities Hue, Value and Chroma*. Geo. H. Ellis Co., 1907. 50
- [96] A. Ford and A. Roberts, *Colour Space Conversions*. London: Westminster University, 1998. 50, 60, 67
- [97] R. Gonzalez and R. Woods, *Digital Image Processing*. Pearson, Prentice Hall, 1992. 50, 86
- [98] A. R. Smith, "Color gamut transform pairs," in *Proceedings of the 5th Annual Conference on Computer Graphics and Interactive Techniques - Special Interest Group on Computer Graphics and Interactive Techniques (SIGGRAPH'78)*, Atlanta, Georgia, USA, August, 23-25. ACM Press, 1978, pp. 12-19. 61, 62, 63
- [99] G. Meyer and D. Greenberg, "Color-defective vision and computer graphics displays," *Computer Graphics and Applications*, vol. 8, no. 5, pp. 28-40, 1988. 61, 80
- [100] C. Poynton, *Digital Video and HDTV: Algorithms and Interfaces*, ser. The Morgan Kaufmann Series in Computer Graphics. Morgan Kaufmann Publishers, 2003. 64, 72, 86, 90
- [101] S. Cotton, "Colour, colour spaces and the human visual system," 1995. 67
- [102] A. J. Vingrys and P. E. King-Smith, "A quantitative scoring technique for panel tests of color vision," *Investigative Ophthalmology & Visual Science*, vol. 29, no. 1, pp. 50-63, January 1988. 75, 91
- [103] J. W. Tukey, *Exploratory Data Analysis*. Addison-Wesley, 1977. 76, 93, 96
- [104] D. S. Shafer and Z. Zhang, *Beginning Statistics*. Andy Schmitz, 2012. 76, 93, 94
- [105] S. Abeyasekera, J. Lawson-Macdowell, and I. Wilson, "Converting ranks to scores for an ad hoc assessment of methods of communication available to farmers," DFID-funded work under the Farming Systems Integrated Pest Management Project, Malawi and DFID NRSP project R7033, Methodological Framework for Combining Qualitative and Quantitative Survey Methods., Tech. Rep., 2000. 76, 94
- [106] W. E. Saris and I. N. Gallhofer, *Design, Evaluation, and Analysis of Questionnaires for Survey Research*. John Wiley & Sons, 2007. 76
- [107] V. Smith and J. Pokorny, "Spectral sensitivity of the foveal cone photopigments between 400 and 500 nm," *Vision Research*, vol. 15, no. 2, pp. 161-171, 1975. 84

- [108] D. Travis, *Effective Color Displays: Theory and Practice*. London: Academic Press, 1991. 84
- [109] L. Thurstone, "A law of comparative judgment," *Psychological Review*, vol. 34, no. 4, pp. 273-286, 1927. 93
- [110] U. Reading, "Approaches to the analysis of survey data biometrics advisory and support service to dfid," The University of Reading - Statistical Services Centre, Tech. Rep., 2001. 94
- [111] K. Potter, "Methods for presenting statistical information: The box plot," in *Visualization of Large and Unstructured Data Sets*, ser. GI-Edition Lecture Notes in Informatics (LNI), H. Hagen, A. Kerren, and P. Dannenmann, Eds., 2006, vol. S-4, pp. 97-106. 96

